Control of Deflection in Concrete Structures

Reported by ACI Committee 435

Edward G. Nawy
Chairman

A. Samer Ezeldin
Secretary

Emin A. Aktan	Anand B. Gogate	Maria A. Polak
Alex Aswad	Jacob S. Grossman	Charles G. Salmon
Donald R. Buettner	Hidayat N. Grouni[*]	Andrew Scanlon
Finley A. Charney	C. T. Thomas Hsu	Fattah A. Shaikh
Russell S. Fling	James K. Iverson	Himat T. Solanki
Amin Ghali	Bernard L. Meyers	Maher K. Tadros
Satyendra K. Ghosh	Vilas Mujumdar	Stanley C. Woodson

This report presents a consolidated treatment of initial and time-dependent deflection of reinforced and prestressed concrete elements such as simple and continuous beams and one-way and two-way slab systems. It presents the state of the art in practice on deflection as well as analytical methods for computer use in deflection evaluation. The introductory chapter and four main chapters are relatively independent in content. Topics include "Deflection of Reinforced Concrete One-way Flexural Members," "Deflection of Two-way Slab Systems," and "Reducing Deflection of Concrete Members."

One or two detailed computational examples for evaluating the deflection of beams and two-way action slabs and plates are given at the end of Chapters 2, 3, and 4. These computations are in accordance with the current ACI- or PCI-accepted methods of design for deflection.

CONTENTS

CHAPTER 1—INTRODUCTION

Design for serviceability is central to the work of structural engineers and code-writing bodies. It is also essential to users of the structures designed. Increased use of high-strength concrete with reinforcing bars and prestressed reinforcement, coupled with more precise computer-aided limit-state serviceability designs, has resulted in lighter and more material-efficient structural elements and systems. This in turn has necessitated better control of short-term and long-term behavior of concrete structures at service loads.

This report presents consolidated treatment of initial and time-dependent deflection of reinforced and prestressed concrete elements such as simple and continuous beams and one-way and two-way slab systems. It presents current engineering practice in design for control of deformation and deflection of concrete elements and includes methods presented in "Building Code Requirements for Reinforced Concrete (ACI 318)" plus selected other published approaches suitable for computer use in deflection computation. Design examples are given at the end of each chapter showing how to evaluate deflection (mainly under static loading) and thus control it through adequate design for serviceability. These step-by-step examples as well as the general thrust of the report are intended for the non-seasoned practitioner who can, in a single document, be familiarized with the major state of practice approaches in buildings as well as additional condensed coverage of analytical methods suitable for computer use in deflection evaluation. The examples apply AC1 318 requirements in conjunction with PCI methods where applicable.

The report replaces several reports of this committee in order to reflect more recent state of the art in design. These reports include ACI 435.2R, "Deflection of Reinforced Concrete Flexural Members," ACI 435.1R, "Deflection of Prestressed Concrete Members," ACI 435.3R, "Allowable Deflections," ACI 435.6R, "Deflection of Two-Way Reinforced Concrete Floor Systems," and 435.5R, "Deflection of Continuous Concrete Beams."

The principal causes of deflections taken into account in this report are those due to elastic deformation, flexural cracking, creep, shrinkage, temperature and their long-term effects. This document is composed of four main chapters, two to five, which are relatively independent in content. There is some repetition of information among the chapters in order to present to the design engineer a self-contained treatment on a particular design aspect of interest.

Chapter 2, "Deflection of Reinforced Concrete One-Way Flexural Members," discusses material properties and their effect on deflection, behavior of cracked and uncracked members, and time-dependent effects. It also includes the relevant code procedures and expressions for deflection computation in reinforced concrete beams. Numerical examples are included to illustrate the standard calculation methods for continuous concrete beams.

Chapter 3, "Deflection of Prestressed Concrete One-Way Members," presents aspects of material behavior pertinent to pretensioned and post-tensioned members mainly for building structures and not for bridges where more precise and detailed computer evaluations of long-term deflection behavior is necessary, such as in segmental and cable-stayed bridges. It also covers short-term and time-dependent deflection behavior and presents in detail the Branson effective moment of inertia approach (I_e) used in ACI 318. It gives in detail the PCI Multipliers Method for evaluating time-dependent effects on deflection and presents a summary of

various other methods for long-term deflection calculations as affected by loss of prestressing. Numerical examples are given to evaluate short-term and long-term deflection in typical prestressed tee-beams.

Chapter 4, "Deflection of Two-way Slab Systems," covers the deflection behavior of both reinforced and prestressed two-way-action slabs and plates. It is a condensation of ACI Document 435.9R, "State-of-the-Art Report on Control of Two-way Slab Deflections," of this Committee. This chapter gives an overview of classical and other methods of deflection evaluation, such as the finite element method for immediate deflection computation. It also discusses approaches for determining the minimum thickness requirements for two-way slabs and plates and gives a detailed computational example for evaluating the long-term deflection of a two-way reinforced concrete slab.

Chapter 5, "Reducing Deflection of Concrete Members," gives practical and remedial guidelines for improving and controlling the deflection of reinforced and prestressed concrete elements, hence enhancing their overall long-term serviceability.

Appendix B presents a general method for calculating the strain distribution at a section considering the effects of a normal force and a moment caused by applied loads, prestressing forces, creep, and shrinkage of concrete, and relaxation of prestressing steel. The axial strain and the curvature calculated at various sections can be used to calculate displacements. This comprehensive analysis procedure is for use when the deflections are critical, when maximum accuracy in calculation is desired, or both.

The curvatures and the axial strains at sections of a continuous or simply supported member can be used to calculate the deflections and the change of length of the member using virtual work. The equations that can be used for this purpose are given in Appendix B. The appendix includes examples of the calculations and a flowchart that can be used to automate the analytical procedure.

It should be emphasized that the magnitude of actual deflection in concrete structural elements, particularly in buildings, which are the emphasis and the intent of this Report, can only be estimated within a range of 20-40 percent accuracy. This is because of the large variability in the properties of the constituent materials of these elements and the quality control exercised in their construction. Therefore, for practical considerations, the computed deflection values in the illustrative examples at the end of each chapter ought to be interpreted within this variability.

In summary, this single umbrella document gives design engineers the major tools for estimating and thereby controlling through design the expected deflection in concrete building structures. The material presented, the extensive reference lists at the end of the Report, and the design examples will help to enhance serviceability when used judiciously by the engineer. Designers, constructors, and codifying bodies can draw on the material presented in this document to achieve serviceable deflection of constructed facilities.

CHAPTER 2—DEFLECTION OF REINFORCED CONCRETE ONE-WAY FLEXURAL MEMBERS*

2.1—Notation

A	=	area of concrete section
A_c	=	effective concrete cross section after cracking, or area of concrete in compression
A_s	=	area of nonprestressed steel
A_{sh}	=	shrinkage deflection multiplier
b	=	width of the section
c	=	depth of neutral axis
$C_c,(C_T)$	=	resultant concrete compression (tension) force
C_t	=	creep coefficient of concrete at time t days
C_u	=	ultimate creep coefficient of concrete
d	=	distance from the extreme compression fiber to centroid of tension reinforcement
D	=	dead load effect
E_c	=	modulus of elasticity of concrete
$\overline{E}_c$	=	age-adjusted modulus of elasticity of concrete at time t
E_s	=	modulus of elasticity of nonprestressed reinforcing steel
EI	=	flexural stiffness of a compression member
f_c'	=	specified compressive strength of concrete
f_{ct},f_t'	=	splitting tensile strength of concrete
f_r	=	modulus of rupture of concrete
f_s	=	stress in nonprestressed steel
f_y	=	specified yield strength of nonprestressed reinforcing steel
h	=	overall thickness of a member
I	=	moment of inertia of the transformed section
I_{cr}	=	moment of inertia of the cracked section transformed to concrete
I_e	=	effective moment of inertia for computation of deflection
I_g	=	moment of inertia for gross concrete section about centroidal axis, neglecting reinforcement
K	=	factor to account for support fixity and load conditions
K_e	=	factor to compute effective moment of inertia for continuous spans
k_{sh}	=	shrinkage deflection constant
$K_{(subscript)}$	=	modification factors for creep and shrinkage effects
l	=	span length
L	=	live load effect
$M_{(subscript)}$	=	bending moment
M_a	=	maximum service load moment (unfactored) at stage deflection is completed
M_{cr}	=	cracking moment
M_n	=	nominal moment strength
M_o	=	midspan moment of a simply supported beam
P	=	axial force
t	=	time
T_s	=	force in steel reinforcement
w_c	=	specified density of concrete
y_t	=	distance from centroidal axis of gross section, neglecting reinforcement, to extreme fiber in tension
α	=	thermal coefficient
γ_c	=	creep modification factor for nonstandard conditions
γ_{sh}	=	shrinkage modification factor for nonstandard

---

*Principal authors: A. S. Ezeldin and E. G. Nawy.

$= $ conditions

ϕ $=$ cross section curvature

$=$ strength reduction factor

ϕ_{cracked} $=$ curvature of a cracked member

ϕ_{mean} $=$ mean curvature

$\phi_{\text{uncracked}}$ $=$ curvature of an uncracked member

ϵ_c $=$ strain in extreme compression fiber of a member

ϵ_s $=$ strain in nonprestressed steel

$(\epsilon_{SH})_t$ $=$ shrinkage strain of concrete at time, t days

$(\epsilon_{SH})_u$ $=$ ultimate shrinkage strain of concrete

ρ $=$ nonprestressed tension reinforcement ratio

ρ_b $=$ reinforcement ratio producing balanced strain conditions

ρ' $=$ reinforcement ratio for nonprestressed compression steel

ξ $=$ time dependent deflection factor

δ $=$ elastic deflection of a beam

δ_{cr} $=$ additional deflection due to creep

δ_L $=$ initial deflection due to live load

δ_{LT} $=$ total long term deflection

$\delta_{L\text{-}T}$ $=$ increase in deflection due to long-term effects

δ_{sh} $=$ additional deflection due to shrinkage

δ_{sus} $=$ initial deflection due to sustained load

Δ_y $=$ y-coordinate of the centroid of the age-adjusted section, measured downward from the centroid of the transformed section at t_o

$\Delta f_c(t_o)$ $=$ stress increment at time t_o days

$\Delta f_c(t, t_o)$ $=$ stress increment from zero at time t_o to its full value at time t

$(\Delta \phi)_{\text{creep}}$ $=$ additional curvature due to creep

$(\Delta \phi)_{\text{shrinkage}}$ $=$ additional curvature due to shrinkage

λ $=$ deflection multiplier for long term deflection

μ $=$ multiplier to account for high-strength concrete effect on long-term deflection

η $=$ correction factor related to the tension and compression reinforcement, CEB-FIP

2.2-General

2.2.1 *Introduction*-Wide availability of personal computers and design software, plus the use of higher strength concrete with steel reinforcement has permitted more material efficient reinforced concrete designs producing shallower sections. More prevalent use of high-strength concrete results in smaller sections, having less stiffness that can result in larger deflections. Consquently, control of short-term and long-term deflection has become more critical.

In many structures, deflection rather than stress limitation is the controlling factor. Deflection computations determine the proportioning of many of the structural system elements. Member stiffness is also a function of short-term and long-term behavior of the concrete. Hence, expressions defining the modulus of rupture, modulus of elasticity, creep, shrinkage, and temperature effects are prime parameters in predicting the deflection of reinforced concrete members.

2.2.2 *Objectives*-This chapter covers the initial and

time-dependent deflections at service load levels under static conditions for one-way non-prestressed flexural concrete members. It is intended to give the designer enough basic background to design concrete elements that perform adequately under service loads, taking into account cracking and both short-term and long-term deflection effects.

While several methods are available in the literature for evaluation of deflection, this chapter concentrates on the effective moment of inertia method in *Building Code Requirements for Reinforced Concrete* (ACI 318) and the modifications introduced by ACI Committee 435. It also includes a brief presentation of several other methods that can be used for deflection estimation computations.

2.2.3 *Significance of defection observation*-The working stress method of design and analysis used prior to the 1970s limited the stress in concrete to about 45 percent of its specified compressive strength, and the stress in the steel reinforcement to less than 50 percent of its specified yield strength. Elastic analysis was applied to the design of reinforced concrete structural frames as well as the cross-section of individual members. The structural elements were proportioned to carry the highest service-level moment along the span of the member, with redistribution of moment effect often largely neglected. As a result, stiffer sections with higher reserve strength were obtained as compared to those obtained by the current ultimate strength approach (Nawy, 1990).

With the improved knowledge of material properties and behavior, emphasis has shifted to the use of high-strength concrete components, such as concretes with strengths in excess of 12,000 psi (83 MPa). Consequently, designs using load-resistance philosophy have resulted in smaller sections that are prone to smaller serviceability safety margins. As a result, prediction and control of deflections and cracking through appropriate design have become a necessary phase of design under service load conditions.

Beams and slabs are rarely built as isolated members, but are a monolithic part of an integrated system. Excessive deflection of a floor slab may cause dislocations in the partitions it supports or difficulty in leveling furniture or fixtures. Excessive deflection of a beam can damage a partition below, and excessive deflection of a spandrel beam above a window opening could crack the glass panels. In the case of roofs or open floors, such as top floors of parking garages, ponding of water can result. For these reasons, empirical deflection control criteria such as those in Table 2.3 and 2.4 are necessary.

Construction loads and procedures can have a significant effect on deflection particularly in floor slabs. Detailed discussion is presented in Chapter 4.

2.3-Material properties

The principal material parameters that influence concrete deflection are modulus of elasticity, modulus of rupture, creep, and shrinkage. The following is a presentation of the expressions used to define these parameters

as recommended by ACI 318 and its Commentary (1989) and AC Committees 435 (1978), 363 (1984), and 209 (1982).

2.3.1 *Concrete modulus of rupture*-AC1 318 (1989) recommends Eq. 2.1 for computing the modulus of rupture of concrete with different densities:

$$f_r = 7.5 \ \lambda \sqrt{f_c'}, \text{psi}$$
$$(0.623 \ \lambda \sqrt{f_c'}, \text{MPa})$$
(2.1)

where λ = 1.0 for normal density concrete [145 to 150 pcf (2325 to 2400 kg/m^3)]
        = 0.85 for semi low-density [ll0-145 pcf (1765 to 2325 kg/m^3)]
        = 0.75 for low-density concrete [90 to 110 pcf (1445 to 1765 kg/m^3)]

Eq. 2.1 is to be used for low-density concrete when the tensile splitting strength, f_{ct}, is not specified. Otherwise, it should be modified by substituting $f_{ct}/6.7$ for $\sqrt{f_c'}$, but the value of $f_{ct}/6.7$ should not exceed $\sqrt{f_c'}$.

ACI Committee 435 (1978) recommended using Eq. 2.2 for computing the modulus of rupture of concrete with densities (w_c) in the range of 90 pcf (1445 kg/m^3) to 145 pcf (2325 kg/m³). This equation yields higher values of f_r.

$$f_r = 0.65 \ \sqrt{w_c f_c'}, \text{psi}$$
$$(0.013 \sqrt{w_c f_c'}, \text{MPa})$$
(2.2)

The values reported by various investigators ACI 363, 1984) for the modulus of rupture of both low-density and normal density high-strength concretes [more than 6,000 psi (42 MPa)] range between 7.5 $\sqrt{f_c'}$ and 12 $\sqrt{f_c'}$. ACI 363 (1992) stipulated Eq. 2.3 for the prediction of the modulus of rupture of normal density concretes having compressive strengths of 3000 psi (21 MPa) to 12,000 psi (83 MPa).

$$f_r = 11.7 \ \sqrt{f_c'}, \text{psi}$$
(2.3)

The degree of scatter in results using Eq. 2.1, 2.2 and 2.3 is indicative of the uncertainties in predicting computed deflections of concrete members. The designer needs to exercise judgement in sensitive cases as to which expressions to use, considering that actual deflection values can vary between 25 to 40 percent from the calculated values.

2.3.2 *Concrete modulus of elasticity* -The modulus of elasticity is strongly influenced by the concrete materials and proportions used. An increase in the modulus of elasticity is expected with an increase in compressive strength since the slope of the ascending branch of the stress-strain diagram becomes steeper for higher-strength concretes, but at a lower rate than the compressive strength. The value of the secant modulus of elasticity for normal-strength concretes at 28 days is usually around 4 x 10^6 psi (28,000 MPa), whereas for higher-strength concretes, values in the range of 7 to 8 x 10^6 psi (49,000 to 56,000 MPa) have been reported. These higher values of the modulus can be used to reduce short-term and long-term deflection of flexural members since the compressive strength is higher, resulting in lower creep levels.

Normal strength concretes are those with compressive strengths up to 6,000 psi (42 MPa) while higher strength concretes achieve strength values beyond 6,000 and up to 20,000 psi (138 MPa) at this time.

ACI 435 (1963) recommended the following expression for computing the modulus of elasticity of concretes with densities in the range of 90 pcf (1445 kg/m^3) to 155 pcf (2325 kg/m^3) based on the secant modulus at 0.45 f_c' intercept

$$E_c = 33 \ w_c^{1.5} \sqrt{f_c'}, \text{psi}$$
$$(0.043 \ w_c^{1.5} \sqrt{f_c'}, \text{MPa})$$
(2.4)

For concretes in the strength range up to 6000 psi (42 MPa), the ACI 318 empirical equation for the secant modulus of concrete E_c of Eq. 2.4 is reasonably applicable. However, as the strength of concrete increases, the value of E_c could increase at a faster rate than that generated by Eq. 2.4 ($E_c = w_c^{1.5} \sqrt{f_c'}$), thereby underestimating the true E_c value. Some expressions for E_c applicable to concrete strength up to 12,000 psi (83 MPa) are available. The equation developed by Nilson (Carrasquillo, Martinez, Ngab, et al, 1981, 1982) for normal-weight concrete of strengths up to 12,000 psi (83 MPa) and light-weight concrete up to 9000 psi (62 MPa) is:

$$E_c = (40,000 \ \sqrt{f_c'} + 1,000,000) \left(\frac{w_c}{145}\right)^{1.5}, \text{psi}$$ (2.5)
$$(3.32 \ \sqrt{f_c'} + 6895)\left(\frac{w_c}{2320}\right)^{1.5}, \text{MPa}$$

where w_c is the unit weight of the hardened concrete in pcf, being 145 lb/ft^3 for normal-weight concrete and 100-120 lb/ft^3 for sand-light weight concrete. Other investigations report that as f_c' approaches 12,000 psi (83 MPa) for normal-weight concrete and less for lightweight concrete, Eq. 2.5 can underestimate the actual value of E_c. Deviations from predicted values are highly sensitive to properties of the coarse aggregate such as size, porosity, and hardness.

Researchers have proposed several empirical equations for predicting the elastic modulus of higher strength concrete (Teychenne et al, 1978; Ahmad et al, 1982; Martinez, et al, 1982). ACI 363 (1984) recommended the following modified expression of Eq. 2.5 for normal-weight concrete:

$$E_c = 40,000 \ \sqrt{f_c'} + 1,000,000 \ , \text{psi}$$
(2.6)

Using these expressions, the designer can predict a modulus of elasticity value in the range of 5.0 to 5.7 x 10^6 psi (35 to 39 x 10^3 MPa) for concrete design strength of up to 12,000 psi (84 MPa) depending on the expression used.

When very high-strength concrete [20,000 psi (140 MPa) or higher] is used in major structures or when deformation is critical, it is advisable to determine the stress-strain relationship from actual cylinder compression test results. In this manner, the deduced secant modulus value of E_c at an $f_c = 0.45 \ f_c'$ intercept can be used to predict more accurately the value of E_c for the particular mix and aggregate size and properties. This approach is advisable until an acceptable expression is

Table 2.1 — Creep and shrinkage ratios from age 60 days to the indicated concrete age (Branson, 1977)

Creep, shrinkage ratios	Concrete age					
	2 months	3 months	6 months	1 year	2 years	**>** 5 years
C_t/C_u	0.48	0.56	0.68	0.77	0.84	1.00
$(\epsilon_{sh})_t/(\epsilon_{sh})_u$ -M.C.	0.46	0.60	0.77	0.88	0.94	1.00
$(\epsilon_{sh})_t/(\epsilon_{sh})_u$ -S.C.	0.36	0.49	0.69	0.82	0.91	1.00

M.C. = Moist cured
S.C. = Steam curd

available to the designer (Nawy, 1990).

2.3.3 *Steel reinforcement modulus of elasticity*-AC1 318 specifies using the value $E_s = 29 \times 10^6$ psi (200×10^6 MPa) for the modulus of elasticity of nonprestressed reinforcing steel.

2.3.4 *Concrete creep and shrinkage*-Deflections are also a function of the age of concrete at the time of loading due to the long-term effects of shrinkage and creep which significantly increase with time. ACI 318-89 does not recommend values for concrete ultimate creep coefficient C_u and ultimate shrinkage strain $(\epsilon_{sh})_u$. However, they can be evaluated from several equations available in the literature (ACI 209, 1982; Bazant et al, 1980; Branson, 1977)ACI 435 (1978) suggested that the average values for C_u and $(\epsilon_{sh})_u$ can be estimated as 1.60 and 400×10^{-6}, respectively. These values correspond to the following conditions:

- 70 percent average relative humidity
- age of loading, 20 days for both moist and steam cured concrete
- minimum thickness of component, 6 in. (152 mm)

Table 2.1 includes creep and shrinkage ratios at different times after loading.

ACI 209 (1971, 1982,1992) recommended a time-dependent model for creep and shrinkage under standard conditions as developed by Branson, Christianson, and Kripanarayanan (1971,1977). The term "standard conditions" is defined for a number of variables related to material properties, the ambient temperature, humidity, and size of members. Except for age of concrete at load application, the standard conditions for both creep and shrinkage are

a) Age of concrete at load applications = 3 days (steam), 7 days (moist)
b) Ambient relative humidity = 40 percent
c) Minimum member thickness = 6 in. (150 mm)
d) Concrete consistency = 3 in. (75 mm)
e) Fine aggregate content = 50 percent
f) Air content = 6 percent

The coefficient for creep at time t (days) after load application, is given by the following expression:

$$C_t = \left(\frac{t^{0.6}}{10 + t^{0.6}}\right) C_u \qquad (2.7)$$

where $C_u = 2.35 \, \gamma_{CR}$
$\gamma_{CR} = K_h^c K_d^c K_s^c K_f^c K_{ac}^c K_{to}^c = 1$ for standard conditions.

Each K coefficient is a correction factor for conditions other than standard as follows:

K_h^c = relative humidity factor
K_d^c = minimum member thickness factor
K_s^c = concrete consistency factor
K_f^c = fine aggregate content factor
K_{ac}^c = air content factor
K_{to}^c = age of concrete at load applications factor

Graphic representations and general equations for the modification factors (K-values) for nonstandard conditions are given in Fig. 2.1 (Meyers et al, 1983).

For moist-cured concrete, the free shrinkage strain which occurs at any time t in days, after 7 days from placing the concrete

$$(\epsilon_{SH})_t = \left(\frac{t}{35 + t}\right)(\epsilon_{SH})_u \qquad (2.8)$$

and for steam cured concrete, the shrinkage strain at any time t in days, after l-3 days from placing the concrete

$$(\epsilon_{SH})_t = \left(\frac{t}{55 + t}\right)(\epsilon_{SH})_u \qquad (2.9)$$

where $(\epsilon_{SH})_{u \, Max} = 780 \times 10^{-6} \gamma_{sh}$
$\lambda_{sh} = K_h^s K_d^s K_f^s K_b^s K_{ac}^s$
$= 1$ for standard conditions

Each K coefficient is a correction factor for other than standard conditions. All coefficients are the same as defined for creep except K_B^s, which is a coefficient for cement content. Graphic representation and general equations for the modification factors for nonstandard conditions are given in Fig. 2.2 (Meyers et al, 1983). The above procedure, using standard and correction equations and extensive experimental comparisons, is detailed in Branson (1977).

Limited information is available on the shrinkage behavior of high-strength concrete [higher than 6,000 psi (41 MPa)], but a relatively high initial rate of shrinkage has been reported (Swamy et al, 1973). However, after drying for 180 days the difference between the shrinkage of high-strength concrete and lower-strength concrete seems to become minor. Nagataki (1978) reported that the shrinkage of high-strength concrete containing high-range water reducers was less than for lower-strength concrete.

On the other hand, a significant difference was reported for the ultimate creep coefficient between high-
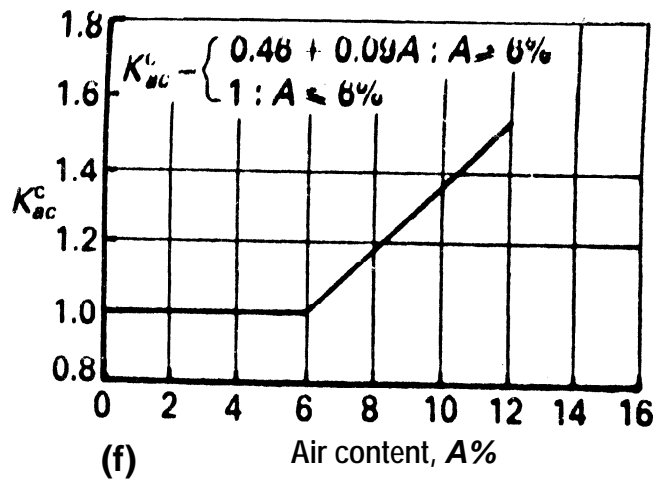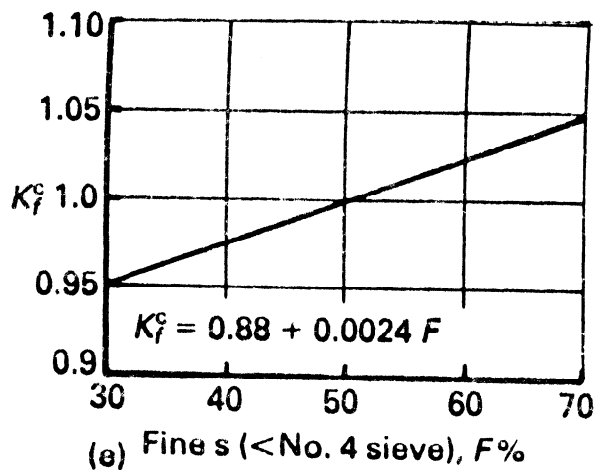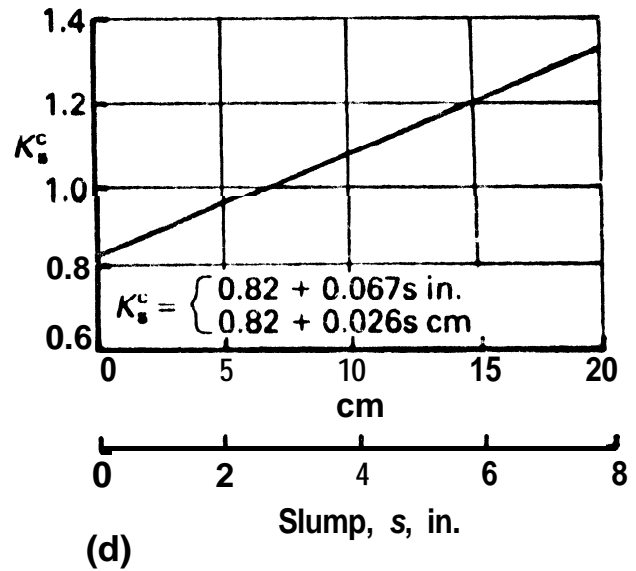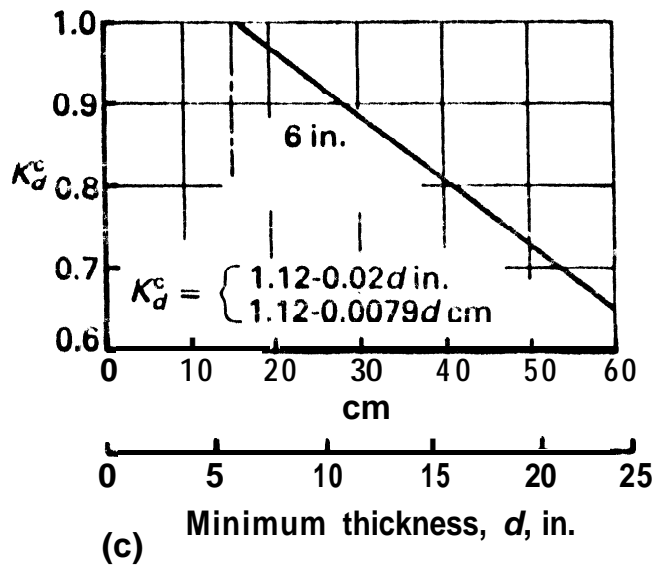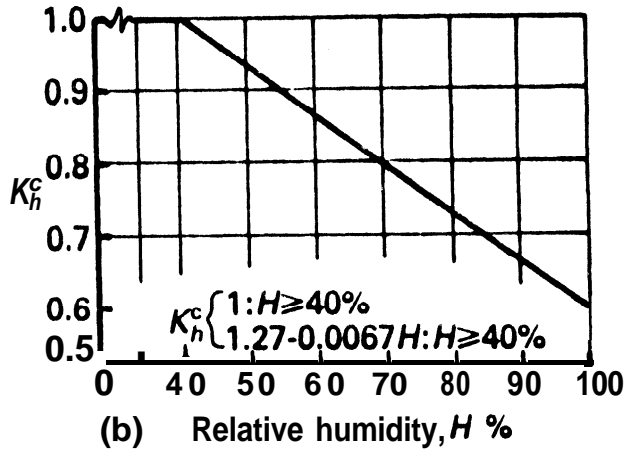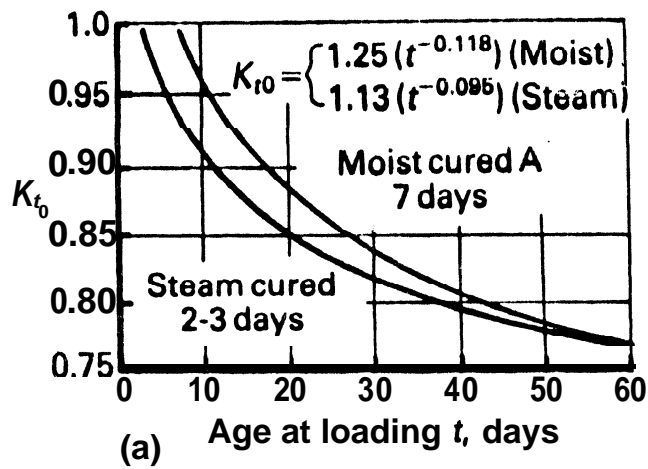
Fig. 2.1-Creep correction factors for nonstandard conditions, ACI 209 method (Meyers, 1983)

$$K_H^s = \begin{cases} 1 : H \leqslant 40 \\ 1.4 - 0.01\,H : 40 \leqslant H \leqslant 80 \\ 3.0 - 0.3\,H : 80 \leqslant H \leqslant 100 \end{cases}$$

(a) Relative humidity, $H\%$

$$K_d^s = \begin{cases} 1.193 - 0.0127\,d \text{ cm)} \\ 1.193 - 0.0322\,d \text{ in.)} \end{cases}$$

(b) Minimum thickness, d, in.

$$K_s^s = \begin{cases} 0.89 + 0.016\,S \text{ cm} \\ 0.89 + 0.04075\,S \text{ in.} \end{cases}$$

(c) Slump, s, in.

$$K_F^s = \begin{cases} 0.3 + 0.014\,F : F \leqslant 50 \\ 0.9 + 0.002\,F \geqslant 50 \end{cases}$$

(d) Fine s ($<$ no. 4 sieve), $F\%$

$$K_B^s = \begin{cases} 0.75 + 0.0034\,B \text{ lb/ft}^3 \\ 0.75 + 0.000214\,B \text{ kg/m}^3 \end{cases}$$
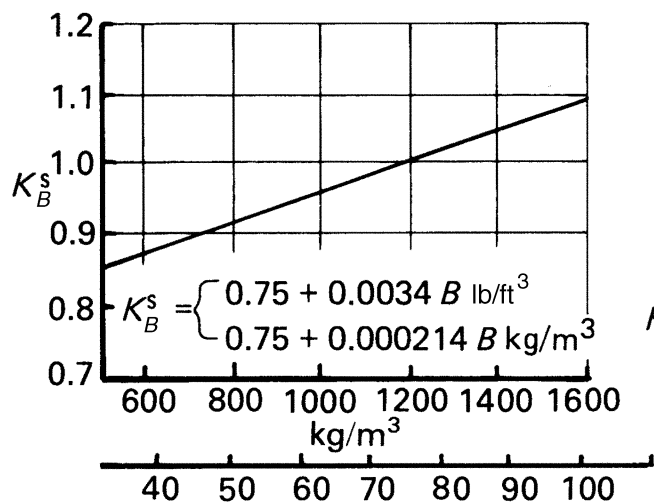
(e) Cement content, B, lb/ft^3

$$K_{AC}^s = 0.95 + 0.008\,A$$
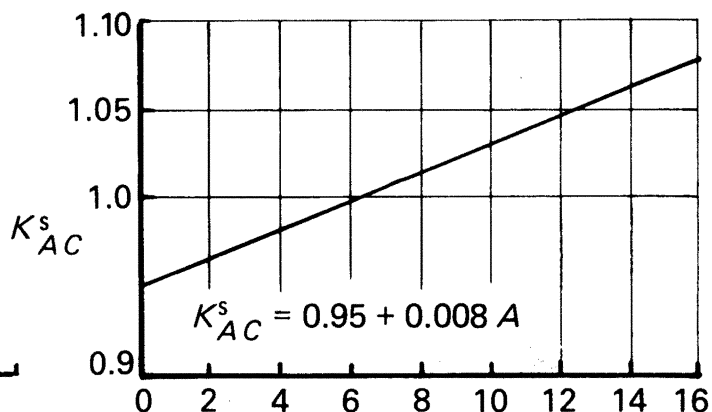
(f) Air content, $A\%$

Fig. 2.2—Shrinkage correction factors for nonstandard conditions, ACI 209 method (Meyers, 1983)

Table 2.2-Recommended tension reinforcement ratios for nonprestressed one-way members so that deflections will normally be within acceptable limits (ACI 435, 1978)

Members	Cross section	Normal weight concrete	Lightweight concrete
Not supporting or not attached to nonstructural elements likely to be damaged by large deflections	Rectangular "T" or box	$\rho \le 35$ percent ρ_b $\rho_w \le 40$ percent ρ_b	$\rho \le 30$ percent ρ_b $\rho_w \le 35$ percent ρ_b
Supporting or attached to nonstructural elements likely to be damaged by large deflections	Rectangular "T" or box	$\rho \le 25$ percent ρ_b $\rho_w \le 30$ percent ρ_b	$\rho \le 20$ percent ρ_b $\rho_w \le 25$ percent ρ_b

For continuous members, the positive region steel ratios only may be used. ρ_b: Refers to the balanced steel ratio based on ultimate strength.

Table 2.3-Minimum thickness of nonprestressed beams and one-way slabs unless deflections are computed (ACI 318, 1989)

		Minimum thickness, h		
	Simply supported	One end continuous	Both ends continuous	Cantilever
Member	Members not supporting or attached to partitions or other construction likely to be damaged by large deflections.			
Solid one-way slabs	$\ell/20$	$1/24$	$\ell/28$	$\ell/10$
Beams or ribbed one-way slabs	$\ell/16$	$\ell/18.5$	$\ell/21$	$\ell/8$

ℓ = Span length

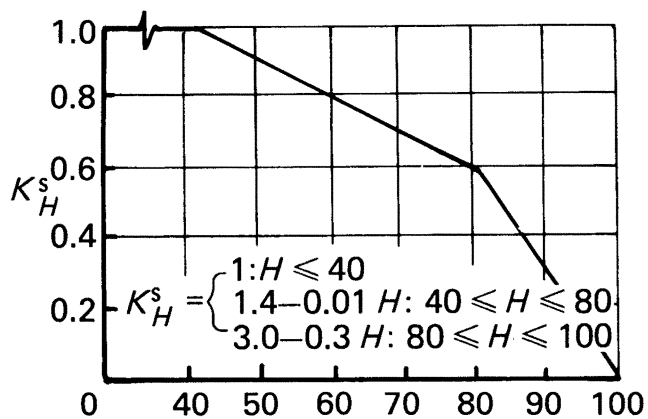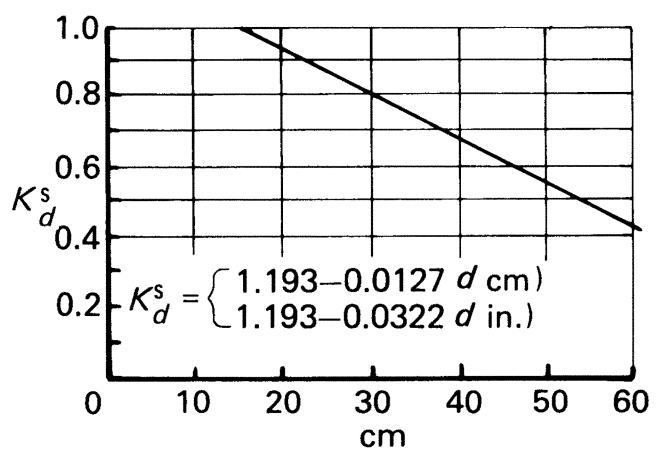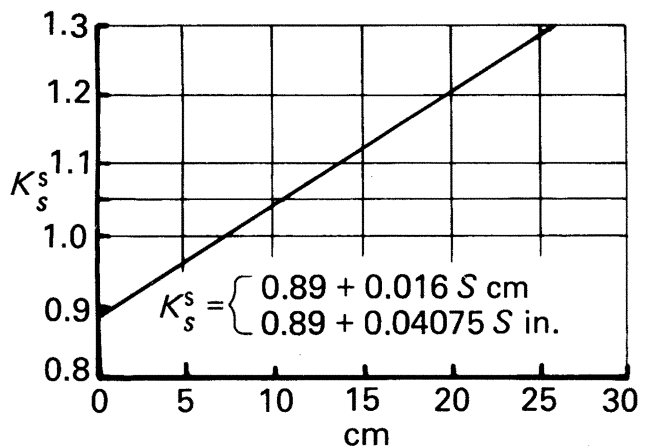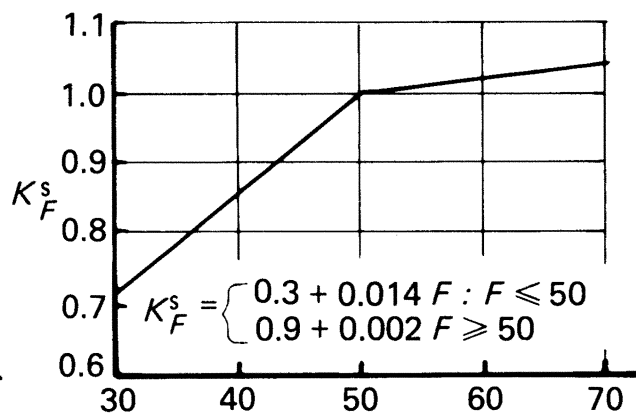Values given shall be used directly for members with normal weight concrete (w_c = 145 pcf) and grade 60 reinforcement. For other conditions. the values shall be modified as follows:

a) For structural lightweight concrete having unit weights in the range 90-120 lb per cu ft. the values shall be multiplied by ($1.65 - 0.005\ w_c$) but not less than 1.09, where w_c is the unit weight in lb per cu ft.

b) For f_y other than 60,000 psi, the values shall be multiplied by ($0.4 + f_y/100,000$).

strength concrete and its normal strength counterpart. The ratio of creep strain to initial elastic strain under sustained axial compression, for high-strength concrete, may be as low as one half that generally associated with low-strength concrete (Ngab et al, 1981; Nilson, 1985).

2.4-Control of deflection

Deflection of one-way nonprestressed concrete flexural members is controlled by reinforcement ratio limitations, minimum thickness requirements, and span/deflection ratio limitations.

2.4.1 *Tension steel reinforcement ratio limitations*-One method to minimize deflection of a concrete member in flexure is by using a relatively small reinforcement ratio. Limiting values of ratio p, ranging from $0.25\rho_b$ to $0.40\rho_b$ are recommended by ACI 435 (1978), as shown in Table 2.2. Other methods of deflection reduction are presented in Chapter 5 of this report.

2.4.2 *Minimum thickness limitations*-Deflections of beams and one way slabs supporting usual loads in buildings, where deflections are not of concern, are normally satisfactory when the minimum thickness provisions in Table 2.3 are met or exceeded. This table (ACI 318, 1989) applies only to members that are not supporting or not attached to partitions or other construction likely to be damaged by excessive deflections. Values in Table 2.3

have been modified by ACI 435 (1978) and expanded in Table 2.4 to include members that are supporting or attached to non-structural elements likely to be damaged by excessive deflections. The thickness may be decreased when computed deflections are shown to be satisfactory. Based on a large number of computer studies, Grossman (1981, 1987) developed a simplified expression for the minimum thickness to satisfy serviceability requirements (Eq. 4.17, Chapter 4).

2.4.3 *Computed deflection limitations--*The allowable computed deflections specified in ACI 318 for one-way systems are given in Table 2.5, where the span-deflection ratios provide for a simple set of allowable deflections. Where excessive deflection may cause damage to non-structural or other structural elements, only that part of the deflection occurring after the construction of the nonstructural elements, such as partitions, needs to be considered. The most stringent span-deflection limit of l/480 in Table 2.5 is an example of such a case. Where excessive deflection may result in a functional problem, such as visual sagging or ponding of water, the total deflection should be considered.

2.5-Short-term deflection

2.5.1 *Untracked members*-Gross moment of inertia I_g -When the maximum flexural moment at service load in

Table 2.4-Minimum thickness of beams and one-way slabs used in roof and floor construction (ACI 435, 1978)

Member	Members not supporting or not attached to nonstructural elements likely to be damaged by large deflections				Members supporting or attached to nonstructural elements likely to be damaged by large deflection			
	Simply supported	One end continuous	Both ends continuous	Cantilever	Simply supported	One end continuous	Both ends continuous	Cantilever
Roof slab	$l/22$	$l/28$	$l/35$	$l/9$	$l/14$	$l/18$	$l/22$	$l/5.5$
Floor slab, and roof beam or ribbed roof slab	$l/18$	$l/23$	$l/28$	$l/7$	$l/12$	$l/15$	$l/19$	$l/5$
Floor beam or ribbed floor slab	$l/14$	$l/18$	$l/21$	$l/5.5$	$l/10$	$l/13$	$l/16$	$l/4$

Table 2.5-Maximum permissible computed beflections (ACI 318, 1989)

Type of member	Deflection to be considered	Deflection limitation
Flat roofs not supporting or attached to nonstructural elements likely to be damaged by large deflections	Immediate deflection due to live load L	$\dfrac{\ell^{*}}{180}$
Floors not supporting or attached to nonstructural elements likely to be damaged by large deflections	Immediate deflection due to live load L	$\dfrac{\ell}{360}$
Roof or floor construction supporting or attached to nonstructural elements likely to be damaged by large deflections	That part of the total deflection occurring after attachment of nonstructural elements (sum of the long-time deflection due to all sustained loads and the innediate deflection due to any additional live load)[†]	$\dfrac{\ell^{‡}}{480}$
Roof or floor construction supporting or attached to nonstructural elements not likely to be damaged by large deflections		$\dfrac{\ell^{§}}{240}$

* Limit not intended to safeguard against ponding. Ponding should be checked by suitable calculations of deflection, including added deflections due to ponded water, and considering long-term effects of all sustained loads, camber, construction tolerances, and reliability of provisions for drainage.

† Long-time deflection shall be determined in accordance with 9.5.2.5 or 9.5.4.2 but may be reduced by amount of deflection calculated to occur before attachment of nonstructural elements. This amount shall be determined on basis of accepted engineering data relating to time-deflection characteristics of members similar to those being considered.

‡ Limit may be exceeded if adequate measures are taken to prevent damage to supported or attached elements.

§ But not greater than tolerance provided for nonstructural elements. Limit may be exceeded if camber is provided so that total deflection minus camber does not exceed limit.

a beam or a slab causes a tensile stress less than the modulus of rupture, f_r, no flexural tension cracks develop at the tension side of the concrete element if the member is not restrained or the shrinkage and temperature tensile stresses are negligible. In such a case, the effective moment of inertia of the uncracked transformed section, I_t, is applicable for deflection computations. However, for design purposes, the gross moment of inertia, I_g, neglecting the reinforcement contribution, can be used with negligible loss of accuracy. The combination of service loads with shrinkage and temperature effects due to end restraint may cause cracking if the tensile stress in the concrete exceeds the modulus of rupture. In such cases, Section 2.5.2 applies.

The elastic deflection for noncracked members can thus be expressed in the following general form

$$\delta = K \frac{M l^2}{E_c I_g} \qquad (2.10)$$

where K is a factor that depends on support fixity and loading conditions. M is the maximum flexural moment along the span. The modulus of elasticity E_c can be obtained from Eq. 2.4 for normal-strength concrete or Eq. 2.5 for high-strength concrete.

2.5.2 *Cracked members-Effective moment of inertia* I_e -Tension cracks occur when the imposed loads cause bending moments in excess of the cracking moment, thus resulting in tensile stresses in the concrete that are higher than its modulus of rupture. The cracking moment, M_{cr}, may be computed as follows:

$$M_{cr} = \frac{f_r I_g}{y_t} \qquad (2.11)$$

where y_t is the distance from the neutral axis to the tension face of the beam, and f_r is the modulus of rupture of the concrete, as expressed by Eq. 2.1.

Cracks develop at several sections along the member length. While the cracked moment of inertia, I_{cr}, applies to the cracked sections, the gross moment of inertia, I_g, applies to the uncracked concrete between these sections.

Several methods have been developed to estimate the variations in stiffness caused by cracking along the span, These methods provide modification factors for the flexural rigidity EI (Yu et al, 1960), identify an effective moment of inertia (Branson, 1963), make adjustments to the curvature along the span and at critical sections (Beeby, 1968), alter the M/I ratio (CEB, 1968), or use a section-curvature incremental evaluation (Ghali, et al, 1986, 1989).

The extensively documented studies by Branson (1977, 1982, 1985) have shown that the initial deflections δ_i occurring in a beam or a slab after the maximum moment M_a has exceeded the cracking moment M_{cr} can be evaluated using an effective moment of inertia I_e instead of I_g in Eq. 2.10.

2.5.2.1 *Simply supported beams-*ACI 318-89 requires using the effective moment of inertia I_e proposed by Branson. This approach was selected as being sufficiently accurate to control deflections in reinforced and prestressed concrete structural elements. Branson's equation for the effective moment of inertia I_e, for short term deflections is as follows

$$I_e = \left(\frac{M_{cr}}{M_a}\right)^3 I_g + \left[1 - \left(\frac{M_{cr}}{M_a}\right)^3\right] I_{cr} \le I_g \qquad (2.12)$$

where

M_{cr} = Cracking moment
Ma = Maximum service load moment (unfactored) at the stage for which deflections are being considered
I_g = Gross moment of inertia of section
I_{cr} = Moment of inertia of cracked transformed section

The two moments of inertia I_g and I_{cr} are based on the assumption of bilinear load-deflection behavior (Fig. 3.19, Chapter 3) of cracked section. I_e provides a transition between the upper and the lower bounds of I_g and I_{cr}, respectively, as a function of the level of cracking, expressed as M_{cr}/M_a. Use of I_e as the resultant of the other two moments of inertia should essentially give deflection values close to those obtained using the bilinear approach. The cracking moment of inertia, I_{cr}, can be obtained from Fig. 2.3 (PCA, 1984). Deflections should be computed for each load level using Eq. 2.12, such as dead load and dead load plus live load. Thus, the incremental deflection such as that due to live load alone, is computed as the difference between these values at the two load levels. I_e may be determined using M_a at the support for cantilevers, and at the midspan for simple spans. Eq. 2.12 shows that I_e is an interpolation between the well-defined limits of I_g and I_{cr}. This equation has been recommended by ACI Committee 435 since 1966 and has been used in ACI 318 since 1971, the PCI *Handbook* since 1971, and the AASHTO *Highway Bridge Specifications* since 1973. Detailed numerical examples using this method for simple and continuous beams, unshored and shored composite beams are available in Branson (1977). The textbooks by Wang and Salmon (1992), and by Nawy (1990) also have an extensive treatment of the subject.

Eq. 2.12 can also be simplified to the following form:

$$I_e = I_{cr} + \left(\frac{M_{cr}}{M_a}\right)^3 (I_g - I_{cr}) \le I_g \qquad (2.13)$$

Heavily reinforced members will have an I_e approximately equal to I_{cr}, which may in some cases (flanged members) be larger than I_g of the concrete section alone. For most practical cases, the calculated I_e will be less than I_g and should be taken as such in the design for deflection control, unless a justification can be made for rigorous transformed section computations.

2.5.2.2 *Continuous beams--*For continuous members, ACI 318-89 stipulates that I_e may be taken as the average values obtained from Eq. 2.12 for the critical positive and negative moment sections. For prismatic members, I_e may be taken as the value obtained at midspan for continuous spans. The use of midspan section properties for continuous prismatic members is considered satisfactory in approximate calculations primarily because the midspan rigidity including the effect of cracking has the dominant effect on deflections (ACI 435, 1978).

If the designer chooses to average the effective moment of inertia I_e, then according to ACI 318-89, the following expression should be used:

$$I_e = 0.5 \, I_{e(m)} + 0.25 \, (I_{e(1)} + I_{e(2)}) \qquad (2.14)$$

where the subscripts m, 1, and 2 refer to mid-span, and the two beam ends, respectively.

Improved results for continuous prismatic members can, however, be obtained using a weighted average as presented in the following equations:

For beams continuous on both ends,

$$I_e = 0.70 \, I_{e(m)} + 0.15 \, (I_{e(1)} + I_{e(2)}) \qquad (2.15a)$$

For beams continuous on one end only,

$$I_e = 0.85 \, I_{e(m)} + 0.15 \, (I_{e(1)}) \qquad (2.15b)$$

When I_e is calculated as indicated in the previous discussion, the deflection can be obtained using the moment-area method (Fig. 3.9, Chapter 3) taking the moment-curvature (rotation) into consideration or using numerical incremental procedures. It should be stated that the I_e value can also be affected by the type of loading on the member (Al-Zaid, 1991), i.e. whether the load is concentrated or distributed.

2.5.2.3 *Approximate* I_e *estimation--*An approximation of the I_e value (Grossman, 1981) without the need for calculating I_{cr} which requires a priori determination of the area of flexural reinforcement, is defined by Eq. 2.16. It gives I_e values within 20 percent of those obtained from the ACI 318 Eq. (Eq. 2.12) and could be useful for a trial check of the I_e needed for deflection control of the cracked sections with minimum reinforcement $200/f_y$,

For $M_a/M_{cr} \le 1.6$:

$$I_e = \left(\frac{M_{cr}}{M_a}\right)^2 I_g \le I_g \qquad (2.16a)$$

$B = b/(nA_s)$ $r = (n-1)A_s'/(nA_s)$ $I_g = bh^3/12$

Without compression steel

$a = (\sqrt{2dB+1} - 1)/B$

$I_{cr} = ba^3/3 + nA_s(d-a)^2$

With compression steel

$a = [\sqrt{2dB(1+rd'/d) + (1+r)^2} - (1+r)]/B$

$I_{cr} = ba^3/3 + nA_s(d-a)^2 + (n-1)A_s'(a-d')^2$

(a) Rectangular Sections

$C = b_w/(nA_s)$, $f = h_f(b-b_w)/(nA_s)$, $y_t = h - 1/2[(b-b_w)h_f^2 + b_w h^2]/[(b-b_w)h_f + b_w h]$

$I_g = (b-b_w)h_f^3/12 + b_w h^3/12 + (b-b_w)h_f(h-h_f/2-y_t)^2 + b_w h(y_t-h/2)^2$

Without compression steel

$a = [\sqrt{C(2d+h_f f) + (1+f)^2} - (1+f)]/C$

$I_{cr} = (b-b_w)h_f^3/12 + b_w a^3/3 + (b-b_w)h_f(a-h_f/2)^2 + nA_s(d-a)^2$

With compression steel

$a = [\sqrt{C(2d+h_f f+2rd') + (f+r+1)^2} - (f+r+1)]/C$

$I_{cr} = (b-b_w)h_f^3/12 + b_w a^3/3 + (b-b_w)h_f(a-h_f/2)^2 + nA_s(d-a)^2 + (n-1)A_s'(a-d')^2$

(b) Flanged Sections

Fig. 2.3-Moments of inertia of uncracked and cracked transformed sections (PCA, 1984)

STRAIN DIAGRAM   STRESS DIAGRAM   FORCE DIAGRAM

Fig. 2.4-Bending behavior of cracked sections

For $1.6 \leq M_a/M_{cr} \leq 10$:

$$I_e = 0.1 \, K_e \left(\frac{M_a}{M_{cr}}\right) I_g \leq I_g \qquad (2.16b)$$

where

$$K_e = \frac{d}{0.9h} \left| \frac{\sqrt{145/w_c}}{0.4 + \left(\frac{1.4M_a}{\phi M_n}\right)\left(\frac{f_y}{100,000}\right)} \right| \qquad (2.16c)$$

but, I_e computed by Eq. 2.16a and 2.16b should not be less than

$$I_e = 0.35 \, K_e \, I\text{-} \qquad (2.16d)$$

nor less than the value from Eq. 2.16b, 2.16c, and 2.16d, where M_a is the maximum service moment capacity, computed for the provided reinforcement.

2.5.3 *Incremental moment-curvature method*-Today with the easy availability of personal computers, more accurate analytical procedures such as the incremental moment-curvature method become effective tools for computing deflections in structural concrete members [P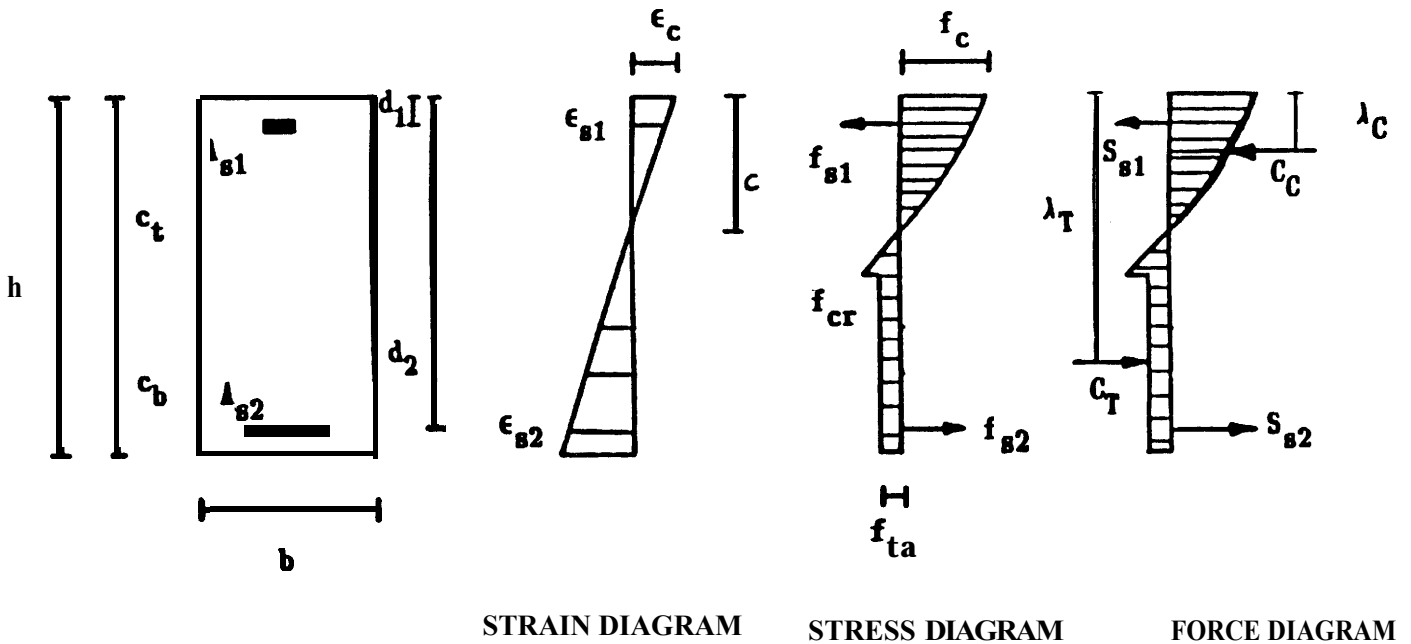ark et al, 1975]. With known material parameters, a theoretical moment-curvature curve model for the cracked section can be derived (see Fig. 2.4). For a given concrete strain in the extreme compression fiber, ϵ_c, and neutral axis depth, c, the steel strains, $\epsilon_{s1}, \epsilon_{s2},...$, can be determined from the properties of similar triangles in the strain diagram. For example:

$$\epsilon_{s1} = \frac{c - d_1}{c} \epsilon_c \qquad (2.17)$$

The stresses, $f_{s1}, f_{s2},...$, corresponding to the strains, $\epsilon_{s1}, \epsilon_{s2},...$, may be obtained from the stress-strain curves. Then, the reinforcing steel forces, $T_{s1}, T_{s2},...$, may be calculated from the steel stresses and areas. For example:

$$T_{s1} = f_{s1} * A_{s1} \qquad (2.18)$$

The distribution of concrete stress, over the compressed and tensioned parts of the section, may be obtained from the concrete stress-strain curves. For any given extreme compression fiber concrete strain, ϵ_c, the resultant concrete compression and tension forces, C_C and C, are calculated by numerically integrating the stresses over their respective areas.

Eq. 2.19 to 2.21 represent the force equilibrium, the moment, and the curvature equations of a cracked section, respectively:

$$T_{s1} + T_{s2} + \ldots + C_C + C_T = 0 \qquad (2.19)$$

$$M = \Sigma \, (A_s)_i \, (f_s)_i \, [c - (d)_i] + C_T \, \lambda_T + C_C \, \lambda_C \qquad (2.20)$$

and

$$\phi = \frac{\epsilon_c}{c} \qquad (2.21)$$

The complete moment-curvature relationship may be determined by incrementally adjusting the concrete strain, ϵ_c, at the extreme compression fiber. For each value of ϵ_c the neutral axis depth, c, is determined by satisfying Eq. 2.19.

Analytical models to compute both the ascending and descending branches of moment-curvature and load-deflection curves of reinforced concrete beams are presented in Hsu (1974, 1983).
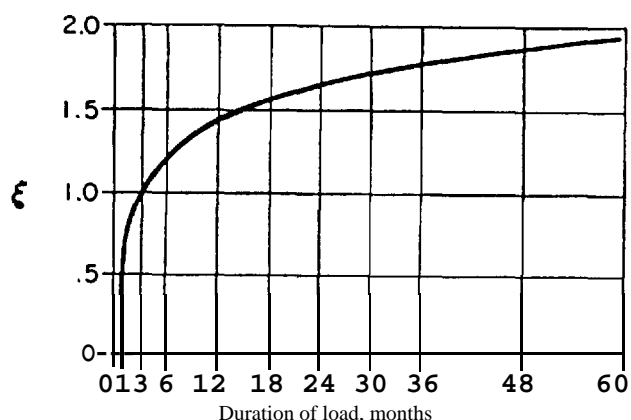
Fig. 2.5-ACI code multipliers for long-term deflections

2.6--Long-term deflection

2.6.1 *ACI method*-Time-dependent deflection of one-way flexural members due to the combined effects of creep and shrinkage, is calculated in accordance with ACI 318-89 (using Branson's Equation, 1971, 1977) by applying a multiplier, λ, to the elastic deflections computed from Equation 2.10:

$$\lambda = \frac{\xi}{1 + 50\,\rho'} \qquad (2.22)$$

where ρ' = reinforcement ratio for non-prestressed compression steel reinforcement

ξ = time dependent factor, from Fig. 2.2 (ACI 318, 1989)

Hence, the total long-term deflection is obtained by:

$$\delta_{LT} = \delta_L + \lambda_t\, \delta_{sus} \qquad (2.23)$$

where

δ_L = initial live load deflection

δ_{sus} = initial deflection due to sustained load

λ_t = time dependent multiplier for a defined duration time *t*

Research has shown that high-strength concrete members exhibit significantly less sustained-load deflections than low-strength concrete members (Luebkeman et al, 1985; Nilson, 1985). This behavior is mainly due to lower creep strain characteristics. Also, the influence of compression steel reinforcement is less pronounced in high-strength concrete members. This is because the substantial force transfer from the compression concrete to compression reinforcement is greatly reduced for high-strength concrete members, for which creep is lower than normal strength concrete. Nilson (1985) suggested that two modifying factors should be introduced into the ACI Code Eq. 2.22. The first is a material modifier, μ_m, with values equal to or less than 1.0, applied to ξ to account for the lower creep coefficient. The second is a section modifier, μ_s, also having values equal to or less than 1.0, to be applied to ρ' to account for the decreasing importance of compression steel in high-strength concrete

members. Comparative studies have shown that a single modifier, μ, can be used to account satisfactorily for both effects simultaneously, leading to the following simplified equation

$$\lambda = \frac{\mu\,\xi}{1 + 50\,\mu\,\rho'} \qquad (2.24)$$

where $0.7 \le \mu = 1.3 - 0.00005\, f_c' \le 1.0$.

This equation results in $\mu = 1.0$ for concrete strength less than 6000 psi (42 MPa), and provides a reasonable fit of experimental data for higher concrete strengths. However, more data is needed, particularly for strengths between 9000 to 12,000 psi (62 MPa to 83 MPa) and beyond before a definitive statement can be made.

2.6.2 *ACI Committee 435 modified method (Branson, 1963, 1977)*-For computing creep and shrinkage deflections separately, Branson's (1963,1977) Eq. 2.25 and 2.26 are recommended by ACI 435 (1966, 1978).

$$\delta_{cr} = \lambda_c\,(\delta_{sus}) \qquad (2.25)$$

$$S_{sh} = k_{sh}\,\phi_{sh}\,l^2 = k_{sh}\left(A_{sh}\,\frac{(\epsilon_{sh})_t}{h}\right)l^2 \qquad (2.26)$$

where

$$\lambda_c = \frac{0.85\,C_t}{1 + 50\,\rho'}$$

C_t and (e,h), may be determined from Eq. 2.7 through 2.9 and Table 2.1.

$$A_{sh} = 0.7(\rho - \rho')^{1/3}\left(\frac{\rho - \rho'}{\rho}\right)^{1/2} \text{ for } \rho - \rho' \le 3.0$$
$$\text{percent}$$
$$= 0.7\,\rho^{1/3} \text{ for } \rho' = 0$$
$$= 1.0 \text{ for } \rho - \rho' > 3.0 \text{ percent}$$

ρ and ρ' are computed at the support section for cantilevers and at the midspan sections for simple and continuous spans.

The shrinkage deflection constant k_{sh} is as follows:

Cantilevers	= 0.50
Simple beams	= 0.13
Spans with one end continuous (multi spans)	= 0.09
Spans with one end continuous (two spans)	= 0.08
Spans with both ends continuous	= 0.07

Separate computations of creep and shrinkage are preferable when part of the live load is considered as a sustained load.

2.6.3 *Other methods*-Other methods for time-dependent deflection calculation in reinforced concrete beams and one-way slabs are available in the literature. They include several methods listed in ACI 435 (1966), the CEB-FIP Model Code (1990) simplified method, and other methods described in Section 3.8, Chapter 3, including the section curvature method (Ghali-Favre, 1986). This section highlights the CEB-FIP Model Code method (1990) and describes the Ghali-Favre approach, referring the reader to the literature for details.

2.6.3.1 *CEB-FIP Model Code simplified method*-On the basis of assuming a bilinear load-deflection relationship, the time-dependent part of deflection of cracked concrete members can be estimated by the fol-

lowing expression [CEB-FIP, 1990]:

$$\delta_{L\text{-}T} = (h/d)^3 \eta (1 - 20\, \rho_{cm})\delta_g \qquad (2.27)$$

where

δ_g = elastic deformation calculated with the rigidity $E_c I_g$ of the gross cross section (neglecting the reinforcement)

η = correction factor (see Fig. 2.6), which includes the effects of cracking and creep

ρ_{cm} = geometrical mean percentage of the compressive reinforcement

The mean percentage of reinforcement is determined according to the bending moment diagram (Fig. 2.6) and Eq. (2.28):

$$\rho_m = \rho_L(l_L/l) + \rho_c\,(l_C/l) + \rho_R(l_R/l) \qquad (2.28)$$

where

$\rho_L,\, \rho_R$ = percentage of tensile reinforcement at the left and right support, respectively

ρ_C = percentage of tensile reinforcement at the maximum positive moment section

$l_L, l_C,$ and l_R = length of inflection point segments as indicated in Fig. 2.6 (an estimate of lengths is generally sufficient)

2.6.3.2 *Section curvature method (Ghali, Favre, and Elbadry 2002)*—Deflection is computed in terms of curvature evaluation at various sections along the span, satisfying compatibility and equilibrium throughout the analysis. Appendix B gives a general procedure for calculation of displacements (two translation components and a rotation) at any section of a plane frame. The general method calculates strain distributions at individual sections considering the effects of a normal force and a moment caused by applied loads, prestressing, creep and shrinkage of concrete, relaxation of prestressed steel, and cracking. The axial strains and the curvatures thus obtained can be used to calculate the displacements.

The comprehensive analysis presented in Appendix B requires more calculations than the simplified methods. It also requires more input parameters related to creep, shrinkage, and tensile strength of concrete and relaxation of prestressing steel. With any method of analysis, the accuracy in the calculation of deflections depends upon the rigor of the analysis and the accuracy of the input parameters. The method presented in Appendix B aims at improving the rigor of the analysis, but it cannot eliminate any inaccuracy caused by the uncertainty of the input parameters.

The comprehensive analysis can be used to study the sensitivity of the calculated deflections to variations in the input parameters. The method applies to the reinforced
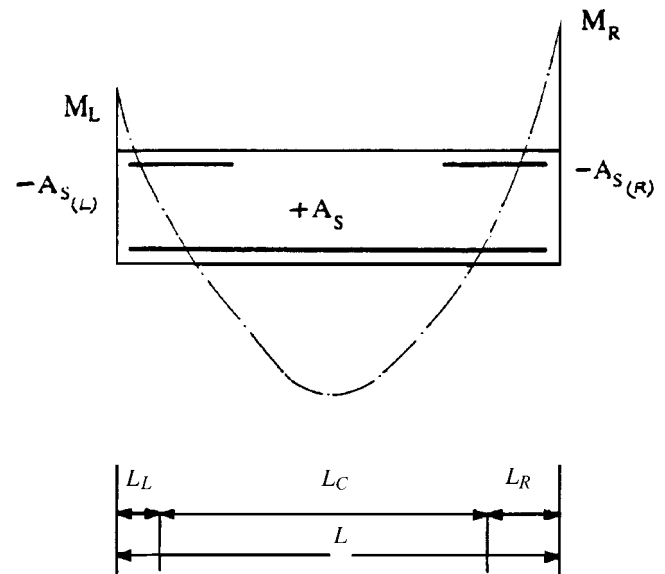
(a) Bending moment diagram defining L_R L_C L_L

ρ_m [%]	0.15	0.2	0.3	0.5	0.75	1.0	1.5
η	10	8	6	4	3	2.5	2

(b) Mean percentage ρ_m of the tensile reinforcement

Fig. 2.6—CEB-FIP simplified deflection calculation method (CEB-FIP, 1990)

concrete members, with or without prestressing, having variable cross sections.

2.6.4 *Finite element method*—Finite element models have been developed to account for time-dependent deflections of reinforced concrete members (ASCE, 1982). Such analytical approaches would be justifiable when a high degree of precision is required for special structures and only when substantially accurate creep and shrinkage data are available. In special cases, such information on material properties is warranted and may be obtained experimentally from tests of actual materials to be used and inputting these in the finite element models.

2.7—Temperature-induced deflections

Variations in ambient temperature significantly affect deformations of reinforced concrete structures. Deflections occur in unrestrained flexural members when a temperature gradient occurs between its opposite faces. It has been standard practice to evaluate thermal stresses and displacements in tall building structures. Movements of bridge superstructures and precast concrete elements are also computed for the purpose of design of support bearings and expansion

joint designs. Before performing an analysis for temperature effects, it is necessary to select design temperature gradients. Martin (1971) summarizes design temperatures that are provided in various national and foreign codes.

An ACI 435 report on temperature-induced deflections (1985) outlines procedures for estimating changes in stiffness and temperature-induced deflections for reinforced concrete members. The following expressions are taken from that report.

2.7.1 *Temperature gradient on unrestrained cross section*—With temperature distribution $t(y)$ on the cross section, thermal strain at a distance y from the bottom of the section can be expressed by

$$\in_t(y) = \alpha t(y) \tag{2.29}$$

To restrain the movement due to temperature $t(y)$, a stress is applied in the opposite direction to $\in_t(y)$:

$$f(y) = E_c \alpha t(y) \tag{2.30}$$

The net restraining axial force and moment are obtained by integrating over the depth:

$$P = \int_A f dA = \int_0^h [\alpha E_c t(y) b(y)] dy \tag{2.31}$$

$$M = \int_A f(y-n) dA = \int_0^h [\alpha E_c t(y) b(y)(y-n)] dy \tag{2.32}$$

In order to obtain the total strains on the unrestrained cross section, P and M are applied in the opposite direction to the restraining force and moment. Assuming plane sections remain plane, axial strain $\in_a$ and curvature ϕ are given by:

$$\in_a = \frac{P}{AE_c} = \frac{\alpha}{A} \int_0^h [t(y) b(y)] dy \tag{2.33}$$

$$\phi = \frac{M}{E_c I} = \frac{\alpha}{I} \int_0^h [t(y) b(y)(y-n)] dy \tag{2.34}$$

The net stress distribution on the cross section is given by:

$$f_n(y) = \frac{P}{A} \pm \frac{M(y-n)}{I} - E_c \alpha t(y) \tag{2.35}$$

For a linear temperature gradient varying from 0 to Δt, the curvature is given by:

$$\phi = \frac{\alpha \Delta t}{h} \tag{2.36}$$

In the case of a uniform vertical temperature gradient constant along the length of a member, deflections for simply supported (δ_{ss}) and cantilever beams (δ_{cont}) are calculated as:

$$\delta_{ss} = \frac{\phi l^2}{8} = \frac{\alpha \Delta t}{h} \frac{l^2}{8} \tag{2.37}$$

$$\delta_{cont} = \frac{\phi l^2}{2} = \frac{\alpha \Delta t}{h} \frac{l^2}{h} \tag{2.38}$$

The deflection-to-span ratio is given by:

$$\frac{\delta}{l} = \frac{\alpha \Delta t}{k} \frac{l}{h} \tag{2.39}$$

where $k = 8$ for simply supported beams and 2 for cantilever beams.

2.7.2 *Effect of restraint on thermal movement*—If a member is restrained from deforming under the action of temperature changes, internal stresses are developed. Cracking that occurs when tensile stresses exceed the concrete tensile strength reduces the flexural stiffness of the member and results in increased deflections under subsequent loading. Consequently, significant temperature effects should be taken into account in determining member stiffness for deflection calculation. The calculation of the effective moment of inertia should be based on maximum moment conditions.

In cases where stresses are developed in the member due to restrain of axial deformations, the induced stress due to axial restraint has to be included in the calculation of the cracking moment in a manner analogous to that for including the prestressing force in prestressed concrete beams.

APPENDIX A2
Example A2.1: Deflection of a four-span beam

A reinforced concrete beam supporting a 4-in. (100 mm) slab is continuous over four equal spans $1 = 36$ ft (10.97 m) as shown in Fig. A2.1 (Nawy, 1990). It is subjected to a uniformly distributed load $w_D = 700$ lb/ft (10.22 kN/m), including its self-weight and a service load $w_L = 1200$ lb/ft (17.52 kN/m). The beam has the dimensions $b = 14$ in. (355.6 mm), $d = 18.25$ in. (463.6 mm) at midspan, and a total thickness $h = 21.0$ in. (533.4 mm). The first interior span is reinforced with four No. 9 bars
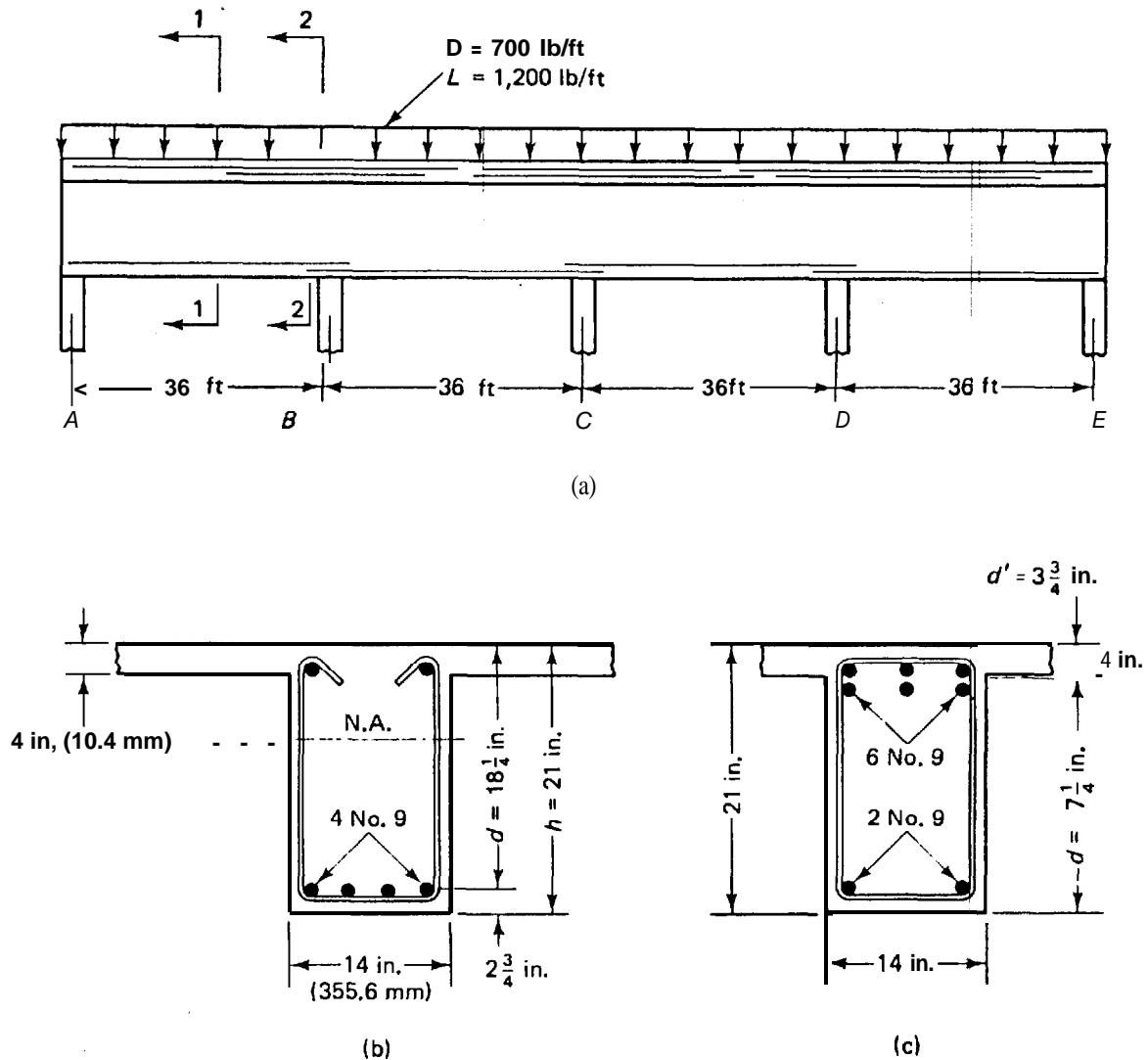
Fig. A2.1-Details of continuous beam in Ex. A2.1 (Nawy, 1990, courtesy Prentiss Hall)

at midspan (28.6 mm diameter) at the bottom fibers and six No. 9 bars at the top fibers of the support section.

Calculate the maximum deflection of the continuous beam using the ACI 318 method.

Given:

f'_c = 4000 psi (27.8 MPa), normal weight concrete
f_y = 60,000 psi (413.7 MPa)
50 percent of the live load is sustained 36 months on the structure.

Solution-ACI Method
Note: All calculations are rounded to three significant figures.
Material properties and bending moment values

E_c = 57,000 = $\sqrt{f'_c}$ = 57,000 $\sqrt{4000}$ = 3.6 x 10^6 psi (24,800 MPa)

E_s = 29 x 10^6 psi (200,000 MPa)

modular ratio $n = E_s/E_c = \dfrac{29 \times 10^6}{3.6 \times 10^6}$ = 8.1

modulus of rupture f_r = 7.5 $\sqrt{f'_c}$ = 7.5 $\sqrt{4000}$ = 474 psi

(3.3 MPa)

For the first interior span, the positive moment = 0.0772 wl^2

$+ M_D$ = 0.0772 x 700(36.0)^2 x 12 = 840,000 in.-lb

$+ M_L$ = 0.0772 x 1200(36.0)^2 x 12 = 1,440,000 in.-lb

$+(M_D + ML)$ = 0.0772x 1900(36.0)^2 x 12 = 2,280,000 in.-lb

negative moment = 0.107 wl^2

$- M_D$ = 0.1071 x 700(36.0)^2 x 12 = 1,170,000 in.-lb

$- M_L$ = 0.1071 x 1200(36.0)^2 x 12 = 2,000,000 in.-lb

$-(M_D + M_L)$ = 0.1071 x 1900(36.0)^2 x 12 = 3,170,000 in.-lb

Effective moment of inertia I_e

Fig. A2.2 shows the theoretical midspan and support
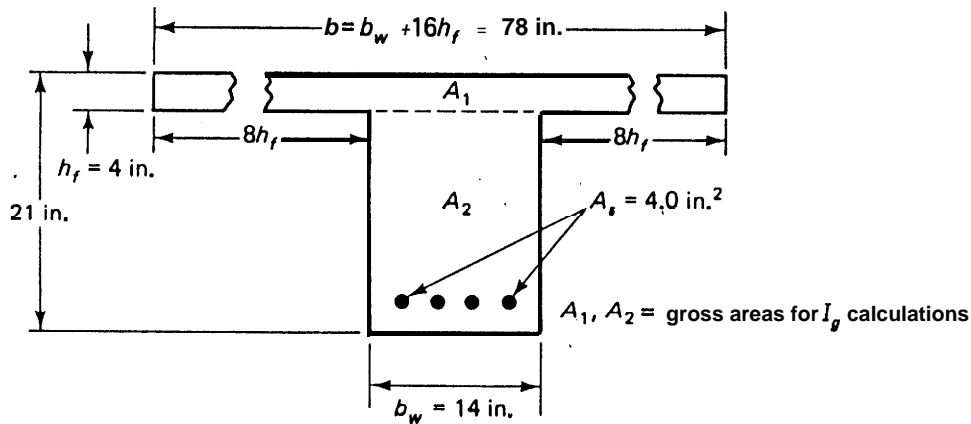
(a)
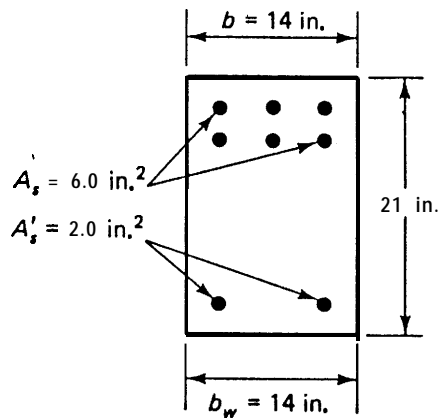
(b)

Fig. A2.2-Gross moment of inertia I_g *cross sections in Ex. A2.1*

cross sections to be used for calculating the gross moment of inertia I_g.

1. Midspan section:
Width of T-beam flange $= b_w + 16h_f = 14.0 + 16 \times 4.0$
$= 78$ in. (1981 mm)
Depth from compression flange to the elastic centroid is:

$$y' = (A_1y_1 + A_2y_2)/(A_1 + A_2)$$

$$= \frac{78(4 \times 2) + 14 \times (21-4) \times 12.5}{78 \times 4 + 14 \times 17} = 6.54 \text{ in.}$$

$$y_t = h - y' = 21.0 - 6.54 = 14.5 \text{ in.}$$

$$I_g = \frac{78(4)^3}{12} + 78 \times 4(6.54 - 4/2)^2$$
$$+ \frac{14(21-4)^3}{12} + 14(21-4)\left(14.46 - \frac{21-4}{2}\right)^2$$
$$= 21.000 \text{ in.}^4$$

$$M_{cr} = \frac{f_r I_g}{y_t} = \frac{474.3 \times 21,000}{14.46} = 690,000 \text{ in.-lb}$$

Depth of neutral axis:

$(A_s = $ four No. 9 bars $= 4.0$ in^2).
To locate the position, c, of the neutral axis, take moment of area of the transformed flanged section, namely

$$b_w(c - h_f)^2 - 2nA_s(d - c) + bh_f(2c - h_f) = 0$$
or
$$14(c - 4.0)^2 - 2 \times 8.1 \times 4.0(18.25 - c) + 78 \times 4(2c - 4.0) = 0$$
or $c^2 + 4.17c - 157.0 = 0$

to give $c = 3.5$ in. Hence the neutral axis is inside the flange and the flange section is analyzed as a rectangular section.

For rectangular sections,

$$\frac{78c^2}{2} + 8.1 \times 4 \times c - 8.1 \times 4 \times 18.25 = 0$$

Therefore, $c = 3.5$ in.

$$I_{cr} = \frac{78(3.5)^3}{3} + 0.8 \times 4 (18.25 - 3.5)^2 = 8160 \text{ in.}^4$$

Ratio M_{cr}/M_a:

$$D \text{ ratio} = \frac{690,000}{840,000} = 0.82$$

$D + 50$ percent L ratio $= \dfrac{690,000}{840,000 + 0.5 \times 1,440,000}$
$= 0.44$

$D + L$ ratio $= \dfrac{690,000}{2,280,000} = 0.30$

Effective moment of inertia for midspan sections:

$$I_e = \left(\frac{M_{cr}}{M_a}\right)^3 I_g + \left[1 + \left(\frac{M_{cr}}{M_a}\right)^3\right] I_{cr}$$

I_e for dead load $= 0.55 \times 21,000 + 0.45 \times 8160$
$\qquad = 15,200$ in.^{4}
I_e for $D + 0.5L = 0.086 \times 21,000 + 0.914 \times 8160$
$\qquad = 9276$ in.^{4}
I_e for $D + L \quad = 0.027 \times 21,000 + 0.973 \times 8160$
$\qquad = 8500$ in.^{4}

If using the simplified approach to obtain I_e (Section 2.5.2.3) values of 14,200 in⁴(7 percent smaller), 9200 in⁴ (1 percent smaller), and 8020 in⁴ (6 percent smaller), are obtained respectively.

2. Support section:

$$I_g \quad \frac{bh^3}{12} \quad \frac{14(21)^3}{12} = 10,800 \text{ in.}^4$$

$$y_t = \frac{21}{2} = 10.5 \text{ in.}$$

$$M_{cr} = f_r I_g / y_t = \frac{470 \times 10,800}{10.5} = 483,000 \text{ in.-lb}$$

Depth of neutral axis:
$A_s \quad =$ six No. 9 bars $= 6.0$ in.^{2} (3870 mm^2)
$A_s' \quad =$ two No. 9 bars $= 2.0$ in.^{2} (1290 mm^2)
$d \quad = 21.0 - 3.75 = 17.30$ in. (438 mm)

Similar calculation for the neutral axis depth c gives a value $c = 7.58$ in.
Hence,

$$I_{cr} = \frac{bc^3}{3} + nA_s(d - c)^2 + (n - 1)A_s'(c - d')^2$$

Ratio M_{cr}/M_a:

$$D \text{ ratio} = \frac{483,000}{1,170,000} = 0.41$$

$$D + 50 \text{ percent } L \text{ ratio} =$$
$$\frac{483,000}{1,170,000 + 0.5 \times 2,000,000} = 0.22$$

$$D + L \text{ ratio} = \frac{483,000}{3,170,000}$$

Effective moment of inertia for support section:
I_e for dead load $= 0.07 \times 10,800 + 0.93 \times 6900$
$\qquad = 7170$ in.^{4}
I_e for $D + 0.5L = 0.01 \times 10,800 + 0.99 \times 6900$
$\qquad = 6940$ in.^{4}
I_e for $D + L \quad = 0.003 \times 10,800 + 0.99 \times 6900$
$\qquad = 6910$ in.^{4}

Average effective I_e *for continuous span*
average $\quad I_e = 0.85 I_m + 0.15 I_{ec}$
dead load: $I_e = 0.85 \times 15,200 + 0.15 \times 7170$
$\qquad = 14,000$ in.^{4}

$D + 0.5L: I_e = 0.85 \times 9260 + 0.15 \times 6940$
$\qquad = 8900$ in.^{4}
$D + L$: $I_e = 0.85 \times 8500 + 0.15 \times 6910 = 8260$ in.^{4}

Short-term deflection

The maximum deflection for the first interior span is:

$$\delta = \frac{0.0065wl^4}{EI}$$

l assumed $= l_n$ for all practical purposes

$$\delta = \frac{0.0065(36 \times 12)^4}{36 \times 10^6} \times \frac{w}{I_e} \times \frac{1}{12} = 5.240 \frac{w}{I_e} \text{ in.}$$

Initial dead-load deflection:

$$\delta_D = \frac{5.240(700)}{14.000} = 0.26 \text{ in., say } 0.3 \text{ in.}$$

Initial live-load deflection:

$$\delta_L = \delta_{L+D} \quad \delta_D$$

$$\delta_L = \frac{5.240(1900)}{8260} - \frac{5.240(700)}{14,000}$$
$$= 1.21 - 0.26 = 0.95 \text{ in., say } 1 \text{ in.}$$

Initial 50 percent sustained live-load deflection:

$$\rho' = \frac{A_s'}{bd} = 0 \text{ (at midspan in this case)}$$

multiplier $\lambda = \xi / (1 + 50\rho')$
From Fig. 2.5
$T = 1.75$ for 36-month sustained load
$T = 2.0$ for 5-year loading
Therefore,
$\lambda_\infty = 2.0$ and $\lambda_t = 1.75$

The total long-term deflection is

$$\delta_{LT} = \delta_L + \lambda_\infty \delta_D + \lambda_t \delta_{LS}$$
$$\delta_{LT} = 0.95 + 2.0 \times 0.26 + 1.75 \times 0.5 = 0.95 + 1.41$$
$$= 2.34 \text{ in. (60 mm), say } 2.4 \text{ in.}$$

Deflection requirements (Table 2.5)

$$\frac{l}{180} = \frac{36 \times 12}{180} = 2.4 \text{ in.} > \delta_L = 1.0 \text{ in., O.K}$$

$$\frac{l}{360} = 1.2 \text{ in.} > \delta_L = 1.0 \text{ in., O.K.}$$

$$\frac{l}{480} = 0.9 \text{ in.} < \delta_{LT} = 2.4 \text{ in., N.G.}$$

$$\frac{l}{240} = 1.8 \text{ in.} < \delta_{LT} = 2.4 \text{ in., N.G.}$$

Hence, the continuous beam is limited to floors or roofs not supporting or attached to nonstructural elements such as partitions.

Application of CEB-FIP method to obtain long-term deflection due to sustained loads:

midspan $\rho = \dfrac{+A_s}{bd} = \dfrac{4 \times 1.0}{78 \times 18.25} = 0.0028 = \rho_c$

support $\rho = \dfrac{-A_s}{b_w d} = \dfrac{6 \times 1.0}{14 \times 18.25} = 0.0235 = \rho_L = \rho_R$

$$\left(\frac{h}{d}\right)^3 = \left(\frac{21}{18.25}\right)^3 = 1.52$$

$$\rho_m = \rho_L\left(\frac{l_L}{l}\right) + \rho_c\left(\frac{l_c}{l}\right) + \rho_R\left(\frac{l_R}{l}\right)$$

Assuming that the location of the inflection points as defined by l_L and l_R for negative moment region, and l_c for the positive moment region in Figure 2.16 are as follows:

$L_l/L = L_R/L = 0.21$ and $L_c/L = (1 - 0.21 \times 2) = 0.58$
Also, assume $\rho_L = \rho_R$
Hence,

$\rho_m = 2(0.0235 \times 0.2) + 0.0028 \times 0.58$
$= 0.0094 + 0.0017 = 0.0111 = 1.11$ percent

From Fig. 2.6, $\eta = 2.4$
From AD Method Solution: $I_g = 21,000$ in.^{4}
Short-term deflection,

$$\delta = \frac{0.0069wl^4}{E_c I_g} = 5.240\,\frac{w}{I_g}$$

$+\dfrac{5.240(700 + 1200)}{21,000} = 0.47$ in., say 0.5 in.

Long-Term increase in deflection due to sustained load:

$$\delta_{L-T} = \left(\frac{h}{d}\right)^3 \eta (1 - 20\rho_c)\delta$$

$= 1.52 \times 2.4(1 - 20 \times 0.0111)0.5$
$= 1.35$ in., say 1.4 in. (35 mm).
         (1.41 in. by the ACI procedure solution)

Example A2.2: Temperature-induced deflections

These design examples illustrate the calculation procedures for temperature induced deflections.

Example (a): Simply supported vertical wall panel — Linear temperature gradient
        $\Delta t = 40$ F (4.4 C)
        $\alpha = 0.0000055$ in./in./F
        $h = 4$ in. (101 mm)
    a) Single story span: $L = 12$ ft. (3.66 m)
        $\delta = (0.0000055 \times 40 \times 144^2)/(4 \times 8)$
            $= 0.14$ in. (3.6 mm), say 0.2 in.
    b) Two story span: $L = 24$ ft. (7.32 m)
        $\delta = (0.0000055 \times 40 \times 288^2)/(4 \times 8)$
            $= 0.57$ in. (14.5 mm), say 0.6 in.
Example (b): Simply supported tee section — Linear Temperature gradient over depth
        $\Delta t = 40$ F (4.4 C)
        $\alpha = 0.0000055$ in./in./F
        $h = 36$ in. (914 mm)
        $L = 60$ ft. (18.4 m) · simply supported
        $\delta = (0.0000055 \times 40 \times 720^2)/(36 \times 8)$

$= 0.40$ in. (10 mm), say 0.5 in.
Example (c): Simply supported tee section — Constant temperature over flange depth
        $I = 69319$ in^4 (2.88 $\times 10^{10}$ mm^4)
        $n = 26.86$ in (682 mm)
        $\Delta t = 40$ F (4.4 C)
        $\alpha = 0.0000055$ in./in./F
        $h = 36$ in. (914 mm)
        $L = 60$ ft. (18.4 m)

$$\phi = (\alpha/I)\int_0^{36} t(y)\, b(y)\, (y - n)dy$$

$$= (\alpha/I)\int_{33}^{36} (40 \times 96)\, (y - 26.86)dy$$

$= (88,013 \times 0.0000055)/69319$
$= 0.00000698$
$\delta = (\phi L^2)/8 = (0.00000698 \times 720^2)/8$
$= 0.45$ in. (11.4 mm), say 0.5 in.

CHAPTER 3-DEFLECTION OF PRESTRESSED CONCRETE ONE-WAY FLEXURAL MEMBERS*

3.1-Notation

A_c = area of section
A_g = gross area of concrete section
A_s = area of nonprestressed reinforcement
A_{ps} = area of prestressed reinforcement in tension zone
b = width of compression face of member
b_w = web width
c = depth of compression zone in a fully-cracked section
cgc = center of gravity of concrete section
cgs = center of gravity of reinforcement
C = creep coefficient, defined as creep strain divided by initial strain due to constant sustained stress
C_1 = PCI multiplier for partially prestressed section
C_2 = PCI multiplier for partially prestressed section
C_t = creep coefficient at a specific age
C_u = ultimate creep coefficient for concrete at loading equal to time of release of prestressing
d = distance from extreme compression fiber to centroid of prestressing steel
d' = distance from extreme compression fiber to centroid of compression reinforcement
d_p = distance from extreme compression fiber to centroid of prestressed reinforcement
e_c = eccentricity of prestress force from centroid of section at center of span
e_{cr} = eccentricity of prestress force from centroid of cracked section
e_e = eccentricity of prestress force from centroid of section at end of span
E_c = modulus of elasticity of concrete
E_{ci} = modulus of elasticity of concrete at time of initial prestress
E_s = modulus of elasticity of nonprestressed reinforcement

E_{ps} = modulus of elasticity of prestressed reinforcement

ES = stress loss due to elastic shortening of concrete

f_c' = specified compressive strength of concrete

f_d = concrete stress at extreme tensile fibers due to unfactored *dead* load when tensile stresses and cracking are caused by external load

f_t' = strength of concrete in tension

f_l = calculated stress due to live load

f_{max} = stress in extreme tension fibers due to effective prestress, if any, plus maximum unfactored load, using uncracked section properties

f_{ce} = compressive stress in concrete due to effective prestress only after losses when tensile stress is caused by applied external load

f_{pe} = effective prestress in prestressing reinforcement after losses

f_{pi} = stress in prestressing reinforcement immediately prior to release

f_{pJ} = stress in pretensioning reinforcement at jacking (5-10 percent higher than f_{pi})

f_{pu} = specified tensile strength of prestressing tendons

f_{py} = yield strength of the prestressing reinforcement

f_r = modulus of rupture of concrete $7.5\sqrt{f_c'}$

f_{TL} = final calculated total stress in member

f_y = specified yield strength of nonprestressed reinforcement

h = overall thickness of member

h_f = depth of flange

I_{cr} = moment of inertia of cracked section transformed to concrete

I_e = effective moment of inertia for computation of deflection

I_g = moment of inertia of gross concrete section about centroid axis

I_t = moment of inertia of transformed section

K_{CR} = coefficient for creep loss in Eq. 3.7

L = span length of beam

M_a = maximum service unfactored *live load* moment

M_{cr} = moment due to that portion of applied *live load* that causes cracking

M_L = moment due to service live load

M_n = nominal flexural strength

M_{SD} = moment due to superimposed dead load

n = modular ratio of normal reinforcement $(= E_s/E_c)$

n_p = modular ratio of prestressing reinforcement $(= E_{ps}/E_c)$

P_e = effective prestressing force after losses

P_i = initial prestressing force prior to transfer

r = radius of gyration $= \sqrt{I_g/A_g}$

REL = stress loss due to relaxation of tendons

SH = stress loss due to shrinkage of concrete

t_o = initial time interval

t = time at any load level or after creep or shrinkage are considered

y_g = distance from extreme compression fibers to centroid of A_g

y_t = distance from centroid axis of gross section, neglecting reinforcement to extreme tension fibers

α = length parameter that is a function of tendon profile used

δ = deflection or camber

ϵ_c = maximum usable strain in the extreme compression fiber of a concrete element (0.003 in./in.)

ϵ_{cr} = strain at first cracking load

ϵ_{ps} = strain in prestressed reinforcement at ultimate flexure

ϵ_{SH} = unit shrinkage strain in concrete

$(\epsilon_{SH})_t$ = shrinkage strain at any time t

$(\epsilon_{SH})_u$ = average value of ultimate shrinkage strain

ϵ_u = ultimate strain

ϕ = curvature (slope of strain diagram)

ϕ_c = curvature at midspan

ϕ_e = curvature at support

γ = correction factor for shrinkage strain in nonstandard conditions (see also Sec. 2.3.4)

Δf_{pCR} = stress loss due to creep in concrete

Δf_{pSH} = stress loss due to concrete shrinkage

Δf_{pR} = stress loss due to relaxation of tendons

3.2-General

3.2.1 *Introduction*-Serviceability behavior of prestressed concrete elements, particularly with regard to deflection and camber, is a more important design consideration than in the past. This is due to the application of factored load design procedures and the use of high-strength materials which result in slender members that may experience excessive deflections unless carefully designed. Slender beams and slabs carrying higher loads crack at earlier stages of loading, resulting in further reduction of stiffness and increased short-term and long-term deflections.

3.2.2 *Objectives*-This chapter discusses the factors affecting short-term and long-term deflection behavior of prestressed concrete members and presents methods for calculating these deflections.

In the design of prestressed concrete structures, the deflections under short-term or long-term service loads may often be the governing criteria in the determination of the required member sizes and amounts of prestress. The variety of possible conditions that can arise are too numerous to be covered by a single set of fixed rules for calculating deflections. However an understanding of the basic factors contributing to fhese deformations will enable a competent designer to make a reasonable estimate of deflection in most of the cases encountered in prestressed concrete design. The reader should note that the word *estimate* should be taken literally in that the properties of concrete which affect deflections (particularly long term deflections) are variable and not determinable with precision. Some of these properties have

values to which a variability of $\pm$ 20 percent or more in the deflection values must be considered. Deflection calculations cannot then be expected to be calculated with great precision.

3.2.3 *Scope*-Both short-term and long-term *transverse* deflections of beams and slabs involving prestressing with high-strength steel reinforcement are considered. Specific values of material properties given in this chapter, such as modulus of elasticity, creep coefficients, and shrinkage coefficients, generally refer to normal weight concrete although the same calculation procedures apply to lightweight concrete as well. This chapter is intended to be self-contained.

Finally several of the methods described in this chapter rely solely on computer use for analysis. They do not lend themselves to any form of hand calculation or approximate solutions. The reader should not be deluded into concluding that such computer generated solutions from complex mathematical models incorporating use of concrete properties, member stiffness, extent of cracking and effective level of prestress somehow generate results with significantly greater accuracy than some of the other methods presented. This is because of the range of variability in these parameters and the difficulty in predicting their precise values at the various loading stages and load history. Hence, experience in evaluating variability of deflections leads to the conclusion that satisfying basic requirments of detailed computer solutions using various values of assumed data can give upper and lower bounds that are not necessarily more rational than present code procedures.

3.3-Prestressing reinforcement

3.3.1 *Types of reinforcement*-Because of the creep and shrinkage which occurs in concrete, effective prestressing can be achieved only by using high-strength steels with strength in the range of 150,000 to 270,000 psi (1862 MPa) or more. Reinforcement used for prestressed concrete members is therefore in the form of stress-relieved or low-relaxation tendons and high-strength steel bars. Such high-strength reinforcement can be stressed to adequate prestress levels so that even after creep and shrinkage of the concrete has occurred, the prestress reinforcement retains adequate remaining stress to provide the required prestressing force. The magnitude of normal prestress losses can be expected to be in the range of 25,000 to 50,000 psi (172 MPa to 345 MPa).

Wires or strands that are not stress-relieved, such as straightened wires or oil-tempered wires, are often used in countries outside North America.

3.3.1.1 *Stress-relieved wires and strands*-Stress-relieved strands are cold-drawn single wires conforming to ASTM A 421 and stress-relieved tendons conform to ASTM A 416. The tendons are made from seven wires by twisting six of them on a pitch of 12 to 16 wire diameters around a slightly larger, straight control wire. Stress-relieving is done after the wires are twisted into the strand. Fig. 3.1 gives a typical stress-strain diagram for wire and tendon prestressing stegl reinforcement,

3.3.1.2 *High-tensile-strength prestressing bars*—High-tensile-strength alloy steel bars for prestressing are either smooth or deformed to satisfy ASTM A 722 requirements and are available in nominal diameters from 5/8 in. (16 mm) to 13/8 in. (35 mm). Cold drawn in order to raise their yield strength, these bars are stress relieved to increase their ductility. Stress relieving is achieved by heating the bar to an appropriate temperature, generally below 500 C. Though essentially the same stress-relieving process is employed for bars as for strands, the tensile strength of prestressing bars has to be a minimum of 150,000 psi (1034 MPa), with a minimum yield strength of 85 percent of the ultimate strength for smooth bars and 80 percent for deformed bars

3.3.2 *Modulus of elasticity*-In computing short-term deflections, the cross-sectional area of the reinforcing tendons in a beam is usually small enough that the deflections may be based on the gross area of the concrete. In this case, accurate determination of the modulus of elasticity of the prestressing reinforcement is not needed. However, in considering time-dependent deflections resulting from shrinkage and creep at the level of the prestressing steel, it is important to have a reasonably good estimate of the modulus of elasticity of the prestressing reinforcement.

In calculating deflections under working loads, it is sufficient to use the modulus of elasticity of the prestressing reinforcement rather than to be concerned with the characteristics of the entire stress-strain curve since the reinforcement is seldom stressed into the inelastic range. In most calculations, the assumption of the modulus value as 28.5×10^6 psi (PCI *Design Handbook,* Fourth Edition) can be of sufficient accuracy considering the fact that the properties of the concrete which are more critical in the calculation of deflections are not known with great precision. The ACI Code states that the modulus of elasticity shall be established by the manufacturer of the tendon, as it could be less than 28.5×10^6 psi.

When the tendon is embedded in concrete, the freedom to twist (unwind) is lessened considerably and it thus is unnecessary to differentiate between the modulus of elasticity of the tendon and that of single-wire reinforcement (AC1 Committee 435, 1979).

3.3.3 *Steel relaxation*-Stress relaxation in prestressing steel is the loss of prestress that occurs when the wires or strands are subjected to essentially constant strain over a period of time. Fig. 3.2 relates stress relaxation to time t in hours for both stress-relieved and low-relaxation tendons.

The magnitude of the decrease in the prestress depends not only on the duration of the sustained prestressing force, but also on the ratio f_{pi}/f_{py} of the initial prestress to the yield strength of the reinforcement. Such a loss in stress is termed intrinsic stress relaxation.

If f_{pR} is the remaining prestressing stress in the steel tendon after relaxation, the following expression defines f_{pR} for stress-relieved steel:
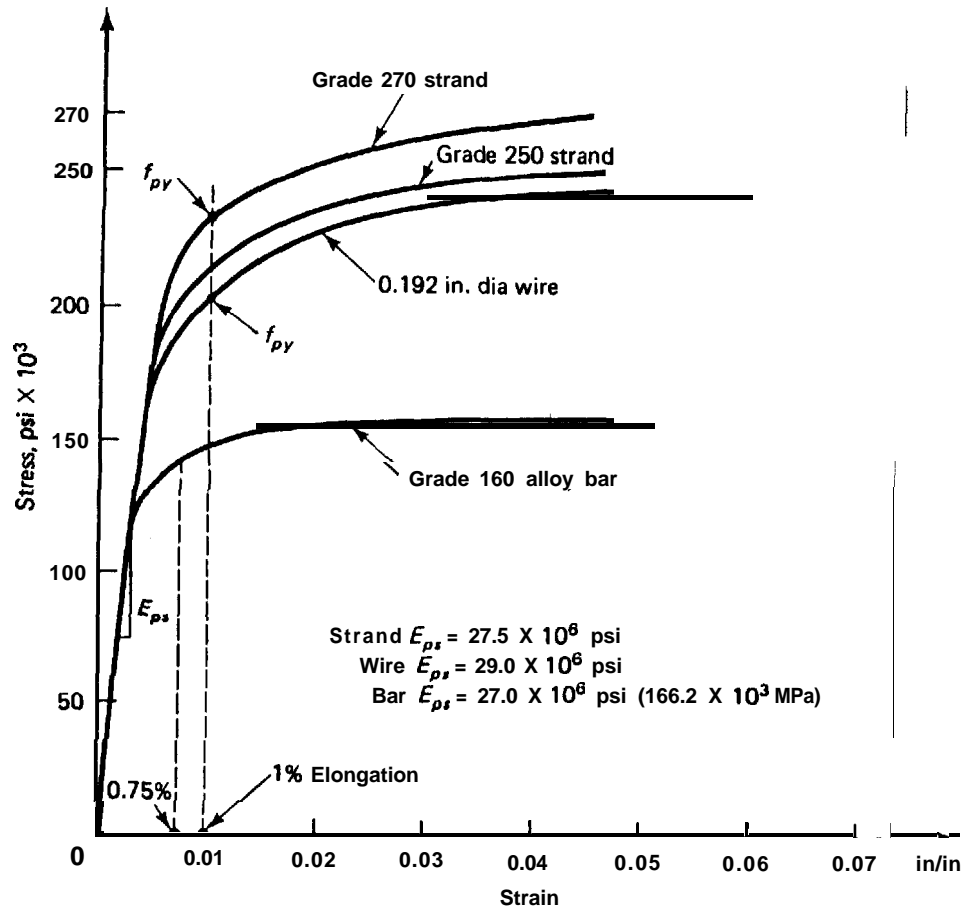
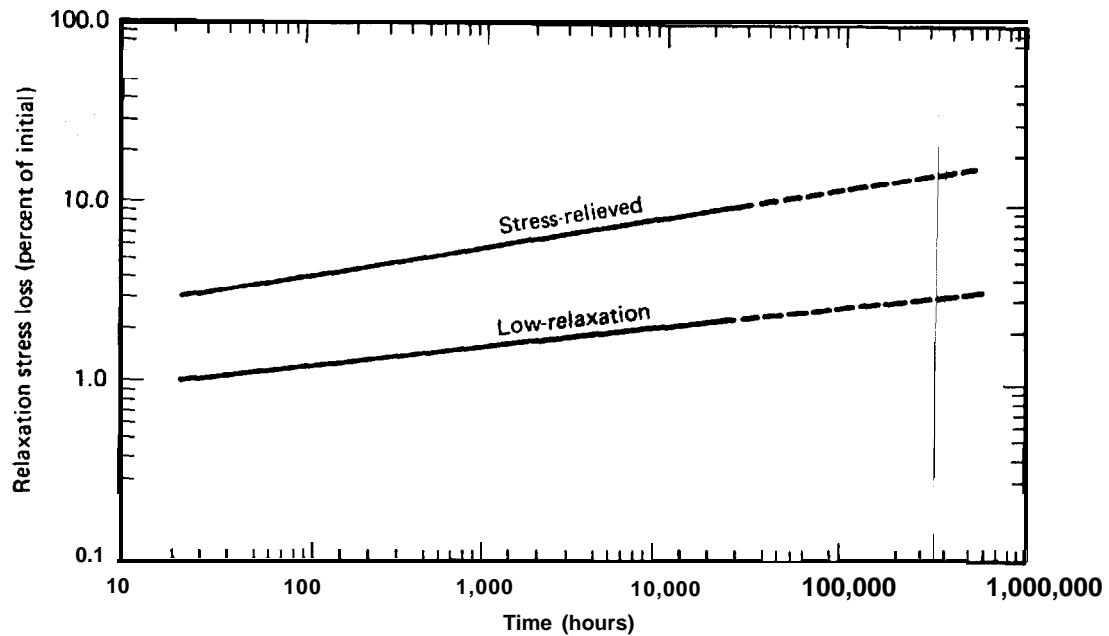Fig. 3.1-Typical stress-strain diagram for prestressing steel reinforcement

Fig. 3.2-Relaxation loss versus time for stress-relieved low-relaxation strands at 70 percent of the ultimate (Post-Tensioning Institute Manual, fourth edition)
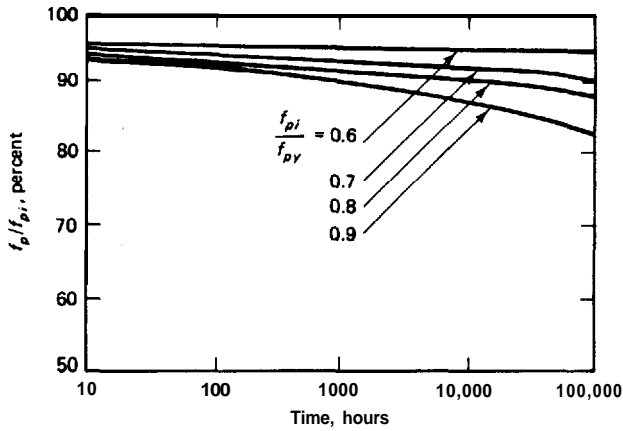
Fig. 3.3-Stress relaxation relationship in stress-relieved strands (Post Tensioning Manual, fourth edition)

$$\frac{f_{pR}}{f_{pi}} = 1 - \left(\frac{log t}{10}\right)\left(\frac{f_{pi}}{f_{py}} - 0.55\right) \qquad (3.1)$$

In this expression, $log t$ in hours is to the base 10, and the ratio f_{pi}/f_{py} must not be less than 0.55. Also, for low-relaxation steel, the denominator of the log term in the equation is divided by 45 instead of 10. A plot of Eq. 3.1 is given in Fig. 3.3. In that case, the intrinsic stress-relaxation loss becomes

$$\Delta f_{pR} = f_{pi} \frac{log t}{45}\left(\frac{f_{pi}}{f_{py}} - 0.55\right) \qquad (3.2)$$

where f_{pi} is the initial stress in steel.

If a step-by-step loss analysis is necessary, the loss increment at any particular stage can be defined as

$$\Delta f_{pR} = f_{pi}\left(\frac{log t_2 - log t_1}{10}\right)\left(\frac{f_{pi}}{f_{py}} - 0.55\right) \qquad (3.3)$$

where t_1 is the time at the beginning of the interval and t_2 is the time at the end of the interval from jacking to the time when the loss is being considered. Therefore, the loss due to relaxation in stress-relieved wires and strands can be evaluated from Eq. 3.3, provided that $f_{pi}/f_{py} \geq 0.55$, with $f_{py} \approx 0.85 f_{pu}$ for stress-relieved strands and $0.90 f_{pu}$ for low-relaxation tendons.

It is possible to decrease stress relaxation loss by subjecting strands that are initially stressed to 70 percent of their ultimate strength f_{pu} to temperatures of 20 C to 100 C for an extended time in order to produce a permanent elongation, a process called *stabilization.* The prestressing steel thus produced is termed *low-relaxation* steel and has a relaxation stress loss that is approximately 25 percent of that of normal stress-relieved steel.

Fig. 3.2 gives the relative relaxation loss for stress-

relieved and low-relaxation steels for seven-wire tendons held at constant length at 29.5 C. Fig. 3.4 shows stress relaxation of stabilized strand at various tension and temperature levels.

It should be noted that relaxation losses may be critically affected by the manner in which a particular wire is manufactured. Thus, relaxation values change not only from one type of steel to another but also from manufacturer to manufacturer. Factors such as reduction in diameter of the wire and its heat treatment may be significant in fixing the rate and amount of relaxation loss that may be expected. Nevertheless, sufficient data exists to define the amount of relaxation loss to be expected in ordinary types of prestressing wires or strands currently in use.

3.4-Loss of prestress

3.4.1 *Elastic shortening loss-*A concrete element shortens when a prestressing force is applied to it due to the axial compression imposed. As the tendons that are bonded to the adjacent concrete simultaneously shorten, they lose part of the prestressing force that they carry.

In pretensioned members, this, force results in uniform longitudinal shortening. Dividing the reduction in beam length by its initial length gives a strain that when multiplied by the tendon modulus of elasticity gives the stress loss value due to elastic shortening. In post-tensioned beams, elastic shortening varies from zero if all tendons are simultaneously jacked to half the value in the pretensioned case if several sequential jacking steps are applied.

3.4.2 *Loss of prestress due to creep of concrete-*The deformation or strain resulting from creep losses is a function of the magnitude of the applied load, its duration, the properties of the concrete including its mix proportions, curing conditions, the size of the element and its age at first loading, and the environmental conditions. Size and shape of the element also affect creep and subsequent loss of prestress. Since the creep strain/stress relationship is essentially linear, it is feasible to relate the creep strain ϵ_{CR} to the elastic strain ϵ_{EL} such that the ultimate creep coefficient C_u can be defined as

$$C_u = \frac{\epsilon_{CR}}{\epsilon_{EL}} \qquad (3.4)$$

The creep coefficient at any time t in days can be taken as

$$C_t = \frac{t^{0.60}}{10 + t^{0.60}} C_u$$

(See Eq. 2.7 of Chapter 2; also Branson, et. al, 1971, 1977 and ACI 209, 1971, 1992)

The value of C_u usually ranges between 2 and 4, with an average of 2.35 for ultimate creep. The loss of pre-
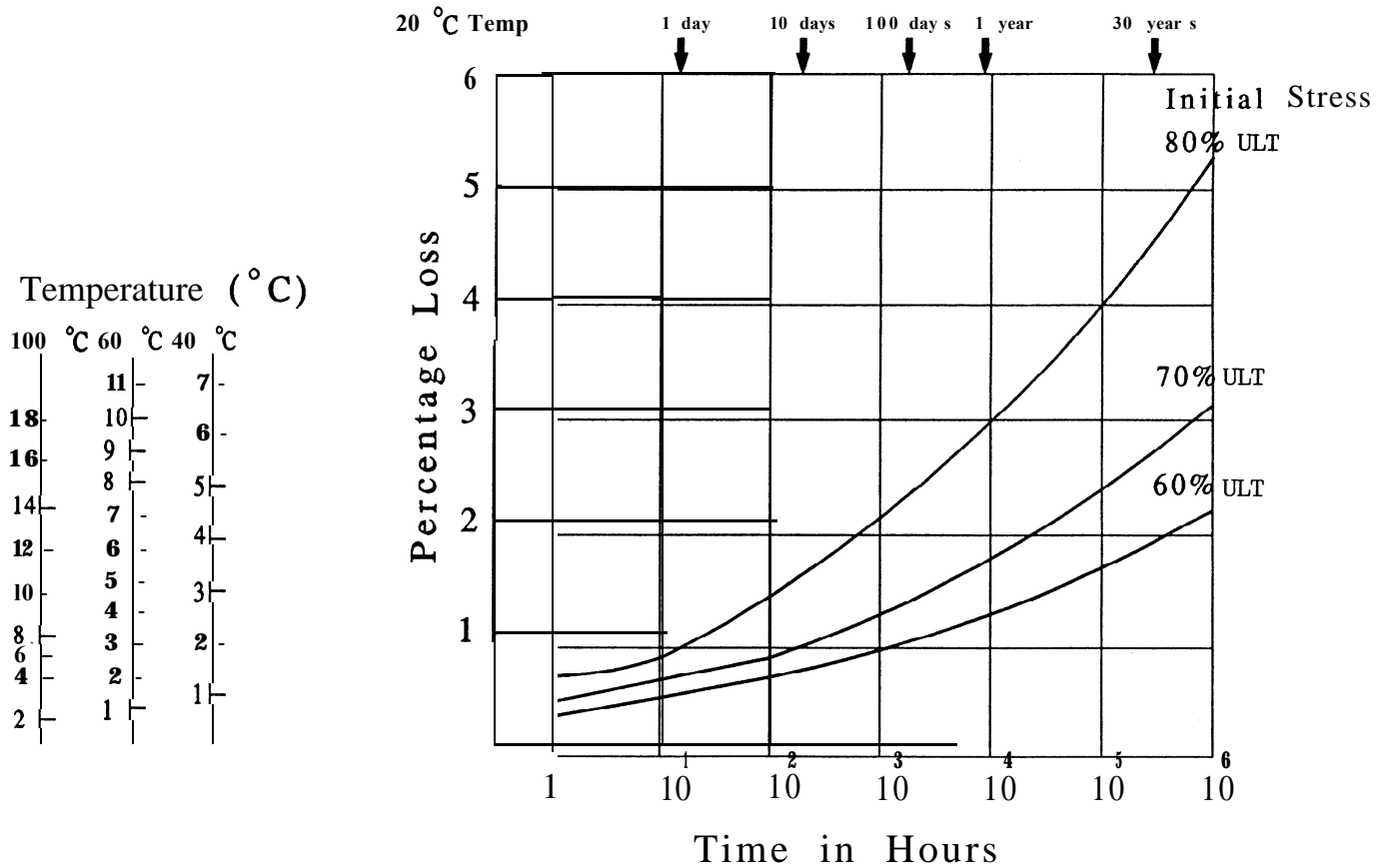
Fig. 3.4-Stress relaxation of stabilized strand at various tensions and temperatures (courtesy STELCO Inc., Canada)

stress for bonded prestressed members due to creep can be defined as

$$\Delta f_{pCR} = C_u \frac{E_{ps}}{E_c} f_{cs} \tag{3.6}$$

where f_{cs} is the stress in the concrete at the level of the centroid of the prestressing tendon. In general, this loss is a function of the stress in the concrete at the section being analyzed. In post-tensioned, nonbonded draped tendon members, the loss can be considered essentially uniform along the whole span. Hence, an average value of the concrete stress between the anchorage points can be used for calculating the creep in post-tensioned members. A modified ACI-ASCE expression for creep loss can be used as follows:

$$\Delta f_{pCR} = K_{CR} \frac{E_{ps}}{E_c} (\bar{f}_{cs} - f_{csd}) \tag{3.7}$$

where

K_{CR} = 2.0 for pretensioned members
= 1.60 for post-tensioned members
(both for normal weight concrete)

$\bar{f}_{cs}$ = stress in concrete at the *cgs* level of the reinforcement immediately after transfer

f_{csd} = stress in concrete at the *cgs* level of the reinforcement due to all superimposed dead loads applied after prestressing is accomplished

K_{CR} should be reduced by 20 percent for lightweight concrete.

Fig. 3.5 shows normalized creep strain plots versus time for different loading ages while Fig. 3.6 illustrates in a three-dimensional surface the influence of age at loading on instantaneous and creep deformations. Fig. 3.7 gives a schematic relationship of total strain with time excluding shrinkage strain for a specimen loaded at a one day age.

3.4.3 *Loss of prestress due to shrinkage of concrete*-As with concrete creep, the magnitude of the shrinkage of concrete is affected by several factors. They include mix proportions, type of aggregate, type of cement, curing time, time between the end of external curing and the application of prestressing, and the environmental conditions. Size and shape of the member also affect shrinkage. Approximately 80 percent of shrinkage takes place in the first year of life of the structure. The average value of ultimate shrinkage strain in both moist-cured and stream-cured concrete is given as 780 x 10^{-6} in./in. in the ACI 209R-92 Report. This average value is affected by the duration of initial moist curing, ambient relative humidity, volume-surface ratio, temperature; and con-
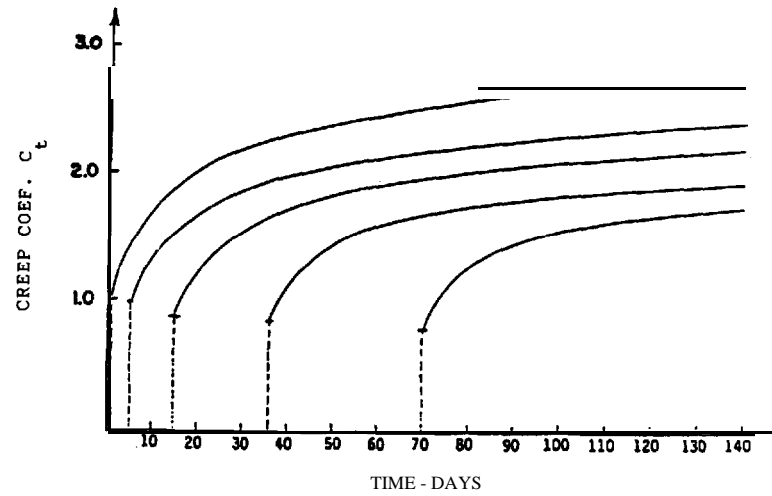
Fig. 3.5-Creep curves for different loading ages at same stress level
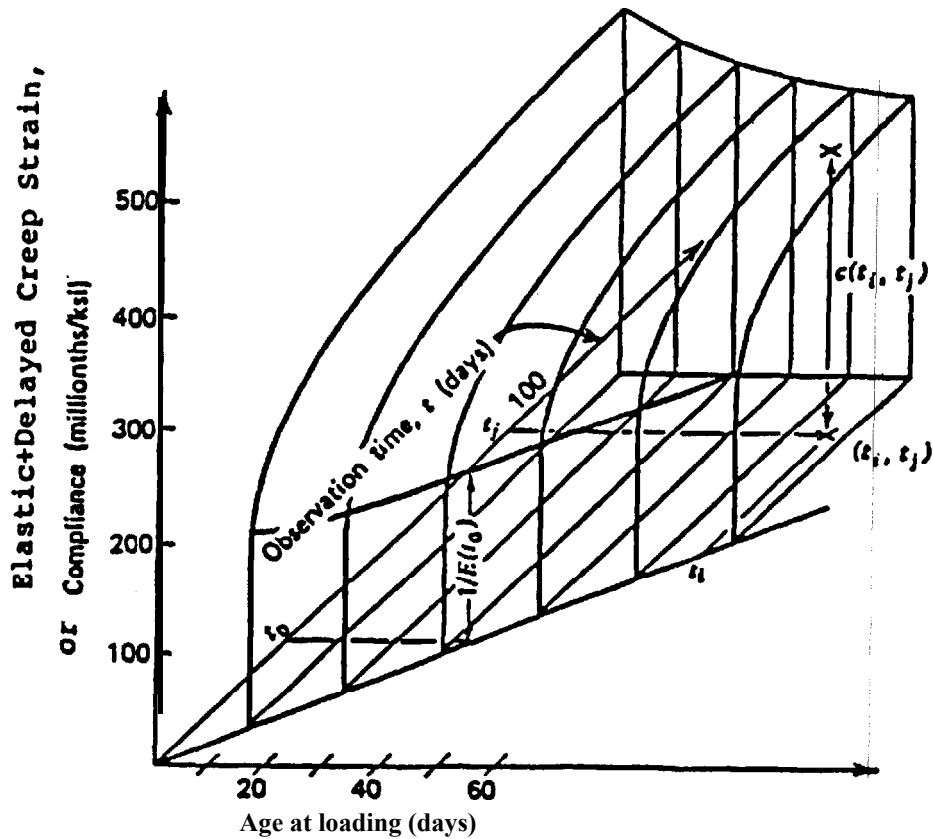
Fig. 3.6-Influence of age at loading on instantaneous and creep deformations (3-D surface)

crete composition. To take such effects into account, the average value of shrinkage strain should be multiplied by a correction factor γ_{SH} as follows

$$\epsilon_{SH} = 780 \times 10^{-6} \gamma sH \qquad (3.8)$$

Components of γ_{SH} are given in Sec. 2.3.4.

The Prestressed Concrete Institute stipulates for standard conditions an average value for nominal ultimate shrinkage strain $(\epsilon_{SH})_u = 820 \times 10^{"}$ in./in. (mm/mm), (PCI *Handbook,* 1993). If ϵ_{SH} is the shrinkage strain after

adjusting for relative humidity at volume-to-surface ratio V/S, the loss in prestressing in pretensioned members is

$$\Delta f_{pSH} = \epsilon_{SH} \times E_{ps} \qquad (3.9)$$

For post-tensioned members, the loss in prestressing due to shrinkage is somewhat less since some shrinkage has already taken place before post-tensioning. If the relative humidity is taken as a percent value and the V/S ratio effect is considered, the PCI general expression for loss in prestressing due to shrinkage becomes
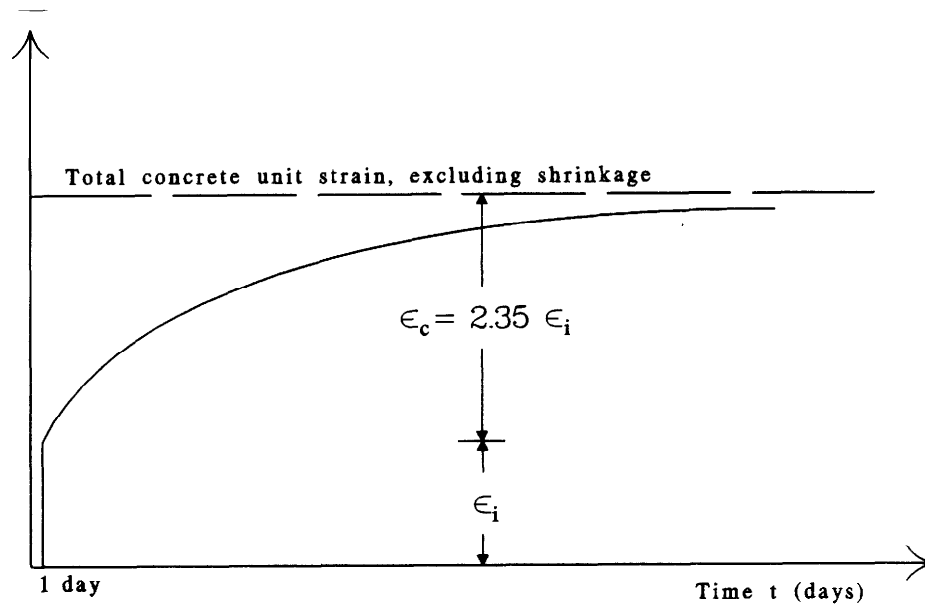
Fig. 3.7-Typical concrete strain versus time curve for constant stress applied at release time

$$\Delta f_{pSH} = 8.2 \ x \ 10^{-6} K_{SH} E_{ps}\left(1 \ -0.06 \frac{V}{S}\right)(100 - RH) \quad (3.10)$$

where $K_{SH} = 1.0$ for pretensioned members. Table 3.1 gives the values of K_{SH} for post-tensioned members.

Adjustment of shrinkage losses for standard conditions as a function of time t in days after seven days for moist curing and three days for steam curing can be obtained from the following expressions (Branson, et.al, 1971):

a) Moist curing, after seven days:

$$(\epsilon_{SH})_t = \frac{t}{35 + t} (\epsilon_{SH})_u \qquad (3.11a)$$

where $(\epsilon_{SH})_u$ is the ultimate shrinkage strain, t = time in days after shrinkage is considered.

b) Steam curing, after one to three days:

$$(\epsilon_{SH})_t = \frac{t}{55 + t} (\epsilon_{SH})_u \qquad (3.11b)$$

Fig. 3.8 schematically shows shrinkage strain versus time.

It should be noted that separating creep from shrinkage calculations as presented in this chapter is an ac-cepted engineering practice. Also, significant variations occur in the creep and shrinkage values due to variations in the properties of the constituent materials from the various sources, even if the products are plant-produced such as pretensioned beams. Hence, it is recommended that information from actual tests be obtained especially on manufactured products, large span-to-depth ratio cases and/or if loading is unusually heavy (Aswad, 1985, 1989, 1992).

3.4.4 *Friction losses in post-tensioned beams*-Relaxation losses are covered in 3.3.3. Loss of prestressing occurs in post-tensioned members due to friction between the tendons and the surrounding concrete ducts. The magnitude of this loss is a function of the tendon form or alignment, called the curvature effect, and the local deviations in the alignment, called the wobble effect. The values of the loss coefficients are affected by the types of tendons and the duct alignment. Whereas the curvature effect is predetermined, the wobble effect is the result of accidental or unavoidable misalignment, since ducts or sheaths cannot be perfectly held in place. Section 186.2 of ACI 318-89 and Table R18.6.2 of the Commentary to the code give the friction coefficients that apply to the friction loss in the various types of prestressing wires and tendons.

Table 3.1---Values of K_{SH} for post-tensioned members

Time from end of moist curing to application of prestress, days	1	3	5	7	10	20	30	60
K_{SH}	0.92	0.85	0.80	0.7	0.73	0.64	0.58	0.45

Source: Prestressed Concrete Institute

Fig. 3.8-Shrinkage strain versus time curve

3.5-General approach to deformation considerations - Curvature and deflections

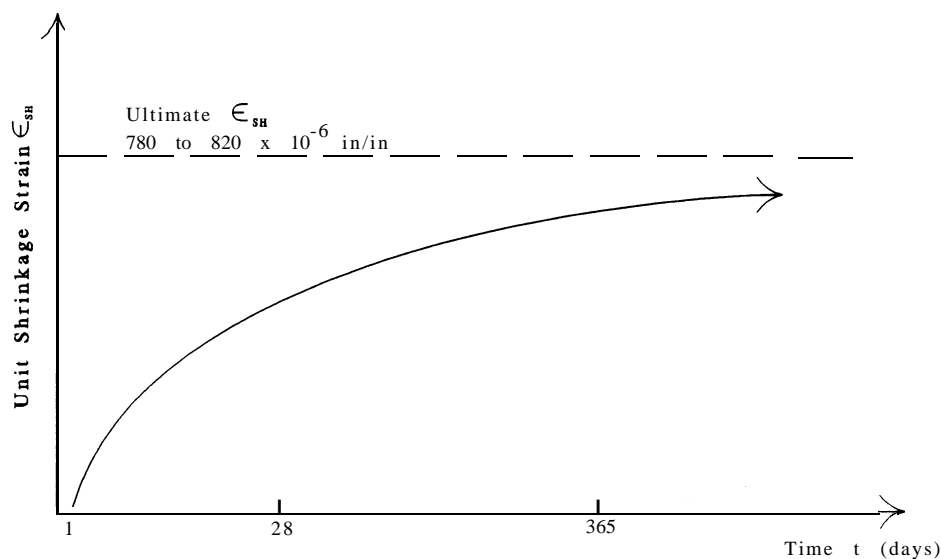In beam-like structures the curvature at any section, defined as $\phi = 1/R$, is the key element in calculating rotations and deflections. Based on geometry of the deflected shape, the two following expressions are derived, see Fig. 3.9.

$$\theta_{AB} = \int_{A}^{B} \phi \, dx \qquad (3.12a)$$

$$\delta_{BA} = \int_{B}^{A} \phi x \, dx \qquad (3.12b)$$

where ϕ is the curvature, θ is the rotation and δ is the tangential deviation (deflection). These two expressions are generalizations of the familiar Mohr or moment-areas theorems, and are applicable whether sections are cracked or uncracked. When the material is linearly elastic, ϕ can be replaced by M/EI. Software programs use Simpson's rule to approximate the above integrals. Fig. 3.9(c) shows how the deflection y at any section can be calculated.

Based on these fundamental principles, the designer can calculate the curvature and rotation incrementally at any section and hence the deflection or camber of the prestressed beam at the critical sections.

Short-term deflections are defined as those occurring instantaneously under the application of any internal or external force. The time element is assumed to be unimportant, no matter what the rate of loading, provided the load is applied within a matter of hours.

In general, the principal variables affecting short-term deflections of a prestressed concrete beam are the magnitude and distribution of the load, the magnitude and eccentricity of the prestress, the length of the span, the size and configuration of the cross section, boundary conditions and the properties of the concrete. More specifically, the effect of critical variables may be summarized by the magnitude of the strain or stress gradient or the curvature at a section and its variation along the span.

The initial curvature at a particular section (Fig. 3.10) is defined by

$$\phi_i = \frac{\epsilon_{bi} - \epsilon_{ti}}{h} = \frac{M}{E_c I} \qquad (3.13)$$

in which tensile strains are considered positive, and M is the moment at the section.

In most cases, the amount of prestressing steel reinforcement has a negligible effect on section properties for short-term deflections due to gravity loads.

3.5.1 *Beams subjected to prestressing only*-Stress and strain distributions over the depth of a cross section of a rectangular bonded beam immediately after application of the prestressing force are shown in Fig. 3.10. It is assumed that there is a linear relationship between concrete stress and strain. Under normal conditions both of these assumptions are reasonably correct. The stress at any level is given by the well-known relationships:

$$f = -\frac{P}{A} \pm \frac{My}{I} \qquad (3.14)$$

and

$$M = Pe \qquad (3.15)$$

for use in Eq. 3.13 and where P is the prestressing force.

The stress and strain distributions in Fig. 3.11 depict the conditions existing after a given time. The normal
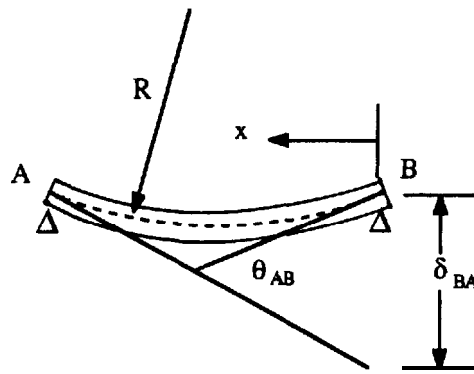
(a) General Beam Deformation
    Curvature $\phi = 1/R$
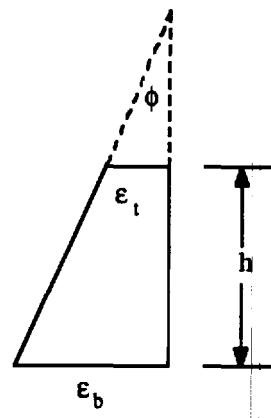
(b) Beam Strain at Any Section
    (Curavture $\phi = (\varepsilon_b - \varepsilon_t)/h$)
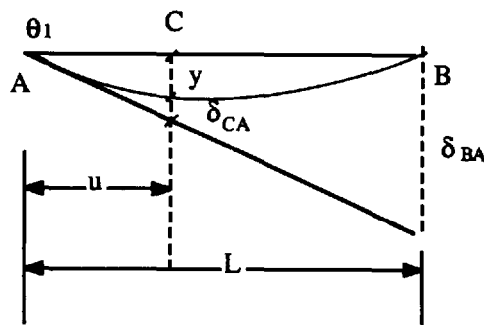
$$\theta = \delta_{BA}/L$$

$$\delta = \int \phi \, x \, dx$$

$$y = \theta_1 u - \delta_{CA}$$

(c) Beam Elastic Curve Deflection y and Tangential Deviation δ_{CA} δ_{BA}

Fig. 3.9-Beam elastic curve deformation

STRESS

STRAIN

(a)   **(b)**   **(c)**
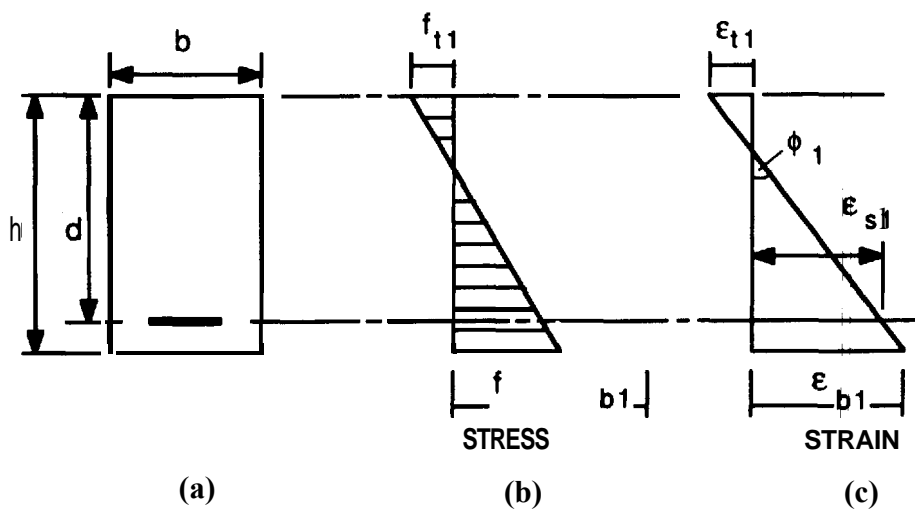
Fig. 3.10-Stress and strain distribution immediately after application of prestress
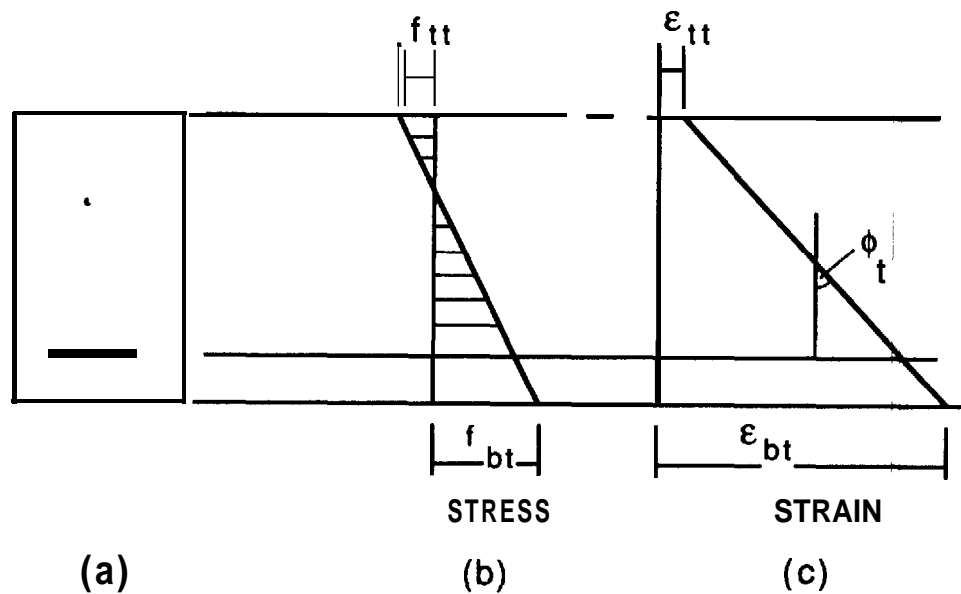
Fig. 3.11-Stress and strain distribution at a time t *after initial application of prestress*
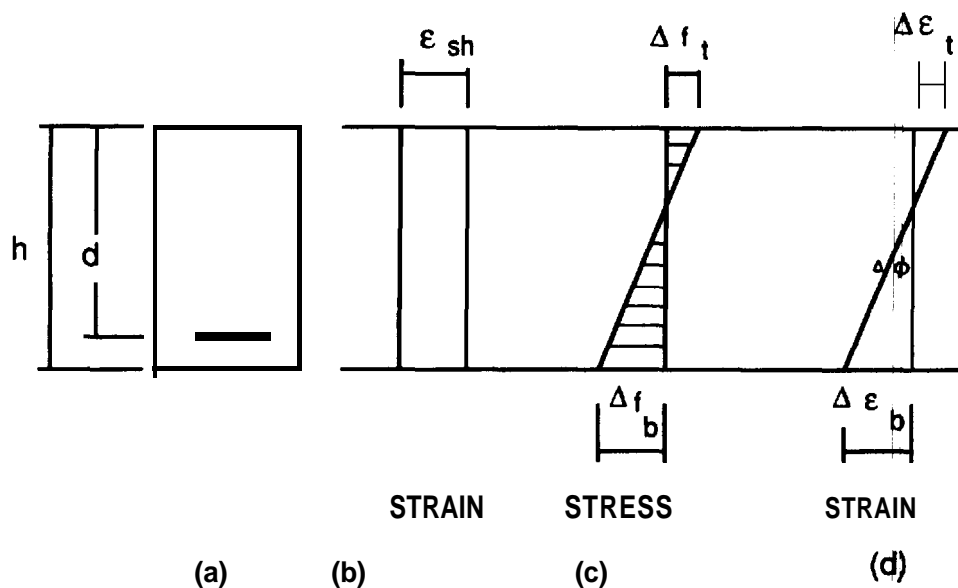
Fig. 3.12-Stress and strain due to shrinkage

stresses on the section decrease as a result of a reduction in the prestressing force while there is a general shift to the right in the strain distribution accompanied by an increase in the strain gradient.

These changes are caused by an interaction between creep and shrinkage of the concrete and relaxation of the reinforcement. All of these effects progress with time and continuously impact on each other. However, to simplify the calculation, it is preferable to treat these three types of strains separately.

Consider first the effect of shrinkage strains. It is assumed that each element of concrete in the cross-section shrinks equally. Thus, the shrinkage strain distribution after a time *t* is given in Fig. 3.12b. The distribution of shrinkage strain causes a reduction in the reinforce-

ment strain which corresponds to a reduction in the prestress. The loss in prestress causes a change in the stress distribution over the depth of the section as indicated in Fig. 3.12c and the corresponding change in the strain distribution, Fig. 3.12d. Thus, the change in curvature is

$$\Delta \phi = \frac{\Delta \epsilon_b - \Delta \epsilon_c}{h} \qquad (3.16)$$

The effect of the relaxation losses in the steel reinforcement is quite similar to that of shrinkage. At a time *t* there is a finite loss in the prestressing force which creates a change in the curvature as explained above. The effects of the creep of the concrete are not as simple, since the reduction in steel stress causes changes in the
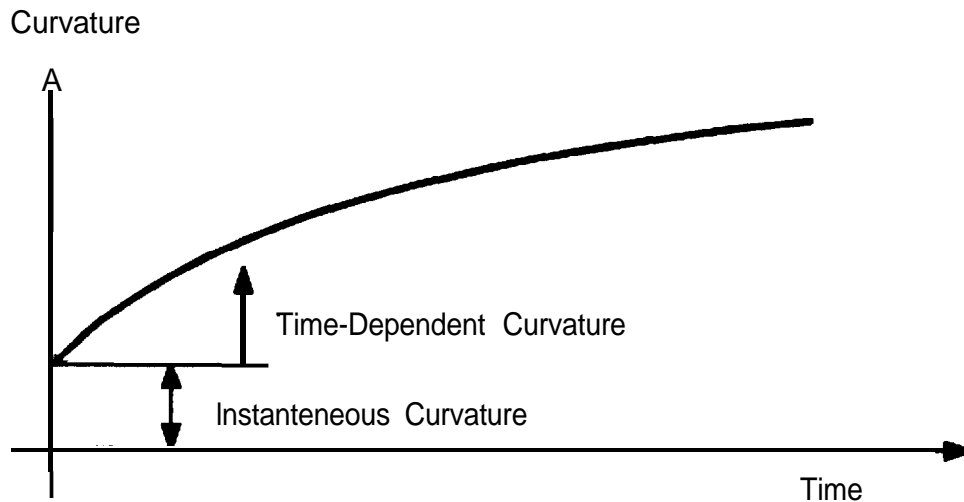
Fig. 3.13-Curvature versus time for a beam subjected to prestress only
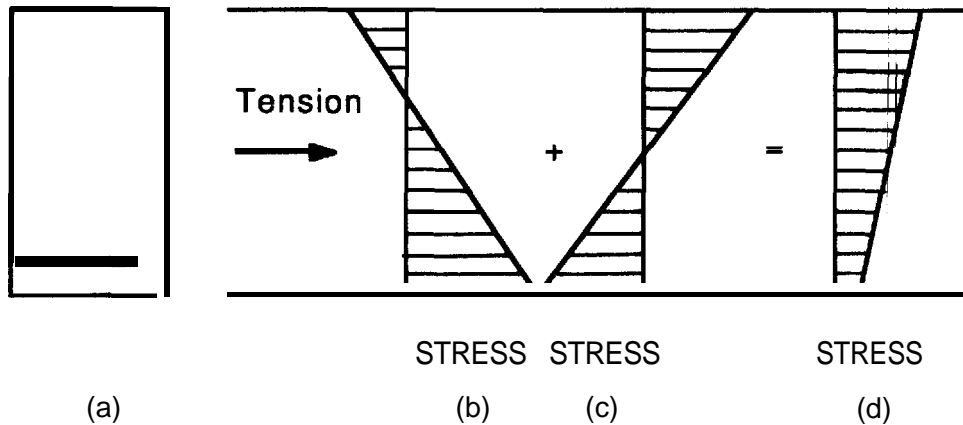
Fig. 3.14-Stress distribution due to prestress and transverse loads

rate of creep strain. It is assumed that the amount of creep strain at a given time is proportional to the stress. Thus, the change in strain caused by creep is directly proportional to the instantaneous strain distribution (Fig. 3.10c), which is directly related to the stress distribution. This change in the strain distribution involves a contraction at the level of the steel, hence, a reduction in prestress. The reduction in prestress caused by creep, shrinkage, and relaxation decreases the normal stress, which in turn reduces the rate of creep.

A qualitative curvature versus time curve is shown in Fig. 3.13. As in the case of short-term deflections, the magnitude of the deflection may be estimated by the magnitude of the stress gradient over the depth of the section after release of prestress. If the stress gradient is very small, then shrinkage and relaxation are bound to dominate, in which case the beam may deflect downward. However, under usual circumstances the stress gradient is large and creep dominates the deflection thus causing the beam to move upward causing increased camber in a simply supported case (ACI 435, 1979).

3.5.2 *Beams subjected to prestressing and external loads*

--If the beam considered in the preceding paragraph is subjected to gravity load, the stress distribution across the section at a given point along the span may be as indicated in Fig. 3.14d. Provided neither the concrete nor the reinforcement is strained into the inelastic range, the stress distribution caused by the prestressing force (Fig. 3.14b) can be superimposed on the stress distribution caused by the transverse load on the uncracked transformed section (Fig. 3.14c) to obtain the total stress distribution shown in Fig. 3.14d.

The strain distribution shown in Fig. 3.15b corresponds to the stress distribution in Fig. 3.14c. It depicts the strains that would occur in an uncracked section under the influence of only the transverse load. The short-term curvature is

$$\phi_i = \frac{\epsilon_{bi} - \epsilon_{ti}}{h}$$

(3.17)

where the subscripts *b* and *t* define the bottom and top fibers respectively.
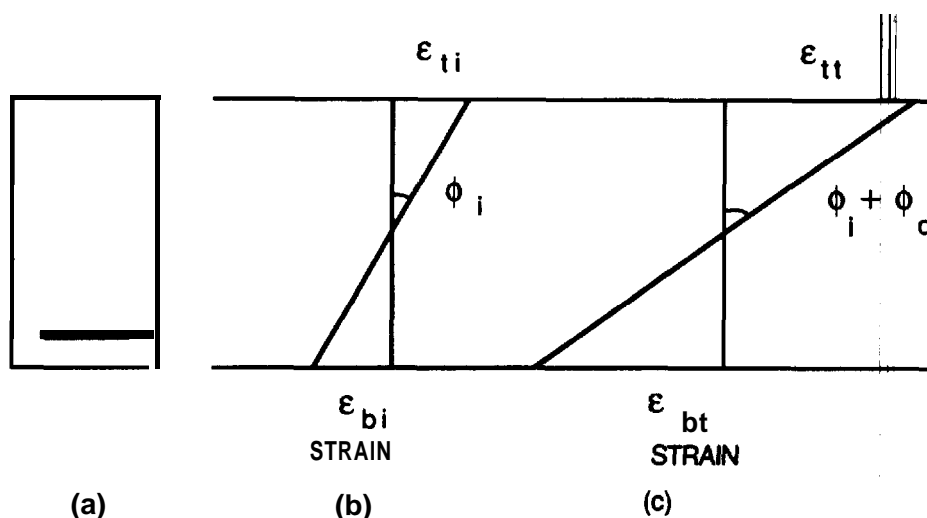
Fig. 3.15-Strain distribution due to transverse loading only
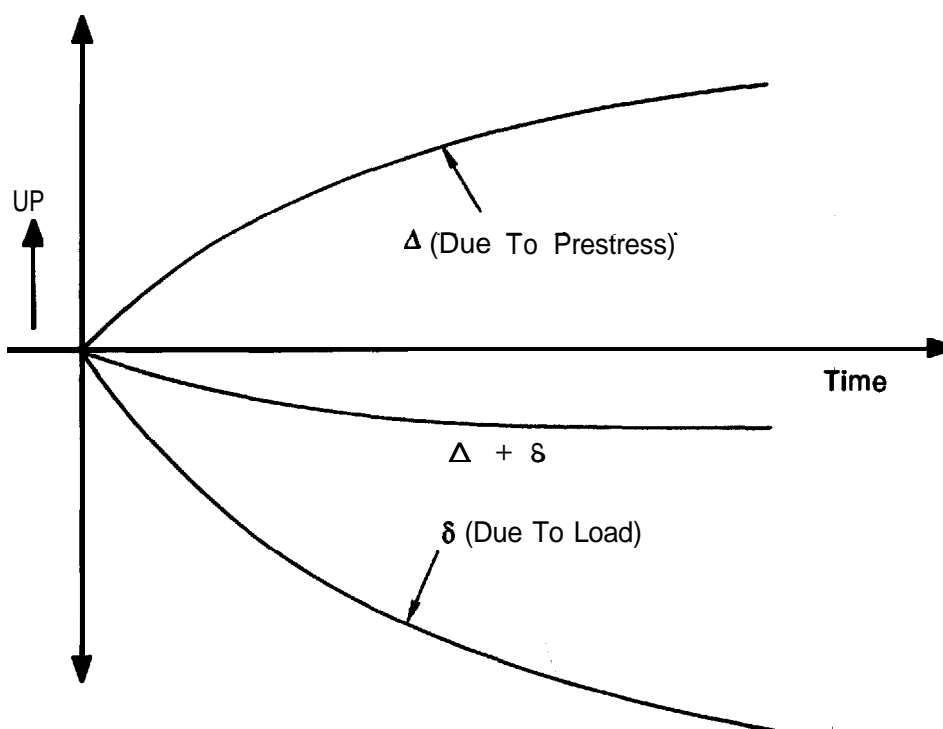
Deflection

Fig. 3.16-Deflection versus time due to prestress and transverse loads

The changes in the curvature or in the deflection of the beam caused by the combined prestress and the transverse load are henceforth determined by superposition. Both of these curvature distributions will change with time. The deflections corresponding to these two imaginary systems are shown in Fig. 3.16.

To get the net deflection, the deflections caused by the prestress and transverse load can be added as indicated by the (A-G) curve. It is seen that the magnitude of the beam deflection (and whether it deflects upward or downward) depends on the relative effect of the prestress and of the transverse loads. Ideally, a beam can be designed to have a small camber at midspan at the ser-

vice load level or at a fraction of the service load level.

3.5.3 *Moment-curvature relationship*--The instantaneous moment-curvature relationship for a prestressed cross section is illustrated in Fig. 3.1 7. Concrete can sustain tensile stresses and contribute to the carrying capacity of a member until cracking occurs at a moment M_{cr}. A moment M_a larger than the cracking moment M_{cr} produces curvature that can be defined as follows:

$$\phi_{cr} = \frac{(M_a - Pe_{cr})}{E_c I_{cr}} \tag{3.18}$$

where P is the prestressing force, and e_{cr} is its eccentricity
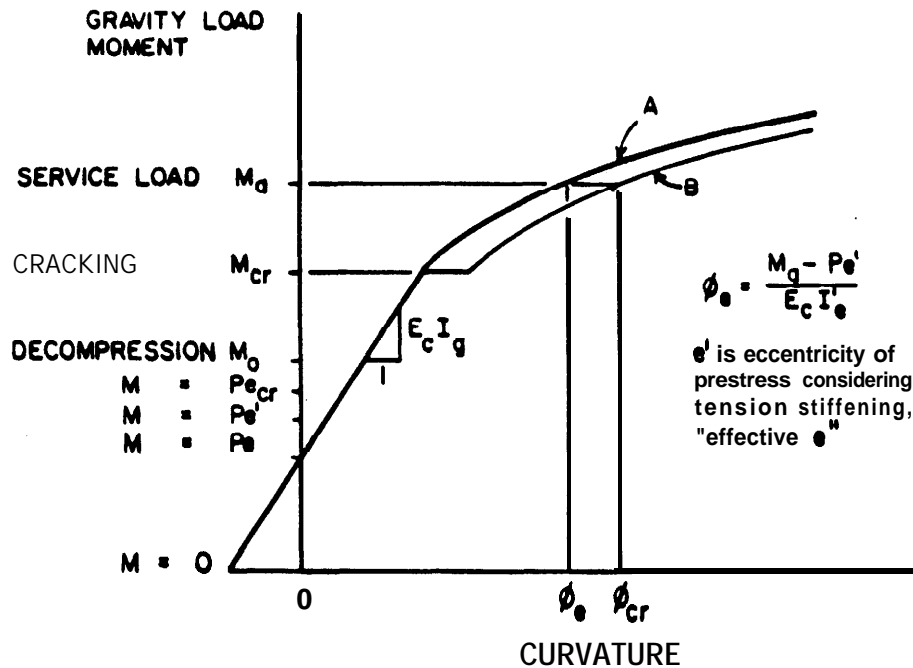
Fig. 3.17 Moment versus curvature relationship in prestressed section

relative to the centroid of the cracked section. The drop in rigidity due to cracking is represented by the horizontal line at the M_{cr} level. For the prestressed section, both I_{cr} and y_{cr} (and in turn e_{cr}) are dependent on the loading level, with the M-ϕ becoming nonlinear after cracking. It is important to note that the shift in the centroid of the cross section upon cracking results in larger prestressing force eccentricity, e_{cr} than the uncracked member eccentricity. This fact is particularly significant in flanged members, such as double tees which are characterized by the relatively low steel area ratio ρ_f, and because concrete tensile strength is not zero, cracking does not extend to the neutral axis. In addition, uncracked concrete which exists between cracks in the tension zone, contributes to the stiffness of the member (tension stiffening). Taking this into account, the M-4 diagram becomes continuous, as indicated by line A in Fig. 3.17 and as is usually accepted in engineering practice (ACI 318, 1989) and verified by numerous tests (Aswad, 1992).

3.6-Short-term deflection and camber evaluation in prestressed beams

Several methods to estimate short-term and long-term deflections of prestressed concrete structural members are presented in this article. Included are procedures for uncracked members and cracked members.

3.6.1 *Uncracked members-*When a concrete section is subjected to a flexural stress which is lower than the modulus of rupture of concrete f_r, the section is assumed to be uncracked and thus its behavior is linear. Under this condition, the deflection is calculated by the basic principles of mechanics of elastic structures. In prestressed concrete construction, the immediate deflection,
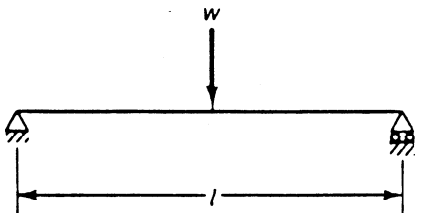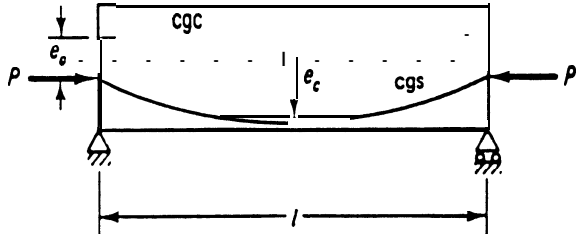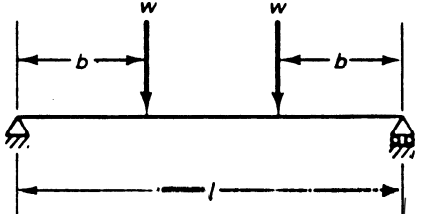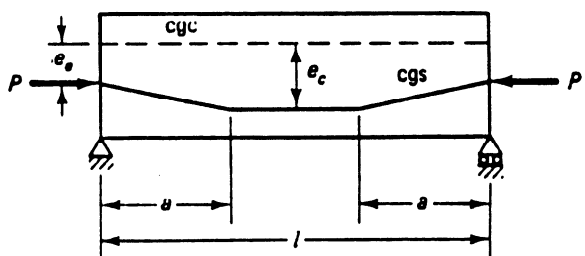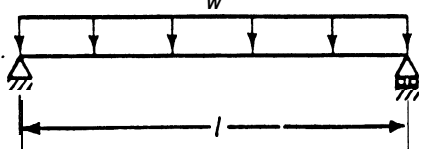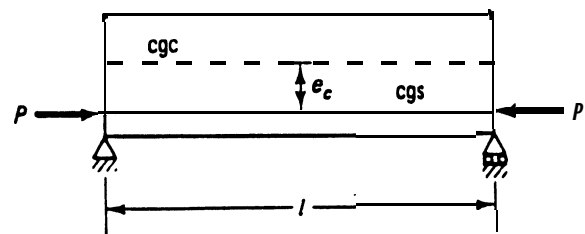
or camber, due to the effects of initial prestressing P_i and member self-weight is generally in the elastic uncracked range. Therefore, the elastic formulas presented in Table 3.2 could be used to calculate the instantaneous deflection of the members. The value of P_i is equal to the jacking force less the initial prestress loss due to anchorage set, elastic shortening, and the relatively small relaxation loss occurring between jacking and release time. Since P_i varies from section to section a weighted average may be used. An average initial loss of 4-10 percent can be reasonably used in order to get f_{pi}.

Unless test results are available, the modulus of elasticity of concrete can be estimated from the expression recommended in ACI 318 (See Chapter 2, Section 2.3). For uncracked sections, it is customary to use the gross moment of inertia I_g for pretensioned members and the net moment of inertia I_n for post-tensioned members with unbonded tendons.

3.6.2 *Cracked members — Effective* I_e *method--*In prestressed concrete members, cracks can develop at several sections along the span under maximum load. The cracked moment of inertia I_{cr} applies at cracked sections while the gross moment of inertia applies in between cracks. ACI 318 (Section 18.4.2c) requires that a bilinear moment-deflection relationship be used to calculate instantaneous deflections when the magnitude of tensile stress in service exceeds $6\sqrt{f_c'}$. A value of $12\sqrt{f_c'}$ is permitted when the immediate and long-term deflections are within the allowable limits. I_g is used for the portion of moment not producing such tensile stress, while for the remaining portion of moment, I_{cr} is used.

The effective moment of inertia I_e for simply sup-

Table 3.2-Short-term deflection in prestressed concrete beams (subscript c indicates midspan, subscript e, support)

Load deflection	Prestress camber

Load deflection (point load at midspan):

$$\delta = \frac{wl^3}{48EI} = \phi_c \frac{l^2}{12}$$

Prestress camber:

$$\delta = -\frac{Pl^2}{8EI}\left[e_e + \frac{5}{6}(e_c - e_e)\right]$$

$$= \phi_c \frac{l^2}{8} + (\phi_e - \phi_c)\frac{l^2}{48}$$

Load deflection (two point loads):

$$\delta = \frac{wb}{24EI}(3l^2 - 4b^2)$$

$$= \phi_c \frac{3l^2 - 4b^2}{24}$$

Prestress camber:

$$\delta = -\frac{Pl^2}{8EI}\left[e_c + (e_s - e_c)\frac{4}{3}\frac{a^2}{l^2}\right]$$

$$= \phi_c \frac{l^2}{8} + (\phi_e - \phi_c)\frac{a^2}{6}$$

Load deflection (uniform load):

$$\delta = \frac{5wl^4}{384EI} = \phi_c \frac{5l^2}{48}$$

Prestress camber:

$$\delta = -\frac{Pe_c l^2}{8EI} = \phi_c \frac{l^2}{8}$$
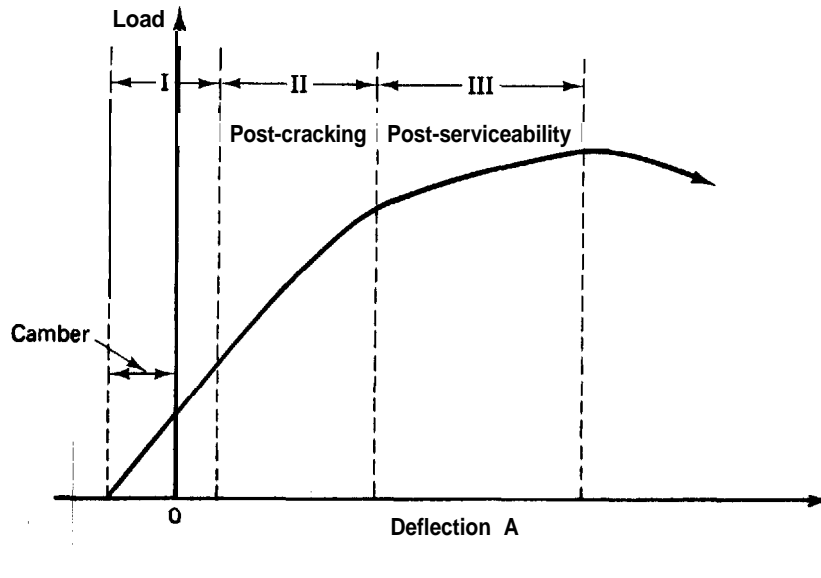
*Fig. 3.18-Load-deflection relationship in prestressed beam: Region **I**, precracking stage; Region **II**, postcracking stage; Region III, post-serviceability stage*

ported beams, cantilevers, and continuous beams between inflection points is given in ACI 318-89, Section 9.5.2.3, but with the modified definitions of M_{cr} and M_a for prestressed concrete as follows:

$$I_e = \left(\frac{M_{cr}}{M_a}\right)^3 I_g + \left[1 - \left(\frac{M_{cr}}{M_a}\right)^3\right] I_{cr} \le I_g \quad (3.19a)$$

or

$$I_e = \left(\frac{M_{cr}}{M_a}\right)^3 (I_g - I_{cr}) + I_{cr} \le I_g \quad (3.19b)$$

where

$$\left(\frac{M_{cr}}{M_a}\right) = \left(1 - \frac{f_{TL} - f_r}{f_L}\right) \quad (3.19c)$$

The value of fr in Eq. 3.19c is taken as $7.5\sqrt{f_c'}$.

λ = reduction factor for sand lightweight concrete

= 0.85 and 0.70 for all lightweight concrete

f_r = modulus of rupture = $7.5\lambda\sqrt{f_c}$

f_{TL} = total calculated stress in member

f_L = calculated stress due to live load

I_{cr} = moment of inertia of the cracked section, from Eq. 3.21, Section 3.6.3

I_g = gross moment of inertia

M_{cr} = moment due to that portion of unfactored *live* load moment M_a that causes cracking

M_a = max unfactored *live* load moment

y_t = distance from neutral axis to tensile face

The effective moment of inertia I_e in Eq. 3.19a and b thus depends on the maximum moment M_a due to live load along the span in relation to the cracking moment capacity M_{cr} of the section due to that portion of the live load that caused cracking.

In the case of beams with two continuous ends ACI 318-89 allows using the midspam I_e. However, more accurate values can be obtained when the section is *uncracked* using the following expressions as discussed in Chapter 2, Section 2.5.

$$\text{Avg. } I_e = 0.70 I_m + 0.15(I_{e1} + I_{e2}) \quad (3.20a)$$

and for continuous beams with one end continuous,

$$\text{Avg. } I_e = 0.85 I_m + 0.15(I_{cont. end}) \quad (3.20b)$$

where I_m is the midspan section moment of inertia and I_{e1} and I_{e2} are the end-section moments of inertia.

In this method, I_e is first determined and the deflection is then calculated by substituting I_e for I_g in the elastic deflection formulas.

3.6.3 *Bilinear computation method*-In graphical form, the load deflection relationship follows Stages I and II of Fig. 3.18. The idealized diagram reflecting the relation between moment and deflection for the I_g and I_{cr} zones is shown in Fig. 3.19.

ACI 318 requires that computation of deflection in the cracked zone in the bonded tendon beams be based on the transformed section whenever the tensile stress f_t in the concrete exceeds the modulus of rupture f_r. Hence, δ_{cr} is evaluated using the transformed I_{cr} utilizing the contribution of the reinforcement in the bilinear method of deflection computation. The cracked moment of inertia can be calculated by the PCI approach for fully prestressed members by means of the

Fig. 3.19-Bilinear moment-defection relationship

Fig. 3.20-Moment-deflection relationship by different I_e *methods. Point A:prestress camber minus dead load deflection; Point B: zero defection; Point C: decompression (Branson and Shaik 1985, ACI SP-86)*

$$I_{cr} = n_p A_{ps} d_p^2 (1 - 1.6\sqrt{n_p \rho_p} = Cbd_p^3 \qquad (3.21a)$$

where C can be obtained from Table 3.3 and $n_p = E_{ps}/E_c$ and $\rho_p = A_{ps}/bd$. If nonprestressed reinforcement is used to carry tensile stresses, namely, in "partial prestressing," Eq. 3.21a is modified to give

$$I_{cr} = (n_p A_{ps} d_p^2 + n_s A_s d^2)(1 - 1.6\sqrt{n_p \rho_p + n_s \rho}) \qquad (3.21b)$$

where $n_s = E_s/E_c$ for the nonprestressed steel d = effective depth to center of mild steel or nonprestressed strand steel. Table 3.3 (PCI, 1993) provides coefficients for rapid calculation of cracked moments of inertia.

Fig. 3.19 shows the moment-deflection relationship as defined in Eq. 3.19 where I_e = average moment of inertia for $\delta_{total} = \delta_e + \delta_{cr}$ and where δ_e is the elastic deflection based on the gross moment of inertia I_g. Fig. 3.20 is a detailed moment-deflection plot for the various loading stages (Branson and Shaikh, 1984, 1985) where points A, B, and C refer to the calculation on the live-load deflection increment for a partially prestressed beam. The effective moment of inertia I, was applied using several methods, as detailed with numerical examples in the two indicated references.

3.6.4 *Incremental moment-curvature method*--The analysis is performed assuming two stages of behavior, namely, elastic uncracked stage and cracked stage. Basic elastic mechanics of prestressed sections are used to obtain the two points defining the linear uncracked stage. Actual material properties are used for analysis of the cracked section response.

The cracked moment of inertia can be calculated more accurately from the moment-curvature relationship along the beam span and from the stress and, consequently, strain distribution across the depth of the critical sections. As shown in Fig. 3.21 for strain ϵ_{cr} at first cracking,

$$\phi_{cr} = \frac{\epsilon_{cr}}{c} = \frac{M}{E_c I_{cr}}$$

where ϵ_{cr} is the strain at the extreme concrete compression fibers at first cracking and M is the net moment at

Table 3.3—Moment of inertia of transformed section in prestressed members (PSI *Design Handbook*, fourth edition)

$$I_{cr} = nA_{ps}d_p^2\left(1 - 1.6\sqrt{n\rho_p}\right)$$

$$= n\rho_p\left(1 - 1.6\sqrt{n\rho_p}\right) \times bd_p^3$$

$$= C \text{ (from table)} \times bd_p^3$$

where: $\rho_p = \dfrac{A_{ps}}{bd_p}$, $n = \dfrac{E_s}{E_c}$

$E_s = 28.5 \times 10^6$ psi

$E_c = 33w_c^{1.5}\sqrt{f_c'}$ (ACI Sect. 8.5.1)

$w_c = 145$ lb/ft^3...Normal weight concrete

$w_c = 115$ lb/ft^3...Sand-lightweight concrete

Values of Coefficient, C

| ρ_p	f_c', psi					
	3000	4000	5000	6000	7000	8000
Normal Weight Concrete						
.0005	.0041	.0036	.0032	.0029	.0027	.0026
.0010	.0077	.0068	.0061	.0056	.0052	.0049
.0015	.0111	.0098	.0089	.0082	.0076	.0072
.0020	.0143	.0126	.0115	.0106	.0099	.0093
.0025	.0173	.0153	.0139	.0129	.0120	.0113
.0030	.0201	.0179	.0163	.0151	.0141	.0133
.0035	.0228	.0203	.0185	.0172	.0161	.0152
.0040	.0254	.0226	.0207	.0192	.0180	.0170
.0045	.0278	.0248	.0227	.0211	.0198	.0188
.0050	.0300	.0270	.0247	.0230	.0216	.0205
.0055	.0322	.0290	.0266	.0248	.0233	.0221
.0060	.0343	.0309	.0284	.0265	.0250	.0237
.0065	.0362	.0327	.0302	.0282	.0266	.0253
.0070	.0381	.0345	.0319	.0298	.0281	.0267
.0075	.0398	.0362	.0335	.0314	.0296	.0282
.0080	.0415	.0378	.0350	.0329	.0311	.0296
.0085	.0430	.0393	.0365	.0343	.0325	.0309
.0090	.0445	.0408	.0380	.0357	.0338	.0323
.0095	.0459	.0422	.0393	.0370	.0351	.0335
.0100	.0472	.0435	.0406	.0383	.0364	.0348
Sand-Lightweight Concrete						
.0005	.0056	.0049	.0044	.0040	.0038	.0035
.0010	.0105	.0092	.0083	.0077	.0071	.0067
.0015	.0149	.0132	.0120	.0110	.0103	.0097
.0020	.0190	.0169	.0153	.0142	.0133	.0125
.0025	.0228	.0203	.0185	.0172	.0161	.0152
.0030	.0263	.0235	.0215	.0200	.0187	.0177
.0035	.0296	.0265	.0243	.0226	.0213	.0201
.0040	.0326	.0294	.0270	.0252	.0237	.0224
.0045	.0354	.0320	.0295	.0275	.0260	.0246
.0050	.0381	.0345	.0319	.0298	.0281	.0267
.0055	.0405	.0368	.0341	.0320	.0302	.0288
.0060	.0427	.0390	.0362	.0340	.0322	.0307
.0065	.0448	.0411	.0382	.0360	.0341	.0325
.0070	.0466	.0430	.0401	.0378	.0359	.0343
.0075	.0484	.0447	.0419	.0395	.0376	.0359
.0080	.0499	.0464	.0435	.0412	.0392	.0375
.0085	.0513	.0479	.0451	.0428	.0408	.0391
.0090	.0526	.0493	.0465	.0442	.0422	.0405
.0095	.0537	.0506	.0479	.0456	.0436	.0419
.0100	.0547	.0518	.0492	.0469	.0449	.0432
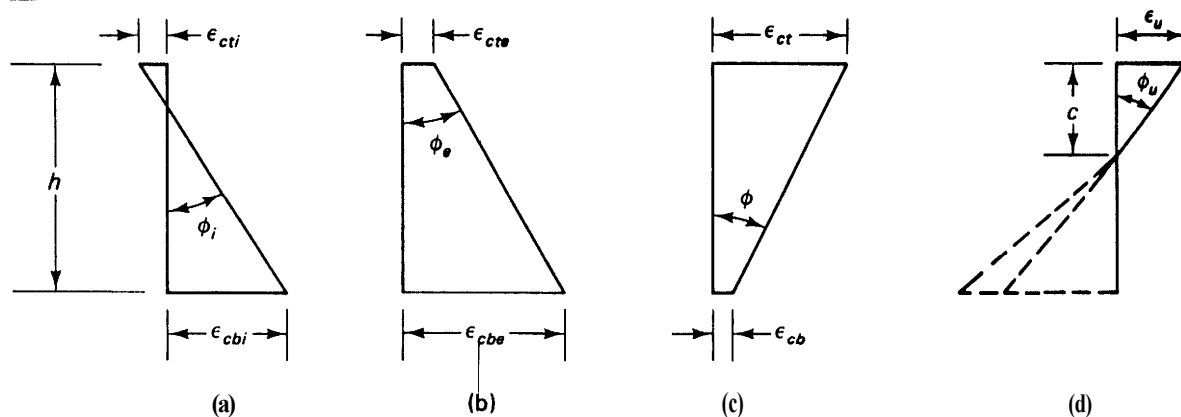
Fig. 3.21-Strain distribution and curvature at controlling loading stages (Nawy, 1989): a) initial prestress; b) effective prestress after losses; c) service load; d) failure. If section is cracked at service load, Fig. 3.21c changes to reflect tensile strain at the bottom fibers (see Fig. A3.2)

the cracking load (see Eq. 3.18), including the pre-stressing primary moment M_1, about the centroid (center-of-gravity of the concrete) of the section under consideration. Eq. 3.21 can be rewritten to give

$$I_{cr} = \frac{Mc}{E_c \epsilon_{cr}} = \frac{Mc}{f}$$

where f is the concrete stress at the extreme compressive fibers on the section. The analysis is performed assuming two stages of behavior, namely, elastic uncracked stage and cracked stage. Basic elastic mechanics of prestressed sections are used to obtain the two points defining the linear uncracked stage. Actual material properties are used for analysis of the cracked section response.

In summary, the distribution of strain across the depth of the section at the controlling stages of loading is linear, as is shown in Fig. 3.21, with the angle of curvature dependent on the top and bottom concrete extreme fiber strains ϵ_{ct} and ϵ_{cb} and whether they are in tension or compression. From the strain distribution, the curvature at the various stages of loading can be expressed as follows:

1) Initial prestress:

$$\phi_i = \frac{\epsilon_{cbi} - \epsilon_{cti}}{h}$$ (3.22a)

2) Effective prestress after losses:

$$\phi_e \frac{\epsilon_{cbe} - \epsilon_{cti}}{h}$$ (3.22b)

3) Service load:

$$\phi = \frac{\epsilon_{ct} - \epsilon_{cb}}{h}$$ (3.22c)

4) Failure:

$$\phi_u = \frac{\epsilon_u}{c}$$ (3.226)

A plus sign for tensile strain and a minus sign for compressive strain are used, so that the bottom fiber strains in Fig. 3.21c can be in tension or compression using the appropriate sign (see Fig. A3.3 of Ex. A3.2).

Fig. 3.21 shows the general strain distribution and curvature at the controlling loading stages defined in Eq. 3.22, in this case an uncracked section at service load. If the section is cracked, as in Ex. A3.2, Fig. 3.21c should reflect tensile strain at the bottom fibers using a plus sign for tensile strain and a minus for compressive strain. It is important to recognize that curvatures ϕ at various load levels and at different locations along the span can be specifically evaluated if the beam is divided into enough small segments. Because of the higher speed personal computers today, a beam may be easily divided into 40 or 100 sections. The trapezoidal rule would be accurate enough, with the only penalty being a few more milli-seconds in computer execution time.

3.7-Long-term deflection and camber evaluation in pre-stressed beams

If the external load is sustained on the prestressed members, the deflection increases with time, mainly be-cause of the effects of creep and shrinkage of concrete and relaxation of the prestressing reinforcement. In such cases, the total deflection can be separated into two parts: the instantaneous elastic part (previously discussed) and the additional long-term part that increases with time.

Several methods are available for camber and deflec-tion calculation, some more empirical and others more refined. This chapter presents in detail the simplified PCI multipliers method even though it is sometimes more conservative, since it is the most commonly used for

Table 3.4-PCI multipliers C, for long-term camber and deflection

	Without composite topping	With composite topping
At erection: 1) Deflection (downward) component-apply to the elastic deflection due to the member weight at release of prestress	1.85	1.85
2) Camber (upward) component-apply to the elastic camber due to prestress at the time of release of prestress	1.80	1.80
Final: *3)* Deflection (downward) component-apply to the elastic deflection due to the member weight at release of prestress	2.70	2.40
4) Camber (upward) component-apply to the elastic camber due to prestress at the time of release of prestress	2.45	2.20
5) Deflection (downward)--apply to the elastic deflection due to the superimposed dead load only	3.00	3.00
6) Deflection (downward)-apply to the elastic deflection caused by the composite topping	—	2.30

Where C_1 = multiplier; A_s = area of nonprestressed reinforcement and A_{ps} = area of prestressed strands.

deflection and camber calculation in normal size and span prestressed beams such as double tees, hollow core slabs and AASHTO type beams. Numerical examples on its use are given in the appendix.

It is worthwhile noting that prestressed building products generally comply with the deflection limits in Table 9.5(b) of ACI 318-89. Industry and local practices, however, may be more stringent, such as requiring that double tee or hollow core slabs should have a slight camber under half of the design live load. It is also good practice to never allow a calculated bottom tension stress due to sustained loads.

Other selected methods are briefly described and reference made to existing literature for details on camber and deflection design examples in those references, that the designer can choose for refined solutions.

3.7.1 *PCI multipliers method*-The determination of long-term camber and deflection in prestressed members is more complex than for nonprestressed members due to the following factors:

1. The long-term effect of the variation in prestressing force resulting from the prestress losses.

2. The increase in strength of the concrete after release of prestress and because the camber and deflection are required to be evaluated at time of erection. The PCI *Design Handbook,* fourth edition, provides a procedure wherein the short term deflections (calculated using conventional procedures) are multiplied by factors (multipliers) for various stages of the deflection (erection, final), for deflections due to prestress dead and applied loads and for composite and noncomposite sections to obtain long term deflections. These multipliers vary from 1.80 to 3.00, as shown in Table 3.4 (PCI *Design Handbook,* 4th ed., 1993).

Shaikh and Branson (1970) propose that substantial reduction can be achieved in long-term deflections by the addition of nonprestressed mild steel reinforcement.

When such reinforcement is used, a reduced multiplier C_2 can be used as follows, to reduce the values in Table 3.4,

$$C_2 = \frac{C_1 + A_s/A_{ps}}{1 + A_s/A_{ps}} \qquad (3.23a)$$

and

$$\delta_{lt} = C_2 \delta_{st} \qquad (3.23b)$$

3.7.2 *Incremental time-steps method*-The incremental time-steps method is based on combining the computations of deflections with those of prestress losses due to time-dependent creep, shrinkage, and relaxation. The design life of the structure is divided into several increasingly larger time intervals. The strain distributions, curvatures, and prestressing forces are calculated for each interval together with the incremental shrinkage, creep, and relaxation losses during the particular time interval.

The procedure is repeated for all subsequent incremental intervals, and an integration or summation of the incremental curvatures is made to give the total time-dependent curvature at the particular section along the span. These calculations should be made for a sufficient number of points along the span to be able to determine with reasonable accuracy the form of the moment-curvature diagram.

The general expression for the total curvature at the end of a time interval can be expressed as

$$= \frac{P_1 e_x}{E_{ci} I_c} + \sum_0^t (P_{n-1} - P_n) \frac{e_x}{E_c I_c} \qquad (3.24)$$
$$- \sum_0^t (C_n - C_{n-1}) P_{n-1} \frac{e_x}{E_c I_c}$$

where
  P_i = initial prestress (at transfer) before losses
  e_x = eccentricity of tendon at any section along the span
  Subscript $n-1$ = beginning of a particular time step
  Subscript n = end of the aforementioned time step
  C_{n-1}, C_n = creep coefficients at beginning and end, respectively, of a particular time step
  $P_n - P_{n-1}$ = prestress loss at a particular time interval from all causes

Obviously, this elaborate procedure is usually justified only in the evaluation of deflection and camber of slender beams or very long-span bridge systems such as segmental bridges, where the erection and assembly of the segments require a relatively accurate estimate of deflections. From Eq. 3.24, the total deflection at a particular section and at a particular time t is

$$\delta_x = \phi_t k \ell^2 \qquad (3.25)$$

where k is a function of the span and geometry of the section and the location of prestressing tendon.

It should be stated that because of the higher speed microcomputers today, a large span structure can be easily evaluated for deflection and camber using this incremental numerical summation method. Detailed examples are given in the textbooks by Nawy, 1989 and Nilson, 1987.

The total camber (↑) or deflection (↓) due to the prestressing force can be obtained from the expression $\phi_T = \phi_{n-1} + \phi_n$ so that

$$\delta_T = \phi_T k \ell^2 \qquad (3.26)$$

where k is an aging coefficient which varies from 0 to 1.0 but may be taken as 0.7 to 0.8 for most applications.

Several investigators have proposed different formats for estimating the additional time-dependent deflection $\Delta\delta$ from the moment curvature relationship modified for creep. Tadros and Dilger recommend integrating the modified curvature along the beam span, while Naaman expressed the long-term deflection in terms of midspan and support curvatures at a time interval t (Tadros, 1983; Naaman, 1985). As an example, Naaman's expression gives, for a parabolic tendon,

$$\Delta\delta(t) = \phi_1(t)\frac{\ell^2}{8} = [\phi_2(t) - \phi_1(t)]\frac{\ell^2}{48} \qquad (3.27)$$

where
  $\phi_1(t)$ = midspan curvature at time t
  $\phi_2(t)$ = support curvature at time in which

$$\phi(t) = \frac{M}{E_{ce}(t)I_c} \qquad (3.28)$$

where
  $E_{ce}(t)$ = time adjusted modulus

$$E_{ce}(t) = \frac{E_c(t_1)}{1 + \chi C_c(t)} \qquad (3.29)$$

in which
  $E_c(t1)$ = modulus of elasticity of concrete at start of interval and χ is an aging coefficient
  $C_c(t)$ = creep coefficient at end of time interval

3.7.3 *Approximate time-steps method*-The approximate time-steps method is based on a simplified form of summation of constituent deflections due to the various time-dependent factors. If C_u is the long-term creep coefficient, the curvature at effective prestress P_e can be defined as

$$\phi_e = -\frac{P_i e_x}{E_c I_c} + (P_i - P_e)\frac{e_x}{E_c I_c}$$
$$- \left(\frac{P_i + P_e}{2}\right)\frac{e_x}{E_c I_c} C_u \qquad (3.30)$$

The final deflection under P_e is

$$\delta_{et} = -\delta_i + (\delta_i - \delta_e) - \left(\frac{\delta_i + \delta_e}{2}\right)C_u \quad (3.31a)$$

or

$$\delta_{et} = \delta_e - \left(\frac{\delta_i + \delta_e}{2}\right)C_u \qquad (3.31b)$$

Adding the deflection δ_D due to self-weight and superimposed dead load δ_{SD}, which are affected by creep, together with the deflection due to live load δ_L gives the final time-dependent increase in deflection due to prestressing and sustained loads, given by

$$\Delta\delta = -\left(\frac{\delta_i + \delta_e}{2}\right)C_u + (\delta D + \delta_{SD})(1 + C_u) \qquad (3.32a)$$

and the final total net deflection becomes

$$\delta_T = -\delta_e - \left(\frac{\delta_i + \delta_e}{2}\right)C_u + (\delta_D + \delta_{SD})(1 + C_u) + \delta_L$$
$$(3.32b)$$

The approximate time-steps method originally presented by Branson and Ozell, 1961, and ACI 435, 1963, tends to yield in most cases comparable results to the PCI multiplier method. Detailed examples are given in the text books by Branson, 1977; Libby, 1984; Nilson,

1987; and Nawy, 1989.

3.7.4 *Axial strain and curvature method (Ghali-Favre)-* This approach gives a procedure for the analysis of instantaneous and long-term stresses and strains in reinforced concrete cross-sections, with or without prestressing but considering cracking. Slope of the strain diagram is set equal to curvature (see Section 2.6.3.2, Chapter 2), which can be used to calculate the change in deflection. The method does not require determination of prestress losses. It introduces, as in the Naaman approach, an aging coefficient that adjusts the modulus of concrete E_c between time limits t_o and t. After cracking, the concrete in tension is ignored and only the concrete in the compression zone of depth c is included in calculating the properties of the transformed section.

A cross-section provided with prestressed and non-prestressed reinforcement of areas A_{ps} and A_s respectively, is subjected at time t_0 to a flexural moment M and to normal force N. Analysis is required for the stresses and strains which occur at the initial time t_0 and at $t >$ to after development of creep and shrinkage in the concrete and relaxation in the prestressed steel reinforcement. M and N are taken as the internal moments and forces due to all external forces plus the prestressing introduced at time t_0. The transformed section is composed of the area of concrete and the **areas** A_{ps} **and** A_s of the reinforcement multiplied by the respective modular ratios, n_{ps} or n; where

$$n_{ps} \ or \ n \ = \ \frac{E_{ps} \ or \ E_s}{E_c(t_0)} \qquad (3.33a)$$

with E_{ps} and E_s being the moduli of elasticity of prestressed and nonprestressed reinforcement and $E_c(t_0)$ the modulus of concrete at t_0.

The term "age-adjusted" transformed section defines a section composed of the area of concrete plus the steel areas A_{ps} and A_s multiplied by the respective age adjusted moduli

$$\bar{n}_{ps} \ or \ \bar{n} \ = \frac{E_{ps} \ or \ E_s}{\bar{E}_c(t, \ t_0)} \qquad (3.33b)$$

and $\bar{E}_c(t, t_0)$ is the age-adjusted modulus of elasticity of concrete. It can be used to relate stress to strain in the same way as the conventional modulus of elasticity in order to determine the total strain, consisting of the sum of the instantaneous and creep strains due to a stress change introduced gradually between t_0 and t. The age-adjusted modulus, as in Eq. 3.29 (Naaman, 1985), is given by:

$$\bar{E}_c(t, \ t_0) \ = \ \frac{E_c(t, \ t_0)}{1 + \chi C_t} \qquad (3.33c)$$

where χ is the aging coefficient, usually assumed equal

to 0.8 and C_t is the creep coefficient. Values of χ and C_t are given as functions of t_0 and t in ACI 209-92. After cracking, the concrete in tension is ignored and only the area of concrete in the compression zone of depth, c, is included in calculating the properties of the trasformed sections. This method is detailed in Ghali and Favre, 1986; Ghali (1986); and Elbadry and Ghali (1989).

3.7.5 *Prestress loss method-*It is assumed in this method that sustained dead load due to self weight does not produce cracking such that the effects of creep, shrinkage, and relaxation are considered only for uncracked cross sections. Additional stress in the concrete caused by live load may result in cracking when the tensile strength of concrete is exceeded. Whether cracking occurs, and the extent to which it occurs when the live load is applied depend upon the magnitude of the prestress losses.

The method recommends stress loss coefficients due to creep, shrinkage and relaxation such that the change in the prestressing force ΔP_c is given by the following:

$$\delta P_c \ = \ -A_{ts}(\Delta f_{pSH} + \Delta f_{pCR} \ - \ A_{ps}\Delta f_{pR}) \quad (3.34a)$$

A set of multipliers, as listed in Table 3.5, are applied to the deflections due to initial prestress, member self weight, superimposed dead load, and time-dependent prestress loss in a similar fashion to the multipliers used in the PCI multipliers method. Thus, total deflection after prestress loss and before application of live load becomes

$$\delta_{TD} = (1 \ + \ C_u)(\delta_D + \delta_i) + \ (1 \ + \ C_u')\delta_{SD} + \\ (1 \ + \ \chi C_u)\delta_{PL} \qquad (3.34b)$$

where

δ_{TD} = total deflection before live load application
δ_D = self-weight deflection
δ_i = initial prestress camber
δ_{SD} = superimposed dead load deflection, and
δ_{PL} = prestress loss deflection

C_u, C_u', χ are taken from Table 3.5. The modulus of elasticity to be used in calculating all of the deflection components due to the causes considered above is E_{ci}, which corresponds to the age of the concrete at prestress transfer, except for the superimposed dead load which is applied at a later age, for which the corresponding elasticity modulus should be used. Examples on the use of this method are given in Tadros and Ghali (1985).

3.7.6 *CEB-FIP model code method-*The CEB-FIP code presents both detailed and simplified methods for evaluating deflection and camber in prestressed concrete elements, cracked or uncracked. The simplified method is discussed in Sec. 2.6.3.1. Details of this approach as well as its code provisions on serviceability are given in CEB-FIP (1990).

Table 3.5-Time-dependent multipliers in Tadros and Ghali, 1985

Load condition	A-Erection time		B-Final time		C = B -A-Long term	
	Formula	Average*	Formula	Average*	Formula	Average*
Initial prestress P_{co}	$1 + C_a$	1.96	$1 + C_u$	2.88	$C_u - C_a$	0.92
Prestress loss ΔP_c	$\alpha_a(1 + \chi C_a)$	1.00	$1 = \chi C_u$	2.32	$1 - \alpha_a + \chi$ $(C_u - \alpha_a C_a)$	1.32
Member weight	$1 + C_a$	1.96	$1 + C_u$	2.88	$C_u - C_a$	0.92
Superimposed dead load†	0	0	$1 + C_u'$	2.50	$1 + C_u'$	2.50
Superimposed dead load‡	1.00	1.00	$1 + C_u'$	2.50	C_u'	1.50

Note: Time-dependent δ = elastic δ x multiplier.
* Assuming $C_a = 0.96$; $C_u = 1.88$; $C_u' = 1.50$; $\chi = 0.7$; and $\alpha_a = 0.6$, which approximately correspond to average conditions with relative humidty = 70 percent, concrete age at release = 1 to 3 days and erection at 40 to 60 days.
† Applied after nonstructural elements are attached to member.
‡ Applied before nonstructural elements are attached to member.

APPENDIX A3

Example A3.1

Evaluate the total immediate elastic deflection and long-term deflection of the beam shown in Fig. A3.1 using (a) applicable moment of inertia I_g or I_e computation, (b) incremental moment-curvature computation. The beam (Nawy, 1989) carries a superimposed service live load of 1100 plf (16.1 kN/m) and superimposed dead load of 100 plf (1.5 kN.m). It is bonded pretensioned, with A_{ps} - fourteen ½ in. diameter seven wire 270 ksi (f_{pu} = 270 ksi = 1862 MPa) stress-relieved tendons = 2.142 in.² Disregard the contribution of the nonprestressed steel in calculating the cracked moment of inertia in this example. Assume that strands are jacked suficiently so that the initial prestress resulting in the P_i at transfer is 405,000 lb. Assume that an effective prestress P_e of 335,000 lb after losses occurs at the first external load application of 30 days after erection and does not include all the time-dependent losses.

Data:

a) Geometrical properties

A_s = 782 in.² (5045 cm²)
I_c = 169,020 in.⁴ (7.04 x 10⁶ cm⁴)
S_b = 4803 in.³ $6.69 x 104 cm³)
S_t = 13,194 in.
W_D = 815 plf, self weight
W_{SD} = 100 plf (91.46 kN/m)
W_L = 1100 plf (16.05 kN/m)

Eccentricities:
e_c = 33.14 in.
e_e = 20.00 in.

Dimensions from neutral axis to extreme fibers:
c_b = 35.19 in.
c_t = 12.81 in.
A_{ps} = 14 x 0.153 = 2.14 in.² (13.8 cm²)

P_i = 405,000 lb (1800 kN) at transfer
P_e = 335,000 lb (1480 kN)

b) Material properties

V/S = 2.33 in.
R H = 70 percent
f_c' = 5000 psi
f_{ci}' = 3750 psi
f_{pu} = 270,000 psi (1862 MPa)
f_{pi} = 189,000 psi (1303 MPa)
f_{pe} = 155,000 psi (1067 MPa)
f_{py} = 230,000 psi
E_{ps} = 28.5 x 10⁶ psi (196 x 10⁶ MPa)

c) Allowable stresses

f_{ci} = 2250 psi
f_c = 2250 psi
f_{ti} = 184 psi (support)
f_t = 849 psi (midspan)

Solution (a)

Note: All calculations are rounded to three significant figures, except geometrical data from the PCI *Design Handbook* (4th edition)

1-Midspan section stresses

e_c = 33.14 in. (872 mm)

Maximum self-weight moment

$$M_D = \frac{815(65)^2}{8} \times 12 = 5,170,000 \text{ in.-lb}$$

a) At transfer, calculated fiber stresses are:

$$f_t = \frac{P_i}{A_c}\left(1 - \frac{e_c c_t}{r^2}\right) - \frac{M_D}{S_t}$$

$$= \frac{405,000}{782}\left(1 - \frac{33.14 \times 12.81}{216}\right) - \frac{5,170,000}{13,194}$$
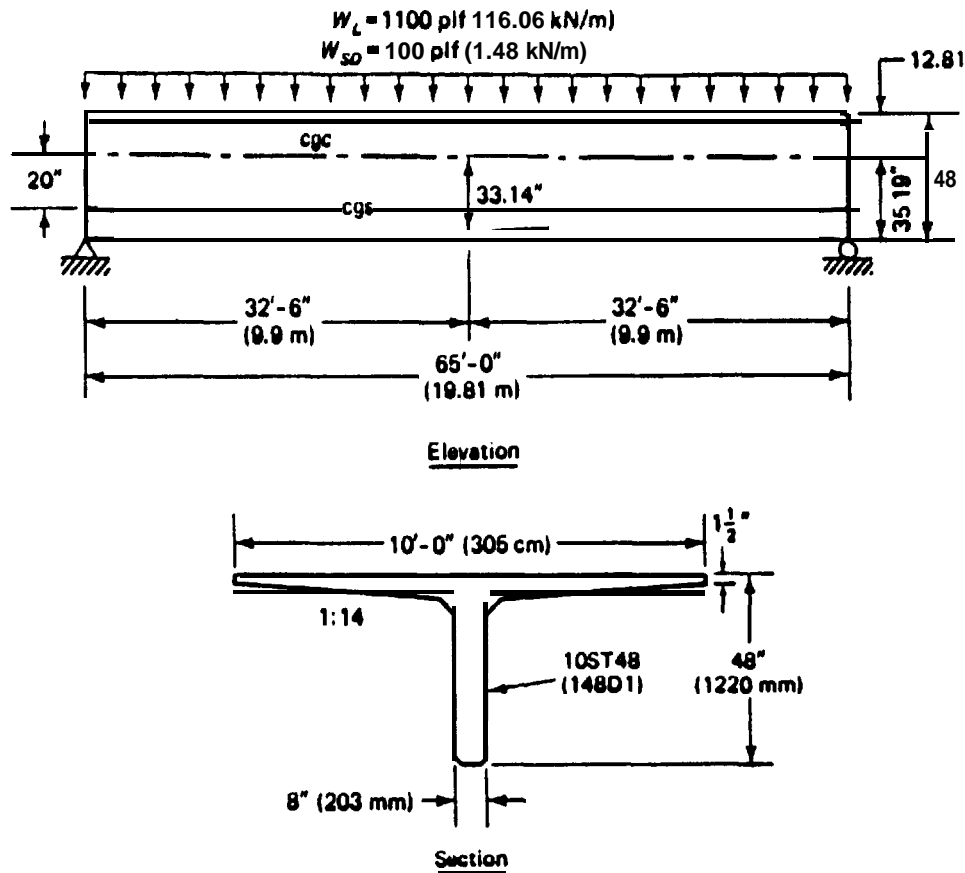
Fig. A3.1-Noncomposite beam geomety Example A3.1 (Nawy, 1989. Courtesy Prentice Hall)

$$= +500 - 392 = 108 \text{ psi } (T) < 184 \text{ psi, OK}$$

$$f_b = -\frac{P_i}{A_c}\left(1 + \frac{e_c c_t}{r^2}\right) + \frac{M_D}{S_b}$$

$$= \frac{405,000}{782}\left(1 + \frac{33.14 \times 35.19}{216}\right) + \frac{5,170,000}{4803}$$

$$= -3310 + 1080 = -2230 \text{ psi} < 2250 \text{ psi, OK}$$

b) At service load

$$M_{SD} = \frac{100(65)^2\,12}{8} = 634,000 \text{ in.-lb (72 kN-m)}$$

$$M_L = \frac{1100(65)^2\,12}{8} = 6,970,000 \text{ in.-lb (788 kN-m)}$$

Live-load $f_t = \dfrac{6,970,000}{13.194} = -530 \text{ psi } (C)$

Live-load $f_b = \dfrac{6,970,000}{4803} = 1450 \text{ psi } (T)$

Total moment $M_r = MD + MSD + M_L$
$= 5,170,000 + 7,610,000$
$= 12,800,000 \text{ in-lb. (1443 kN-m)}$

$$f_t = -\frac{P_e}{A_c}\left(1 - \frac{ec_t}{r^2}\right) - \frac{M_T}{S_t}$$

$$= -\frac{335,000}{782}\left(1 - \frac{33.14 \times 12.81}{216}\right) - \frac{12,800,000}{13,194}$$

$$= +413 - 970 \approx -560 \text{ psi} < f_c = -2250 \text{ psi, OK}$$

$$f_b = -\frac{P_e}{A_c}\left(1 + \frac{ec_b}{r^2}\right) + \frac{M_T}{S_b}$$

$$= \frac{335,000}{782}\left(1 + \frac{33.14 \times 35.19}{216}\right) + \frac{12,800,00}{4803}$$

$$= -2740 + 2670 = -70 \text{ psi } (C), \text{ OK}$$

Hence, the section is uncracked and the gross moment of inertia $I_g = 169,020 \text{ in.}^4$ has to be used for deflection

Summary of fiber stresses (psi)

	Midspan		Support	
	f_t	f_b	f_t	f_b
Prestress P_i only	+500	-3310	+100	-2200
At transfer and W_D	+108	-2230	+100	-2200
At service load	-560	-70	+80	-1810

1 psi = 6.895 MPa

calculation.

2-Support section stresses
$e_e = $　20 in.
Follow the same steps as in the midspan section, with the moment $M = 0$. A check of support section stresses at transfer gave stresses below the allowable, hence O.K.

3-Deflection and camber calculation at transfer
From basic mechanics or from Table 3.1, for $a = \frac{1}{2}$, the camber at midspan due to a single harp or depression of the prestressing tendon is

$$\delta\uparrow = \frac{P\,e_c\,l^2}{8EI} + \frac{P(e_e - eJI^*}{24EI}$$

So

$$E_{ci} = 57,000\sqrt{f_{ci}'} = 57,000\sqrt{3750}$$
$$= 3.49 \times 10^6 \text{ psi (24.1 MPa)}$$

$$E_c = 57,000\sqrt{f_c'} = 57,000\sqrt{5000} = 4.03 \times 10^6 \text{ psi}$$
$$(27.8 \text{ MPa})$$

$$\delta_{pi}\uparrow \frac{405,000 \times 33.14 \times (65 \times 12)^2}{8 \times 3.49 \times 10^6 \times 169,020}$$

$$+ \frac{405,000 \times (20 - 33.14)(65 \times 12)^2}{24 \times 3.49 \times 10^6 \times 169,020}$$

$$= -1.73 + 0.23 = -1.50 \text{ in. (38 m)}$$

This upward deflection (camber) is due to prestress only. The self-weight per inch is $815/12 = 67.9$ lb/in., and the deflection caused by self-weight is $\delta_D\downarrow = 5wl^4/384EI$, or

$$\delta_D = 5 \times 67.9(65 \times 12)^2/384 \times 3.49 \times 10^6 \times 169,020$$
$$= 0.55 \text{ in.}4$$

Thus, the net camber at transfer is -1.50 $\uparrow$ + 0.55 = -0.95 in.$\uparrow$ (24 mm).

4-Total immediate deflection at service load of uncracked beam
a) Superimposed dead load deflection:

using $E_c = 4.03 \times 10^6$ psi

$$\delta_{SD} = 0.55\frac{E_{ci}}{E_c}\left(\frac{100}{815}\right) = 0.55\left(\frac{3.49}{4.03}\right)\left(\frac{100}{815}\right)$$

$$= 0.06 \text{ in. (1.5 mm)} \downarrow$$

b) Live load deflection

$$\delta_L \cdot \frac{5wl^4}{384E_cI_c} = \frac{5(1100)(65 \times 12)^4}{384 \times 4.03 \times 10^6 \times 169,020} \times \frac{1}{12}$$

$$= 0.65 \text{ in.} \downarrow$$

A summary of the instantaneous deflection due to prestress, dead load and live load is as follows:

Camber due to initial prestress= 1.50 in. (38 mm) $\uparrow$
Deflection due to self weight= 0.55 in. (14 mm) $\downarrow$
Deflection due to super-
　imposed dead load= 0.06 in. (2 mm) $\downarrow$
Deflection due to live load= 0.65 in. (17 mm) $\downarrow$
Net deflection at transfer
　= -1.50 + 0.55= -0.95 in. $\downarrow$

In addition to the immediate deflections, there will be additional long-term deflections due to creep and prestress loss after erection. If deflection due to prestress loss from the transfer stage to erection at 30 days is considered, reduced camber is

$$= 1.5\left(\frac{405,000 - 335,000}{405,000}\right)$$

$$= 1.5\left(\frac{75,000}{405,000}\right) = 0.26 \text{ in.} \downarrow$$

Hence, camber only at erection (30 days) can be reasonably assumed

$$= 1.50 - 0.26 = 1.24 \text{ in.} \uparrow$$

Solution (b)
Alternate solution by incremental moment curvature method

P_e at 30 days after transfer is 335,000 lb. So 30 days'

prestress loss $\Delta P = P_i - P_e = 405,000 - 335,000$
$= 70,000$ lb (324 kN)

Strains at transfer due to prestressing
E_{ci} at 7 days $= 3.49 \times 10^6$ psi
(i) Due to prestressing force (P_i)
Midspan: $f_t = +500$ psi
$\qquad f_b = -3310$ psi

$$\epsilon'_c = \frac{+500}{3.49 \times 10^6} = +143 \times 10^{-6} \text{ in./in.}$$

$$\epsilon_{cb} = -949 \times 10^{-6} \text{ in./in.}$$

Support: $f_t = +100$ psi
$\qquad f_b = -2200$ psi
$\qquad \epsilon_{te} = +28 \times 10^{-6}$ in./in.
$\qquad \epsilon_{eb} = -631 \times 10$" in./in.

(1 psi = 6.895 MPa)

(ii) Due to prestressing and self-weight $(P_i + W_D)$
Midspan: $f_t = +108$ psi $\quad \epsilon'_c = 31 \times 10^{-6}$ in./in.
$\qquad f_b = -2230 \qquad \epsilon_{cb} = -640 \times 10^{-6}$ in./in.
Support: same as in (i)

Strain change due to prestress loss
$$-\Delta P = 70,000 \text{ lb}$$

$$E_{ci} = 3.49 \times 10^{-6} \text{ psi}$$

Midspan section:

$$\Delta f_t = -\frac{(-\Delta P)}{A_c}\left(1 - \frac{ec_t}{r^2}\right) = +\frac{70,000}{782}\left(1 - \frac{33.14 \times 12.81}{216}\right)$$
$$= -86 \text{ psi } (C)$$

$$\Delta\epsilon_{tc} = \frac{-86}{3.49 \times 10^6} = -25 \times 10^{-6} \text{ in./in.}$$

$$\Delta f_b = -\frac{(-\Delta P)}{A_c}\left(1 + \frac{ec_b}{r^2}\right) = +\frac{70,000}{782}\left(1 + \frac{33.14 \times 35.19}{216}\right)$$
$$= 573 \text{ psi } (T)$$

$$\Delta\epsilon_{cb} = \frac{573}{3.49 \times 10^6} = +164 \times 10^{-6} \text{ in./in.}$$

Support section:

$$\Delta f_t = -\frac{-\Delta P}{A_c}\left(1 - \frac{ec_t}{r^2}\right) = +\frac{70,000}{728}\left(1 - \frac{20 \times 12.81}{216}\right)$$
$$= -17 \text{ psi } (C)$$

$$\Delta\epsilon_{te} = \frac{-17}{3.49 \times 10^6} = -5 \times 10^{-6} \text{ in./in.}$$

$$\Delta f_b = -\frac{\Delta P}{A_c}\left(1 - \frac{ec_b}{r^2}\right) = +\frac{70,000}{782}\left(1 + \frac{20 \times 35.19}{216}\right)$$
$$= 381 \text{ psi } (T)$$

$$\Delta\epsilon_{cb} = \frac{+381}{3.49 \times 10^6} = +109 \times 10^{-6} \text{ in./in.}$$

Superimposing the strain at transfer on the strain due to prestress loss gives the strain distributions at service load after prestress loss due to prestress only, as shown in Fig. A3.2.
From Fig. A3.2:

Midspan curvature

$$\phi_c = \frac{-785 - 118}{48} \times 10^{-6} = -18.8 \times 10^{-6} \text{ rad/in.}$$

Support curvature

$$\phi_e = \frac{-522 - 23}{48} \times 10^{-6} = -11.4 \times 10^{-6} \text{ rad/in.}$$

From Table 3.2, for $a = \ell/2$, the beam camber after losses due only to P_e is

$$\delta_e \uparrow = \phi_c \left(\frac{\ell^2}{8}\right) + (\phi_e - \phi_c)\frac{\ell^2}{24}$$

$$= -18.8 \times 10^{-6} \frac{(65 \times 12)^2}{8} + (-11.4 + 18.8)$$

$$\times 10^{-6} \frac{(65 \times 12)^2}{24}$$

$$= -1.24 \text{ in.} \uparrow \text{ (32 mm) (camber)}$$

which is identical to the prestressing camber value of $(-1.50 + 0.26) = 1.24$ in.$\uparrow$ in the previous solution.

5-Long term deflection (camber)
Using the PCI multipliers method for calculating deflection at construction erection time (30 days) and at the final service load deflection (5 years) the following are the tabulated values (Nawy, 1989) of long-term deflection and camber obtained using the applicable PCI multipliers in Table 3.3.
If the section is composite after erection, I_{comp} has to be used in calculating δ_L, I_{comp} should also be used in calculating δ_{SD} if the beam is shored during the placement of the concrete topping.
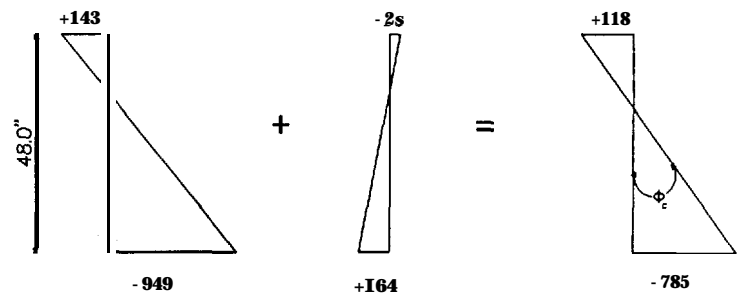
(a) Midspan Section Strains ϵ_c x 10^{-6} rad\in.
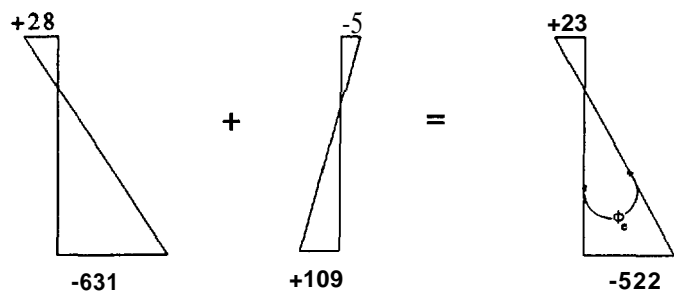
(b) Support Section Strains ϵ_e x 10^{-6} rad\in.

Fig. A3.2-Strain distribution across section depth at prestress transfer in Ex. A3.1)

PCI multipliers from Table 3.3

Load	Transfer δ_p (in.)	Multiplier	Erection δ_{er} (in.)	Multiplier (noncomposite)	Final δ_{net} (in.)
	(1)		(2)		(3)
Prestress	1.50 ↑	1.80	2.70 ↑	2.45	3.68 ↑
W_D	0.55 ↓	1.85	1.02 ↓	2.70	1.49 ↓
Net δ	0.95 ↑		1.68 ↑		2.19 ↑
W_{SD}			0.06 ↓	3.00	0.18 ↓
Net δ			1.62 ↑		2.01 ↑
W_l					0.65 ↓
Final δ	0.95 ↑		1.62 ↑		1.36 ↑

If mild steel reinforcement A_s was also used in this prestressed beam, the reduced multiplier

$$C_2 = \frac{C_1 + A_s/A_{ps}}{1 + A_s/A_{ps}}$$

would be used (Shaikh and Branson, 1970). The C_1 multiplier is reduced due to the mild steel reinforcement controlling creep propagation or widening of the flexural cracks at long-term loading, hence enhancing stiffness. As an example, assume 3 # 5 bars were also used in the pre-stressed beam,

$$\frac{A_s}{A_{ps}} = \frac{3 \times 0.31}{2.14} = 0.43 \text{ giving } C_2 = 2.01$$

Adjusting the values previously tabulated, the original camber becomes = 3.01 in. ↑ instead of the 3.68 in. ↑ shown in the table. Similar adjustments for all deflection components can be made by applying the relevant correction factor.

Fig. A3.3-Double-tee composite beam in Ex. A3.2

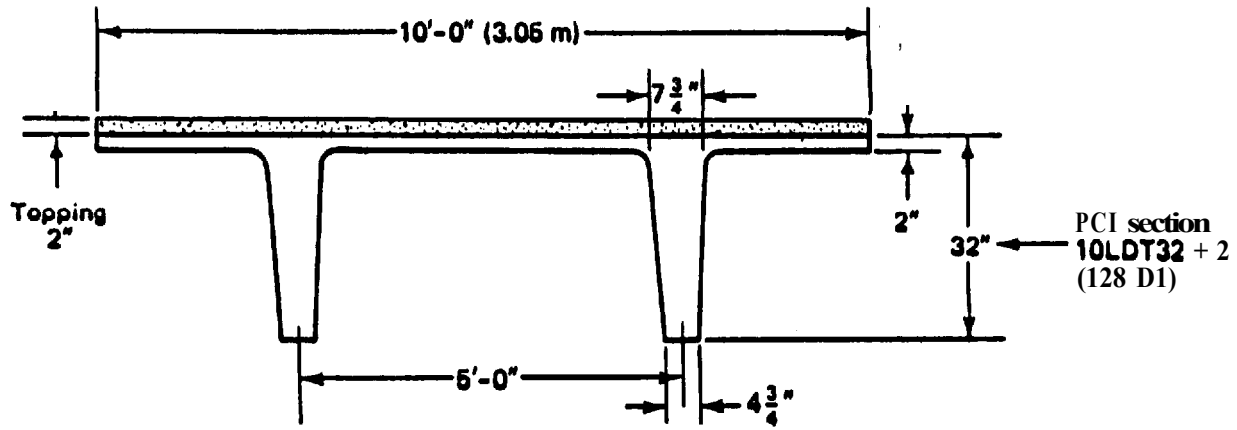|	Noncomposite	Composite
A_c, in.^{2}	615 (3968 cm^2)	855
I_c, in.^{4}	59,720 (24.9 x10^{5}cm^4)	77,118
r^2, in.^{2}	97 (625 cm^2)	90
C_b, in.	21.98 (558 mm)	24.54
C_t, in.	10.02 (255 mm)	9.46
S_b, in.^{3}	2717 (4.5 x 10^{4}cm^3)	3142
S_t, in.^{3}	5960 (9.8 x 10^4 cm^3)	8152
W_D, plf	641 (9.34 kN/m)	891

Example A3.2

A 72-ft (21.9 m) span simply supported unshored roof normal weight concrete composite double-T beam (Fig. A3.3) is subjected to a superimposed topping load W_{SD} = 250 plf (3.65 kN/m) and a service live load W_L = 280 plf (4.08 KN/m). Calculate the camber and deflection of this beam at prestress transfer by (a) the I_e method (b) bilinear method, as well as the time-dependent deflections after 2 in. topping is cast (30 days) and the final deflection (5 years), using the PCI Multipliers method. Given prestress total losses after transfer 18 percent (see table above).

V/S = 615/364 = 1.69 in. (4.3 mm)
RH = 75 percent
Eccentricities e_c = 18.73 in. (476 mm)
        e_e = 12.81 in. (325 mm)
f'_c = 5000 psi (34.5 MPa)
f'_{ci} = 3750 psi (25.7 MPa)
topping f'_c = 3000 psi

f_t at bottom fibers = $12\sqrt{f'_c}$ = 850 psi (5.6 MPa)
A_{ps} = twelve ½ in. dia low-relaxation
      steel depressed at midspan only
f_{pu} = 270,000 psi (1862 MPa), low relaxation
f_{pi} = 189,000 psi (1303 MPa)
f_{PJ} = 200,000 psi (1380 MPa)
E_{ps} = 28.5 x 10^6 psi (19.65 x 10^4 MPa)

Solution:

Note: All calculations are rounded to three significant figures, except geometrical data from the PCI *Design Handbook* (4th ed.).

1-Midspan section stresses

f_{PJ} = 200,00 psi at jacking
f_{pi} assumed = 0.945 f_{PJ} = 189,000 psi at transfer
e_c = 18.73 in. (475 mm)
P_i = 12 x 0.153 x 189,000 = 347,000 lbs

Self-weight moment

$$M_D = \frac{641(72)^2}{8} \times 12 = 4,985,000 \text{ in.-lb}$$

(a) At transfer

$$f^t = -\frac{P_i}{A_c}\left(1 - \frac{e_c c_t}{r^2}\right) - \frac{M_D}{S^t}$$

$$= -\frac{347,000}{615}\left(1 - \frac{18.73 \times 10.02}{97}\right) - \frac{4,980,000}{5960}$$

$= +527 - 836$
$= -309$ psi (C), say 310 psi (C) $< 0.60 f'_c < 0.60$ (3750)
$= 2250$ psi, OK

$$f_b = -\frac{P_i}{A_c}\left(1 + \frac{e_c c_b}{r^2}\right)$$

$$= \frac{347,000}{615}\left(1 + \frac{18.73 \times 21.98}{97}\right) + \frac{4,980,000}{2717}$$

$$= -2960 + 1835$$
$$= -1125 \text{ psi } (C) < -2250 \text{ psi, OK}$$

(b) After unshored slab is cast

At this load level:

f_{pe} = 0.82 f_{pi} = 0.82 x 189,000 = 155,000 psi
P_e = 12 x 0.153 x 155,000 = 285,000 lb.
For the 2 in. slab, W_{SD} = 2/12 x 10 ft x 150 = 250 plf

$$M_{SD} = \frac{250 \ (72)^2}{8} \text{ x } 12 = 1,945,000 \text{ in.-lb}$$

$$M_D + M_{SD} = 4,985,000 + 1,945,000 = 6,930,000 \text{ in.-lb}$$

$$f^t = -\frac{P_e}{A_c}\left(1 - \frac{e_c c^t}{r^2}\right) - \frac{M_D + M_{SD}}{S^t}$$

$$= -\frac{285,000}{615}\left(1 - \frac{18.83 \times 10.02}{97}\right) - \frac{6,930,000}{5960}$$

$$= +433 - 1163 = -730 \text{ psi} < 0.45 f_c' < -2250 \text{ psi, OK}$$

$$f_b = -\frac{P_e}{A_c}\left(1 + \frac{e_c c_b}{r^2}\right) + \frac{M_D + M_{SD}}{S_b}$$

$$= -\frac{285,000}{615}\left(1 + \frac{18.73 \times 21.98}{97}\right) + \frac{6,930,000}{2717}$$

$$= -2430 + 2550 = +120, \text{ psi } (T), \text{ OK}$$

This is a very low tensile stress when the unshored slab is cast and before the service load is applied, $<< 3\sqrt{f_c'}$.

(c) At service load for the precast section

Section Modulus for composite section at the top of the precast section is

$$S_c^t = \frac{77,118}{9.46 - 2} = 10,300 \text{ in.}^3$$

$$M_L = \frac{280(72)^2}{8} \text{ x } 12 = 2,180,000 \text{ in.-lb}$$

$$f^t = -\frac{P_e}{A_c}\left(1 - \frac{e_c c^t}{r^2}\right) - \frac{M_D + M_{SD}}{S^t} - \frac{M_{CSD} + M_L}{S_c^t}$$

M_{CSD} = superimposed dead load = 0 in this case.

$$f^t = -730 - \frac{2,180,000}{10,300}$$

$$= -730 - 211 = -941 \text{ psi } (C), \text{ OK}$$

$$f_b = +120 + \frac{2,180,000}{3142} = +120 + 694$$

$$= +814 \text{ psi } (T) \ (5.4 \text{ MPa}) < f_t = 850 \text{ psi, OK}$$

(d) Composite slab stresses

Precast double-T concrete modulus is

E_c = $57,000\sqrt{f_c'}$ = $57,000\sqrt{5000}$
    = 4.03 x 10^6 psi (2.8 x 10, MPa)

Situ-cast slab Concrete Modulus is

E_c = $57,000\sqrt{3000}$ = 3.12 x 10^6 psi (2.2 x 10^4 MPa)

Modular ratio

$$n_p = \frac{3.12 \times 10^6}{4.03 \times 10^6} = 0.77$$

S_c^t for 2 in. slab top fibers = 8152 in.^{3} from data.
S_{cb} for 2 in. slab bottom fibers = 10,337 in.^{3} from before for top of precast section.

Stress f_{cs}^t at top slab fibers = $n\dfrac{M_L}{S_c^t}$

$$= -0.77 \text{ x } \frac{2,180,000}{8125} = -207 \text{ psi } (C)$$

Stress f_{csb} at bottom slab fibers

$$= -0.77 \text{ x } \frac{2,180,000}{10,337} = -162 \text{ psi } (C)$$

2-Support section stresses

Check is made at the support face (a slightly less conservative check can be made at $50 d_b$ from end).
e_e = 12.81 in.

(a) At transfer

$$f^t = -\frac{347,000}{615}\left(1 - \frac{12.81 \times 10.02}{97}\right) - 0$$

$$= -182 \text{ psi } (C) << -2250 \text{ psi, OK}$$

$$f_b = \frac{347,000}{615}\left(1 + \frac{12.81 \times 21.98}{97}\right) + 0$$

$$= -2200 \text{ psi} < 0.60 f_{ci}' = -2250 \text{ psi, OK}$$

(b) After unshored slab is cast and at service load, the support section stresses both at top and bottom extreme fibers were found to be below the allowable, hence OK.

3-Camber and deflection calculation at transfer

Initial E_{ci} = $57,000\sqrt{3750}$ = 3.49 x 10^6 psi (2.2 x 10^4 MPa).
From before, 28 days E_c = 4.03 x 10^6 psi (2.8 x 10^4 MPa).

Summary of midspan stresses (psi)

	f_t	f_b
Transfer P_e only	+433	-2430
W_D at transfer	-1163	+2550
Net at transfer	-730	+120
External load (W_L)	-211	+694
Net total at service	-941	+814

Due to initial prestress only

$$\delta_i = \frac{P_i e_c l^2}{8E_{ci}I_g} + \frac{P_i(e_e - e_c)l^2}{24E_{ci}I_g}$$

$$= \frac{(-347,000)(18.73)(72 \times 12)^2}{8(3.49 \times 10^6)59,720}$$

$$+ \frac{(-347,000)(12.81 - 18.73)(72 \times 12)^2}{24(3.49 \times 10^6)59,720}$$

$$= -2.90 + 0.30 = -2.6 \text{ in. (66 mm)} \uparrow$$

Self-weight intensity $w = 641/12 = 53.4$ lb/in.

Self-weight $\delta_D = \dfrac{5wl^4}{384E_{ci}I_g}$ for uncracked section

$$= \frac{5 \times 53.4 (72 \times 12)^4}{384(3.49 \times 10^6)59,720} = 1.86 \text{ in. (47 mm)}$$

Thus the net camber at transfer = -2.6 + 1.86 = -0.74 in. (20 mm) ↑

4-Immediate service load deflection
(a) Effective I_e Method
Modulus of rupture

$$f_r = 7.5 \sqrt{f_c'} = 7.5\sqrt{5000} = 530 \text{ psi}$$

f_b at service load = 814 psi (5.4 MPa) in tension (from before).

Hence, the section is cracked and the effective I_e from Eq. 3.19(a) or (b) should be used.

$$d_p = 18.73 + 10.02 + 2 \text{ (topping)} = 30.8 \text{ in. (780 mm)}$$

$$\rho_p = \frac{A_{ps}}{bd_p} = \frac{12(0.153)}{120 \times 30.75} = 4.97 \times 10^{-4}$$

From Eq. 3.21(a),

$$I_{cr} = n_p A_{ps} d_P^2(1 - 1.6\sqrt{n_p \rho_p}) = C b d_p^3$$

where coefficient C can be obtained from Table 3.3.
Use $f_c' = 5000$ psi of the precast section in entering the table as the neutral axis falls within the precast section at $\bar{x} = 3.5$ in. below the top of the composite section.

$C \approx 0.00318$
$\rho_s = 0.000497$
Hence, $I_{cr} = 0.00318 \times 120(30.75)^3 = 11,100$ in.^{3}
$n_p = 28.5 \times 10^6/4.03 \times 10^6 = 7.07$ to be used in Eq. 3-21(a). Equation 3.21(a) gives $I_{cr} = 11,100$ in.^{4}

From Eq. 3.19(c), and the stress values previously tabulated,

$$\frac{M_{cr}}{M_a} = 1 - \frac{f_{TL} - f_r}{f_L} = 1 - \left(\frac{814 - 530}{694}\right) = 0.591$$

$$\left(\frac{M_{cr}}{M_a}\right)^3 = (0.591)^3 = 0.206$$

Hence,
$I_e = 0.206 (77,118) + (1 - 0.206) 11,100$
$\quad = 24,700$ in.^{4}
$W_{SD} = 1/12 (891 - 641) = 20.8$ in./lb
$W_L = (1/12) \times 280 = 23.3$ in/lb

$$\delta_L = \frac{5wl^4}{384E_c I_e} = \frac{5 \times 23.3(72 \times 12)^4}{384(4.03 \times 10^6)24,700}$$

$$= +1.7 \text{ in. (45 mm)} \downarrow \text{ (as an average value)}$$

When the concrete 2 in. topping is placed on the precast section, the resulting topping deflection with $I_g = 59,700$ in.^{4}:

$$\delta_{SD} = \frac{5 \times 20.8(72 \times 12)^4}{384(4.03 \times 10^6)59,700} = 0.63 \text{ in.} \downarrow$$

(b) Bilinear method

$$f_{net} = f_{cb} - 7.5\lambda\sqrt{f_c'} = 814 - 530$$

$$= +284 \text{ psi } (T) \text{ causing cracking}$$

Load	Transfer δ_p, in.	PCI multipliers	δ_{30}, in.	PCI multiplier (composite)	δ_{Final}, in.
	(1)		(2)		(3)
Prestress	-2.60	1.80	-4.68	2.20	-5.71↑
W_D	+1.86	1.85	+3.44	2.40	+4.46↓
	-0.74↑		-1.24↑		-1.25↑
W_{SD}			+0.63↓	2.30	+1.45↓
W_L			+1.88↓		+1.88↓
Final δ	-0.74↑		+1.27↓		+2.07↓

f_L = tensile stress caused by live load alone
= +694 psi (T)

W_{L1} = portion of live load not causing cracking

$$= (f_L - f_{net})\frac{W_L}{f_L} = \frac{694 - 284}{694} \times 280 plf$$
$$= 0.591 \times 280 = 165 \text{ plf} = 13.8 \text{ lb/in.}$$

δ_{L1} due to uncracked I_g

$$\delta_{L1} = \frac{5w_{L1}l^4}{384E_cI_g} = \frac{5 \times 13.8(72 \times 12)^4}{384(4.03 \times 10^6)77,117}$$

$$= 0.32 \text{ in. } \downarrow$$

$W_{L2} = W_L - W_{L1} = 1/12 \ (280-165) = 9.6 \text{ lb/in.}$

$$\delta_{cr} = \frac{5w_{L2}l^4}{384 E_cI_g} = \frac{5 \times 9.6(72 \times 12)^4}{384(4.03 \times 10^6) 11,110}$$

$$= 1.56 \text{ in. } \downarrow$$

Total live load deflection prior to prestress losses =
$\delta_{L1} + \delta_{cr} = 0.32 + 1.56 = 1.88$ in. ↓
From before, $\delta_i = -0.70$
Net short-term deflection prior to prestress loss is
$\delta_{Total} = -0.70 + 1.88 \approx 1.2$ in. ↓

5-Long-term deflection (camber) by PCI multipliers

When the 2 in. concrete topping is placed on the pre-cast section, the resulting topping deflection with $I_g = 59,720$ in.[4] is

$$\delta_{SD} = \frac{5 \times 20.8(72 \times 12)^4}{384(4.03 \times 10^6) 59,720} = +0.63 \text{ in. (16 mm)}$$

Using PCI multipliers at slab topping completion stage (30 days) and at the final service load (5 years), the tabulated deflection values can be gotten from the above table.

Hence, final deflection ≈ 2.1 in (56 mm) ↓.

Allowable deflection = span/l80

$$= \frac{72 \times 12}{180} = 4.8 \text{ in. } > 2.1 \text{ in., OK}$$

CHAPTER 4-DEFLECTION OF TWO-WAY SLAB SYSTEMS*

4.1-Notation
C_u = ultimate creep coefficient
D = plate flexural rigidity per unit width, or dead load
d = effective depth of reinforcement
E = modulus of elasticity
f'_c = compressive strength of concrete
f_r = modulus of rupture
f_y = yield strength of reinforcement
h = plate or slab thickness
I = moment of inertia
k = coefficient
L = live load
M = bending moment
N = number of shored and reshored levels
R = applied load/slab dead load ratio
t = thickness
w, w_u = intensity of transverse load per unit area
x, y = coordinate axes
y_t = distance from neutral axis to extreme tension fiber
v = Poisson's ratio
α = coefficient
δ = deflection
ϕ = curvature
λ = long-time multiplier
$\epsilon_{sh\infty}$ = ultimate shrinkage
ρ = reinforcement ratio

---

* Principle authors: A. Scanlon and C. T. Hsu.

4.2-Introduction

Building Code Requirements for Reinforced Concrete (ACI 318) specifies minimum thickness requirements for control of two-way slab deflections. If the slab thickness equals or exceeds the specified minimum thickness, deflections need not be computed and serviceability in terms of deflection control is deemed to be satisfied.

Experience has shown that, in most cases, the use of ACI minimum thickness equations produces slabs that behave in a satisfactory manner under service loads. ACI 318 does permit a smaller than minimum thickness to be used if deflections are calculated and shown to be within limits specified by the standard. However, the calculation of slab deflections requires careful consideration of a number of factors if realistic estimates of deflections are to be obtained.

This chapter reviews the current state-of-the-art for control of two-way slab deflections. Methods of calculating slab deflections are presented. Effects of two-way action, cracking, creep, and shrinkage are considered. The minimum thickness equations in the current ACI 318 are examined and recent proposals for alternative methods of specifying minimum thickness are reviewed.

4.3-Deflection calculation methods for two-way slab systems

4.3.1 *Immediate deflection of uncracked slabs*-In this section, calculation procedures are given for immediate deflections based on three approaches, namely, classical solutions, simplified crossing beam analogies, and finite element analysis.

4.3.1.1 *Classical solutions*-Immediate deflection of uncracked two-way slab systems loaded uniformly can be determined using plate bending theory for elastic thin plates. Load-deflection response is governed by the plate equation:

$$\frac{\partial^4 \delta}{\partial x^4} + \frac{2\partial^4 \delta}{\partial x^2 \partial y^2} + \frac{\partial^4 \delta}{\partial y^4} = \frac{w}{D} \quad (4.1)$$

where

x,y = orthogonal coordinate axes of the middle surface
δ = deflection of the plate
w = transverse load per unit area
D = flexural rigidity per unit width, $Eh^3/12(1 \cdot v^2)$
E = modulus of elasticity
h = plate thickness
v = Poisson's ratio

The relationship between moments and curvatures is given by

$$\begin{Bmatrix} M_x \\ M_y \\ M_{xy} \end{Bmatrix} = \frac{Eh^3}{12(1 - v^2)} \begin{bmatrix} 1 & v & 0 \\ v & 1 & 0 \\ 0 & 0 & 2(1+v) \end{bmatrix} \begin{Bmatrix} \phi_x \\ \phi_y \\ \phi_{xy} \end{Bmatrix} \quad (4.2)$$

For rectangular plates with uniformly distributed loads, the solution of Eq. (4.2) leads to an expression for maximum deflection in the form

$$\delta = \frac{\alpha w \ell^4}{D} = \frac{\alpha w \ell^4}{Eh^3/12(1 - v^2)} \quad (4.3)$$

where

ℓ = longer span length
w = uniform transverse load
α = coefficient depending on the boundary conditions and aspect ratio

It is noted from Eq. (4.3) that the influence of Poisson's ratio, v, on deflections is quite small. Typical values of v for concrete fall in the range between 0.15 and 0.25. The term $(1 - v^2)$ in the flexural rigidity, D, falls in the range 0.94 to 0.98. The error involved in neglecting Poisson's ratio is, therefore, approximately 2 to 6 percent.

Solutions of the plate equation for various geometries and support conditions have been given by Timoshenko and Woinowsky-Krieger (1959) and by Jensen (1938). Since closed-form solutions of the plate equation are available for only a limited number of cases, alternative solution procedures are required for most practical situations.

4.3.1.2 *Crossing beam methods* — Several approaches have been developed in which the two-way slab system is considered an orthogonal one-way system, thus allowing deflection calculations by beam analogy. Some of the earlier approaches were summarized in ACI 435.6R.

More recently, Rangan (1976) and Scanlon and Murray (1982) described calculation procedures in which the column and middle strips are treated as continuous beams; the middle strip is considered to be supported at its ends by column strips that are run perpendicular to the middle strip.

For two-way systems supported on a rectangular layout of columns, the ACI 318 method of design for strength involves dividing the slab into column strips and middle strips in each of the two orthogonal directions. The total static moment for each span, $M_o = w_u \ell_2 \ell_n^2/8$, is divided between positive and negative moment regions and then between column and middle strips, using either the direct design method or the equivalent frame method. Where w_u is the intensity of load per unit area, ℓ_n is the effective span and ℓ_2 is the dimension in the perpendicular direction. The distribution of moments approximates the elastic distribution for the given loading and therefore can be used to obtain an estimate of immediate deflections. However, the applied moments for strength design use factored loads, while the moments for calculation of immediate deflections require service loads that are unfactored. The bending moments required to calculate deflections or curvatures of columns and middle strips may be the same as the bending moments deter-

Column Strip Oeflection

Middle Strip Oeflection
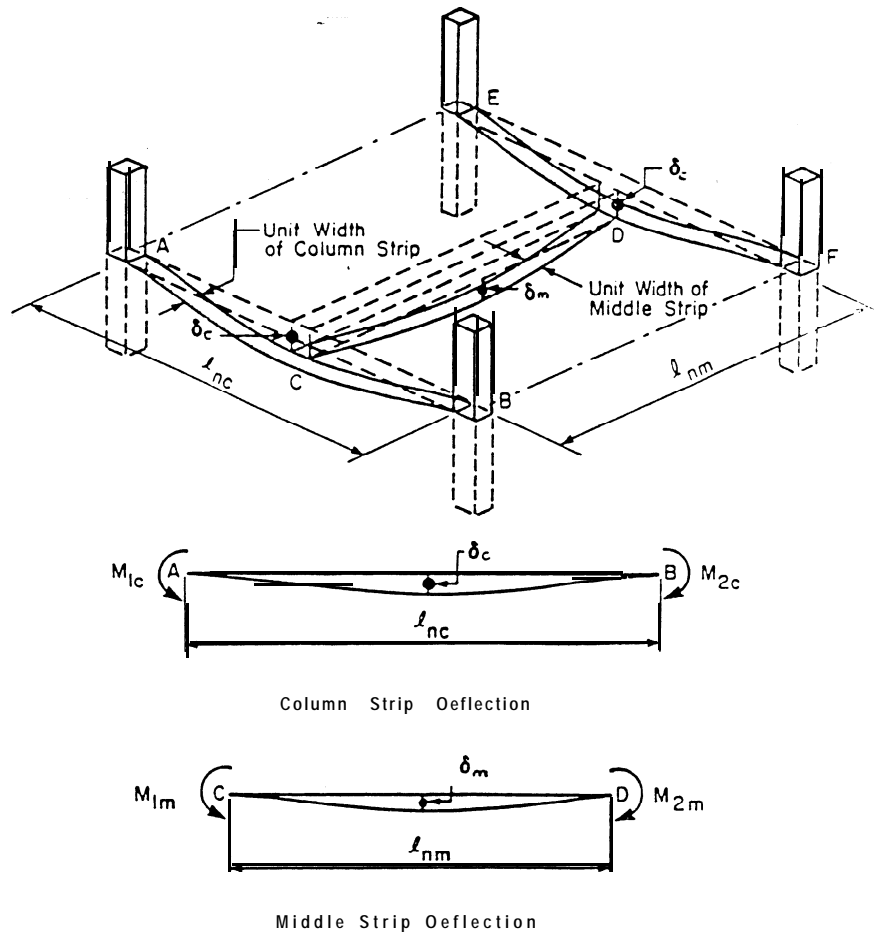
Fig. 4. 1-Crossing beam approach

mined for factored loads according to ACI 318 multiplied by the ratio of service load to factored load.

Fig. 4.1 shows a rectangular panel in a column-supported two-way slab system. The dotted areas represent a set of crossing beams from which column strip deflection, δ_c, and middle strip deflection, δ_m, can be obtained. Each beam can be treated as a strip of unit width for which end moments, midspan moment, and flexural rigidity properties can be obtained. Note that, by definition, end moments are those at the faces of supports, such as column or column capital faces, and that the beam span is the clear span between the faces of such supports.

Once the end moments and midspan moment have been obtained for a column or middle strip, the deflection for the strip can be calculated, using the elastic beam deflection equation:

$$\delta = \frac{5}{48} \frac{\ell_n^2}{EI} [M_m = 0.1(M_1 = M_2)] \qquad (4.4)$$

where

ℓ_n = clear span

M_1, M_2 = end moments per unit width

M_m = midspan moment per unit width

(Positive M_m, M_1, or M_2 produce tension at bottom fiber.)

Using this procedure the deflection of each column strip (δ_c) and of each middle strip (δ_m) can be calculated. The mid-panel deflection, δ_{mp}, is obtained by adding the column and middle strip deflections.

$$\delta_{mp} = \delta_c + \delta_m \qquad (4.5)$$

For cantilever slabs the rotation at the support must be included.

An earlier version of the equivalent frame method for calculating deflections proposed by Vanderbilt, Sozen and Siess (1965) considers the mid-panel deflection as the sum of a column strip deflection, cantilever deflection of a portion of the middle strip extending from the column strip, and the mid-panel deflection of a simply supported rectangular plate. The procedure developed by Nilson and Walters (1975), based on the equivalent frame method, is similar to the method outlined above except that a reference deflection is calculated for the

total panel width. Deflections for column and middle strips are then obtained from this reference deflection using lateral distribution factors based on relative *M/EI* values. A numerical example (Nawy, 1990) calculating the expected deflection limits using this procedure is given in Appendix A4.1. The resulting values are applicable in lieu of Table 4.2.

Ghali (1989) calculates the deflection at midspan of a column or middle strip from values of curvature calculated on the basis of compatibility and equilibrium at the midspan and supports using the relationship:

$$\delta = \frac{\ell^2}{96} (\phi_L = 10\phi_c = \phi_R) \qquad (4.6)$$

where ϕ_L, ϕ_c, ϕ_R are, respectively, the curvatures calculated from analysis of sections at the left end, center, and right end of column and middle strips and ℓ is the distance between the two ends. This relationship is based on the assumption that variation of curvature over the length ℓ is parabolic, The effects of cracking, creep, and shrinkage are accounted for in the analysis for ϕ at each section. In the absence of prestressing, simplification can be made by use of multipliers and graphs (Ghali, 1989; Ghali-Favre, 1986) that also account for the cracking, creep and shrinkage effects.

4.3.1.3 *Finite element method*-The finite element method can be used to analyze plates with irregular support and loading conditions. Effects of beams and columns can be included and a number of general purpose computer programs are available for elastic analysis of plate systems.

The plate is divided into a number of sub-regions or "elements." Within each element the transverse displacement is expressed in terms of a finite number of degrees of freedom (displacements, slopes, etc.) specified at element nodal points. In other words, the continuous displacement function, $a(x,y)$, is approximated by another function with a finite number of degrees of freedom. Based on the assumed displacement function and the given stress-strain, or moment-curvature relationships (such as Eq. 4.2 for elastic plates), the element stiffness matrix can be derived. The stiffness matrix of the entire slab is then assembled. The solution for displacements and internal moments proceeds using the standard matrix analysis techniques applicable for solving equilibrium equations, as outlined in a number of textbooks (e.g. Cook 1974; Gallagher 1975; Zienkiewicz 1977). Although the method is becoming increasingly popular in engineering practice, some skill is required in selecting an appropriate finite element model, developing an appropriate mesh, preparing computer input data, and interpreting the results.

4.3.2 *Effect of cracking*--The procedures outlined above are applicable to linear elastic isotropic plate systems and must be modified for concrete slabs to include the effect of cracking on flexural stiffness. An early

application of classical anisotropic theory to analysis of two-way reinforced concrete slabs is given in the text by Timoshenko and Woinoswky-Krieger (1959). More recently, procedures have been proposed for including cracking in finite element analysis and in the crossing beam analogies for two-way slabs.

The effective moment of inertia, I_e, concept developed originally by Branson (1963) for beams can be applied directly to the column and middle strips in the crossing beam analogies described in Section 2.2.2 for elastic uncracked plates. In Eq. 4.4 the cross-section stiffness, *EI,* becomes $E_c I_e$, using the usual averaging procedures given in ACI 318 for I_e, calculated at both positive and negative moment locations. Kripanarayanan and Branson (1976) presented an extension of the Nilson and Walters equivalent frame procedure to include cracking using the I_e procedure.

A review of the more sophisticated cracking models proposed for finite element analysis of slabs is given in the report of an ASCE Task Committee (1982). A simple generalization of Branson's effective moment of inertia concept to two-way systems has been suggested by Scanlon and Murray (1982) and implemented in a modified version of a linear elastic plate bending finite element by Graham and Scanlon [1986(a)].

4.3.3 *Restraint cracking*-In two-way reinforced concrete slabs built monolithically with supporting column and wall elements, in-plane shortening due to shrinkage and thermal effects is restrained. The restraint is provided by a combination of factors, including embedded reinforcement, attachment to structural supports, and lower shrinkage rates of previously placed adjacent panels when slab panels are placed at different times. Nonlinear distribution of free shrinkage strains across the cross-section may also be a contributing factor.

Service load moments in two-way slabs are often of the same order of magnitude as the code-specified cracking moment, M_{cr}. Deflection calculations made using the code-specified modulus of rupture will often result in an uncracked section being used when cracking may actually be present due to a combination of flexural stress and restraint stress.

ACI 318 specifies the modulus of rupture for deflection calculations as 7.5 $\sqrt{f_c'}$ psi (0.62 $\sqrt{f_c'}$ MPa). Laboratory test data, summarized in ACI 209R, indicate values ranging from 6 to 12 $\sqrt{f_c'}$ psi (0.5 to 1.0 $\sqrt{f_c'}$ MPa).

For slab sections with low reinforcement ratios, approaching minimum reinforcement, the difference between cracked and uncracked flexural stiffness is significant. It is important, therefore, to account for effects of any restraint cracking that may be present. Unfortunately, the extent of restraint cracking is difficult to predict. To account for restraint cracking in two-way slabs, Rangan (1976) suggested that column strip deflections be based on the moment of inertia of a fully cracked section, I_{cr}, and that middle strip deflections be based on $(I_g + I_{cr})/2$. Good agreement was reported between calcu-

lated and field measured deflections.

A more general approach was proposed by Scanlon and Murray (1982). They suggested that the effect of restraint cracking be included by introducing a restraint stress, f_{res}, that effectively reduces the modulus of rupture for calculating M_{cr}, i.e.

$$M_{cr} = \frac{f_e I_g}{y_t} \qquad (4.7)$$

where $f_e = f_r - f_{res}$

A value of $4\sqrt{f_c'}$ psi ($0.33\sqrt{f_c}$ MPa), or about half of the value specified in ACI 318, was proposed for the reduced effective modulus of rupture. This approach was investigated by Tam and Scanlon (1986) and has produced good correlation between calculated deflection and reported mean field-measured deflections [Jokinen and Scanlon 1985; Graham and Scanlon 1986(b)].

Ghali (1989) has also used the idea of reduced modulus of rupture and demonstrates the calculation of restraint stress due to reinforcement in the presence of uniform shrinkage.

An additional consideration is that the moments used in design for strength are based on some redistribution of moments. The distribution of design moments does not reflect the high peaks of moment adjacent to columns that occur in uncracked slabs. Deflection calculations based on moment distributions used for design, therefore, tend to under-predict the effects of cracking.

For slab systems in which significant restraint to in-plane deformations may be present, it is recommended that a reduced effective modulus of $4\sqrt{f_c'}$ psi ($0.33\sqrt{f_c}$ MPa) be used to compute the effective moment of inertia, I_e. A procedure for implementing this approach in finite element analysis is given by Tam and Scanlon (1986).

4.3.4 *Long-term deflections*-Long-term deflections can be estimated by applying a long-term multiplier to the calculated immediate deflection. Values for the long-term multiplier are specified in design codes such as ACI 318 where a value of $2/(l+50\rho')$ is applied to the immediate deflection caused by the sustained load considered. A number of authors have suggested that the ACI 318 long-term multiplier is too low for application to two-way slab systems, being based on poor correlation between reported calculated long-term deflections and field-measured deflections, However, it may be that much of the discrepancy between calculated and measured deflections is due to the effect of restraint cracking described earlier. There is no obvious reason to infer that creep and shrinkage characteristics of two-way slabs are significantly different from one-way slabs and beams. On the other hand, shrinkage warping is more significant in shallow slab systems than in deeper beam sections.

Two approaches are presented next for estimating long-term deflections; namely, by detailed computations and by the ACI multiplier methods.

4.3.4.1 *Detailed calculations*-Effects of creep deflection and shrinkage warping may be considered separately using procedures outlined in ACI 209R (82) (1986), based on the work of Branson, Meyers and Kripanapayanan (1970), and Branson and Christiason (1971).

Deflection due to creep is obtained from

$$\delta_{cp} = k_r C_t \delta_i \qquad (4.8)$$

where
C_t = time dependent creep coefficient representing creep strain at any time t in days after load application

k_r = factor to account for compression reinforcement and neutral axis shift

δ_i = immediate deflection due to dead load plus sustained live load, including effects of cracking

The general form of C_t given by ACI 209 is

$$C_t = \frac{(t)^{0.60}}{10 + (t)^{0.60}} C_u \qquad (4.9)$$

where C_u = ultimate creep coefficient.

ACI Committee report 209R-92 provides typical values of factors applying to moist-cured concrete loaded at 7 days or later (see Chapter 2 for details). For slabs loaded before 7 days, these values may be used for first approximations.

In a two-way slab, shrinkage occurs in all directions. The shrinkage deflection should therefore be calculated for orthogonal column and middle strips, and the results added to give the total mid-panel shrinkage deflection. Although there may be a contribution to shrinkage warping from nonuniform shrinkage strains through the slab cross-section, there is insufficient experimental data available to make specific recommendations for deflection calculations.

Shrinkage warping deflection for a beam is given by

$$\delta_{sh} = K_w \phi_{sh} \ell^2 \qquad (4.10)$$

where
K_w = coefficient depending on end conditions
  = 11/128 (one end continuous)
  = 1/16 (both ends continuous)
  = 1/8 (simple beam)
  = 1/2 (cantilever)

ϕ_s = shrinkage curvature
  = $0.7\varepsilon_{sh}(t)\rho^{1/3}/h$, singly reinforced member
  = $0.7\varepsilon_{sh}(t)(\rho-\rho')^{1/3}(\rho-\rho'/\rho)^{1/2}/h$, doubly reinforced member

Table 4.1—Multipliers recommended by different authors

Source	Modulus of rupture, psi	Immediate	Creep λ_c	Shrinkage λ_{sh}	Total λ_t
Sbarounis (1984)	$7.5\sqrt{f_c'}$	1.0	2.8	1.2	5.0
Branson (1977)	$7.5\sqrt{f_c'}$	1.0	2.0	1.0	4.0
Graham and Scanlon (1986b)	$7.5\sqrt{f_c'}$ $4\sqrt{f_c'}$	1.0 1.0	2.0 1.5	2.0 1.0	5.0 3.5
ACI Code	$7.5\sqrt{f_c'}$	1.0	2.0		3.0

Shrinkage warping deflections can also be determined using the equivalent tension force method outlined in ACI 209R.

The total deflection at any time is obtained by adding immediate deflection due to sustained load, creep deflection due to sustained load, shrinkage warping deflection, and deflection due to the part of the live load that is transient.

Sophisticated finite element models have been developed (ASCE 1982) to account for time-dependent deformations of two-way slabs caused by creep and shrinkage. These models are generally used for research purposes and are considered to be too complex for normal design applications, particularly when the high variability of creep and shrinkage properties is considered.

4.3.4.2 *ACI multiplier*—While deflection calculations can be made for long-term effects of creep and shrinkage, as outlined above, the use of a multiplier applied to the immediate deflection provides a simple calculation procedure that is adequate for most purposes. This approach is used in ACI 318, in which a sustained-load multiplier of 2 is applied to the immediate deflection of a member with no compression reinforcement. Several authors have recommended increasing this factor for two-way slabs, as indicated in Table 4.1, where the total long-time multiplier is expressed as

$$\lambda_t = 1 + \lambda_c + \lambda_{sh} \qquad (4.11)$$

where

λ_c = multiplier for creep

λ_{sh} = multiplier for shrinkage warping

As a first approximation, the additional deflection at intermediate time intervals due to sustained loads can be calculated using the values for ξ (Eq. 9-10 of ACI 318) multiplied by the factor $(\lambda_t - 1)/2$.

It is recommended that in cases where restraint stresses are expected to have an insignificant effect, the multiplier for sustained-load deflection be increased from 2 to 4, as recommended by Sbarounis (1984) and Graham and Scanlon [1986(b)]. In this case, the ACI 318 value for modulus of rupture would be used. In cases

where restraint stresses are likely to have a significant effect on cracking, for example, large slab areas and stiff lateral restraint elements such as structure walls and columns, it is recommended that a reduced modulus of rupture given by $f_r = 4\sqrt{f_c'}$ psi (0.33 $\sqrt{f_c}$ MPa) be used along with a long-term sustained-load multiplier of 2.5.

Values recommended in ACI 209R for ultimate creep and shrinkage coefficients are $C_u = 2.35$, and $\varepsilon_{sh\infty} = 780 \times 10^{-6}$, respectively at standard conditions as discussed in Chapters 2 and 3. Sbarounis (1984) has suggested that at standard conditions the long-term multipliers be modified if the concrete properties are known, and better estimates of ultimate creep, $\overline{C}_u$, and shrinkage, $\overline{\varepsilon}_{sh\infty}$, are available. Thus,

$$\lambda_t = (1 + \lambda_c)\frac{\overline{C}_u}{C_u} + \lambda_{sh}\frac{\overline{\varepsilon}_{sh\infty}}{\varepsilon_{sh\infty}} \qquad (4.12)$$

4.4—Minimum thickness requirements

Because of the complexities involved in calculating two-way slab deflections, engineers have preferred to control deflections by giving minimum slab thickness as a function of span length. Equations such as those in Section 9.5 of ACI 318, as shown in Table 4.2, are based on experience gained over many years. The ACI 318 equations express minimum thickness in terms of clear span between columns, steel yield strength, and flexural stiffness of edge beams. The minimum thickness values are modified for the effects of drop panels and discontinuous edges. ACI 318 permits the use of thinner slabs if deflections are computed and found to satisfy the specified maximum permissible values.

An extensive evaluation of the current ACI minimum thickness equations was reported by Thompson and Scanlon (1986). The study was based on finite element analyses of more than 300 slabs covering a range of thickness values, aspect ratios, edge beam dimensions, construction loads, and other parameters. The main conclusions of the study were as follows:

1) Calculated deflections for slabs designed according to the minimum thickness requirements of ACI 318 were within the permissible limits, when the calculations were

Table 4.2-Maximum permissible computed deflections

Type of member	Deflection to be considered	Deflection limitation
Flat roofs not supporting or attached to nonstructural elements likely to be damaged by large deflections	Immediate deflection due to live load L	$\dfrac{\ell^*}{180}$
Floors not supporting or attached to nonstructural elements likely to be damaged by large deflections	Immediate deflection due to live load L	$\dfrac{\ell}{360}$
Roof or floor construction supporting or attached to nonstructural elements likely to be damaged by large deflections	That part of the total deflection occurring after attachment of nonstructural elements (sum of the long-time deflection due to all sustained loads and the immediate deflection due to any additional live load)[†]	$\dfrac{\ell^{\ddagger}}{480}$
Roof or floor construction supporting or attached to nonstructural elements not likely to be damaged by large deflections		$\dfrac{\ell^{\S}}{240}$

   * Limit not intended to safeguard against ponding. Ponding should be checked by suitable calculations of deflection, including added deflections due to ponded water, and considering long-term effects of all sustained loads, camber, construction tolerances, and reliability of provisions for drainage.

   † Limit may be exceeded if adequate measures are taken to prevent damage to supported or attached elements.

   ‡ Long time deflection shall be determined in accordance with 9.5.2.5 or 9.5.4.2, but may be reduced by amount of deflection calculated to occur before attachment of nonstructural elements. This amount shall be determined on the basis of accepted engineering data relating to time deflection characteristics of members similar to those being considered.

   § But not greater than tolerance provided for nonstructural elements. Limit may be exceeded if camber is provided so that total deflection minus camber does not exceed limit.

based on the ACI 318-specified value of 7.5 $\sqrt{f_c'}$ for modulus of rupture, and ACI 209R Eq. 15-17 for creep and shrinkage deflection. Construction loads due to shoring and reshoring were also considered.

2) When the calculations were based on a reduced modulus of rupture to account for restraint cracking, the ACI 318 limit of $\ell/480$ on incremental deflection was exceeded for slab panels with aspect ratios less than 1.5. An increase of 10 percent over the current minimum thickness value for square panels was suggested to obtain calculated deflections within the allowable limits. The suggested increase in minimum thickness decreases linearly to zero for a panel with an aspect ratio equal to 1.5.

The results of this study suggest that the ACI minimum thickness equations will provide satisfactory serviceability in most cases, confirming the satisfactory performance of slabs designed and built according to the requirements in ACI 318 prior to the 1989 edition. When more stringent than normal deflection limits are required, a thicker slab should be used. Other means to increase the slab stiffness, such as the addition of beams, can also be considered.

Recently, attempts have been made to develop criteria for span-to-depth ratios or minimum thickness of slabs that explicitly include the effects of such parameters as live-to-dead load ratio, permissible deflection-to-span ratio, effect of cracking, sustained load level, and time between construction and installation of nonstructural elements. Two such approaches are described in the following paragraphs.

Gilbert (1985) extended to two-way slabs an expres-

sion developed by Rangan (1982) for maximum allowable span-to-depth ratio for beams. Rangan's equation involves rearranging the basic equation for beam deflection calculations,

$$\delta = \delta_\ell + \delta_{sus} \qquad (4.13)$$

where

δ_ℓ = deflection due to variable part of live load
     = $kw_\ell\ell^4/E_cI_e$
δ_{sus} = total deflection due to sustained load including sustained part of live load
     = $\lambda\,(kw_s\ell^4/E_cI_e)$
λ = long-term multiplier

Replacing I_e by αbd^3, where the term α gives an approximation for I_e as a function of the reinforcement ratio ρ, Eq. 4.13 can be rewritten as

$$\frac{\delta}{\ell} \quad \frac{k(w_\ell + \lambda w_s)\ell^3}{E_c\,\alpha bd^3} \qquad (4.14)$$

If δ/ℓ is given as the maximum permissible deflection-to-span ratio, the corresponding maximum span to effective depth ratio can be obtained from

$$\frac{\ell}{d} < k_1\,\frac{\delta}{\ell}\left|\frac{\alpha bE_c}{w_\ell + \lambda w_s}\right|^{1/3} \qquad (4.15)$$

where

k_1 = a combination of factors to account for support conditions and effect of beam flanges

Gilbert extended Eq. 4.15 by adding a "slab system factor" k_2 to account for two-way action, i.e.

$$\frac{\ell}{d} < k_1 k_2 \, \frac{\delta}{\ell} \left(\frac{\alpha b E_c}{w_\ell + \lambda w_s} \right)^{1/3} \qquad (4.16)$$

The factor k_2 was developed for a variety of conditions from parameter studies using a sophisticated finite element model. Eq. 4.16 involves an iterative procedure since the reinforcement ratio required to determine α, and the dead load are initially unknown.

A somewhat simpler expression for beams was developed by Grossman (1981, 1987); it was based on a large number of computer-generated beam deflection calculations. Grossman's minimum thickness equation is given by

$$h_{\min} > \frac{\ell}{c} \, \frac{\ell}{\delta} \, C_d \geq \frac{\ell}{24} \qquad (4.17)$$

Correction factors are given for variations in support conditions, d/h, f_y, and concrete density. The term c was developed from the computer analyses and depends on the load levels and construction methods used. For heavily-loaded members, a limiting value of $c = 4320$ was proposed by Grossman for heavily loaded members. Smaller thicknesses can be obtained if the required reinforcement ratio for less heavily loaded members is known and is used to obtain a larger revised value of c from Grossman's data.

The term C_d, given by

$$C_d = \frac{\lambda' D + L}{D + L} \qquad (4.18)$$

accounts for both the live-load-to-dead-load ratio, L/D, and the net long-term multiplier λ', for deflections occurring after installation of partitions in buildings.

Although developed for beams only, the equation could be extended to two-way systems using a "slab system factor" similar to that given by Gilbert (1985).

4.5-Prestressed two-way slab systems

4.5.1 *Introduction*-Two-way post-tensioned concrete slabs are widely used for the floor systems of office buildings, parking garages, shopping centers, and lift slabs in residential buildings. Due to its general economy and ability to satisfy architectural requirements, the post-tensioned concrete flat plate has been widely adopted in the United States as a viable structural system. This type of construction has grown over the past 25 years, despite competition from other floor systems. The popularity of this type of construction is primarily due to the economies that result from reduced slab thickness, longer spans, and reduced construction time due to earlier removal of form work. In addition, the use of post-tensioning enables the engineer to better control deflections and cracking at service loads.

4.5.2 *Basic principle for deflection control*--The concept of load balancing [Lin (1963)] is often used to make an appropriate choice of tendon profile, prestressing amounts and tendon distribution in two-way prestressed and post-tensioned floor systems. Service live loads, rather than total dead plus live loads, should be used to evaluate deflection of the slab. Load balancing from the transverse component of the prestressing force would have to be used to neutralize the dead-load deflection or even induce camber if the live load is excessively high. ACI 318 requires that both immediate deflection, due to live load and long-term deflection due to sustained loads be investigated for all prestressed concrete.

4.5.3 *Minimum stab thickness for deflection control*--In choosing the slab thickness, the engineer must consider deflection control, shear resistance, fire resistance, and corrosion protection for the reinforcement. While ACI 318 requires deflection calculations for a preliminary estimate of the two-way slab thickness, it is usual to determine a minimum thickness for deflection control based on traditional span-depth ratios as suggested by the Post-Tensioning Institute (1976). As an approximate guideline, a span-to-depth ratio of 50 and 45 may be used for two-way continuous slabs with and without drop panels, respectively. A minimum drop panel of 1/6 span length each way is recommended. A span-to-depth ratio of 55 for a two-way slab with two-way beams is reasonable. For waffle slabs, a lower value of 35 is recommended. Gilbert (1989) also gave a simple formula to express the maximum span-to-depth ratio of two-way post-tensioned floor systems. The expression provides an initial estimate of the minimum slab thickness required to limit deflections to some preselected maximum value.

4.5.4 *Methods for defection calculations*-Control of deflection in a two-way prestressed and post-tensioned floor system is dealt with in Section 9.5.4 and Chapter 18 of ACI 318. However, unlike the two-way slab construction in a nonprestressed case, there are no provisions containing requirements to determine a minimum thickness for two-way post-tensioned slabs. To compute the deflections, the engineer may apply the methods proposed for nonprestressed construction with appropriate treatment of the effects of prestressing.

The accurate determination of deflections of two-way post-tensioned slabs is a complex operation involving considerations of the boundary conditions, loading patterns and history, changes of stiffness due to local cracking, and loss of prestress due to creep, shrinkage, and relaxation. For practical design purposes, it is usually adequate to use simple approximate expressions to estimate the deflection, such as the crossing beam methods including the equivalent frame approach described earlier, The mid-panel deflection can be approximated as the sum of the center-span deflections of the column strip, in
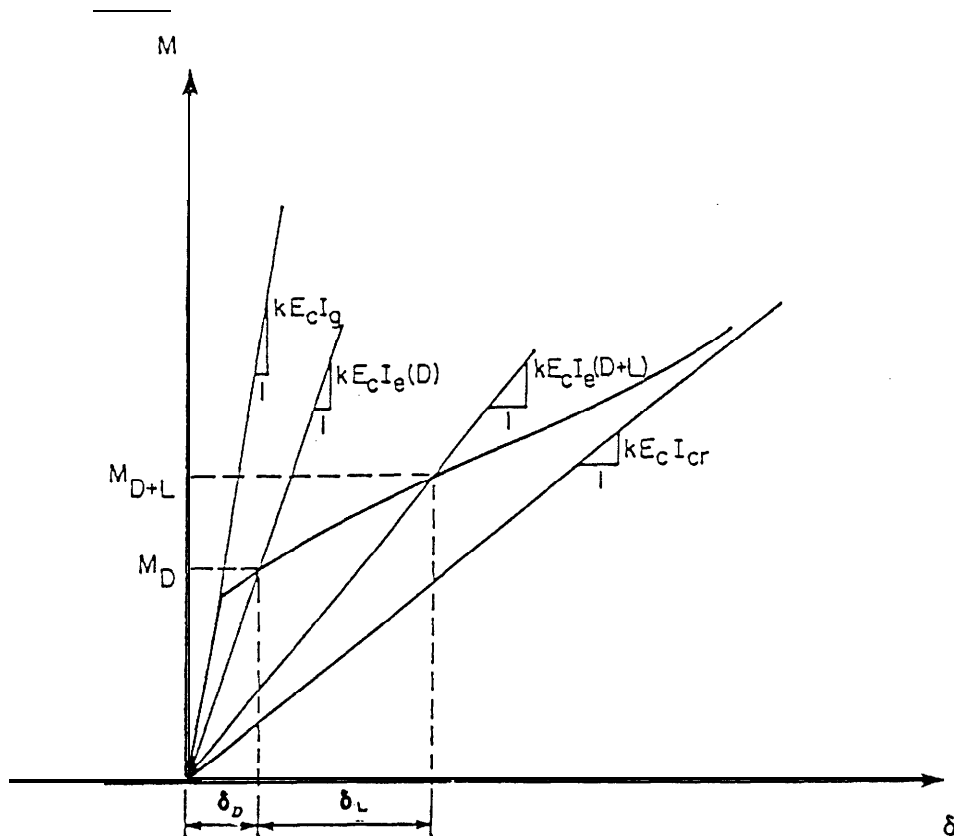
Fig. 4.2-Definition of δ_D *and* δ_L *for monotonic moment-deflection curve*

one direction, and that of the middle strip, in the orthogonal direction. A detailed numerical example is given in Nawy (1989). The use of gross stiffness values to compute deflections is justifiable only if the tensile stresses in the concrete remain below the cracking stress. If cracking is predicted, then the effective moment of inertia may be used to estimate the influence of cracking on the deflection, as discussed in Chapter 3, Section 3.6.2.

Deflections of two-way prestressed systems can also be computed by evaluating curvatures at sections based on compatibility and equilibrium as described in Section 4.3.1.2. The time-dependent changes in strains in prestressed sections are caused by relaxation of prestressed steel in addition to creep and shrinkage of concrete. The sections are subjected to normal force N and bending moment M, producing axial strain as well as curvature. The position of the neutral axis after cracking is dependent on the value (M/N) in addition to geometric properties. Analysis details and a computational example are given in Ghali,1990.

4.6-Loads for deflection calculations

ACI 318 stipulates that calculated deflections must not exceed certain permissible values, expressed as fractions of span length. Components of deflections to be considered are immediate live load deflection and incremental deflection, including that due to live load, after installation of nonstructural elements. The live load component of deflection is normally considered as that due

to total load minus that due to dead load. Under monotonic loading, two effective moment of inertia values should be used to calculate the deflections at the two different load levels, as shown in Fig. 4.2.

For multistory slab construction, however, since the load imposed on the slab during construction often exceeds that due to the specified dead plus live load (Grundy and Kabaila, 1963; etc.), the extent of cracking is usually determined by the construction loads resulting from shoring and reshoring procedures. Under these conditions all values of immediate deflection should be calculated using the effective moment of inertia corresponding to the construction load level, as illustrated in Fig. 4.3. This calculation procedure usually results in a smaller live load deflection and larger dead load deflection, with correspondingly larger sustained load deflection.

A typical load-time history is shown in Fig. 4.4 for a slab in a multistory structure. During construction, the load on the slab increases as new slabs are placed above. When construction above is no longer supported by the slab under consideration, the load decreases to a value corresponding to the slab self-weight plus an allowance for superimposed dead load and sustained portion of live load (load level at t_1 in Fig. 4.4).

A simple procedure to determine slab loads during construction was proposed by Grundy and Kabaila (1963). More refined analysis procedures reported subsequently [e.g., Liu et al (1985), Aguinaga-Zapata and
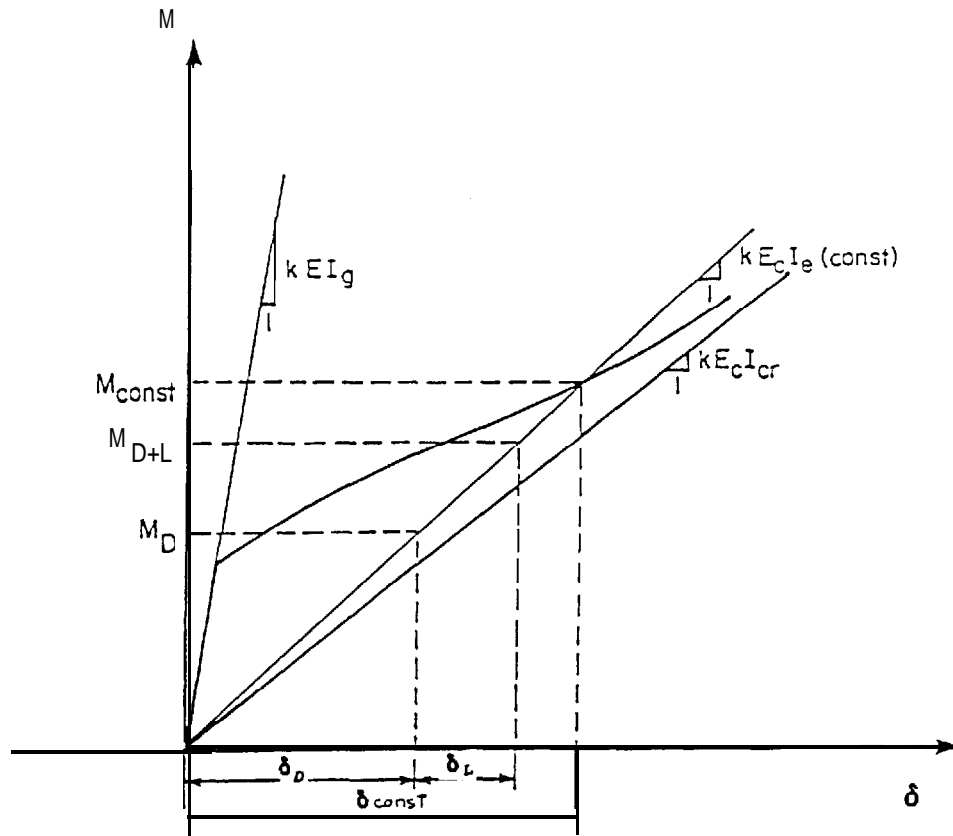
Fig. 4.3-Definition of $\delta_D, \delta_L,$ and δ_{const} when construction loads exceed specified dead plus live load
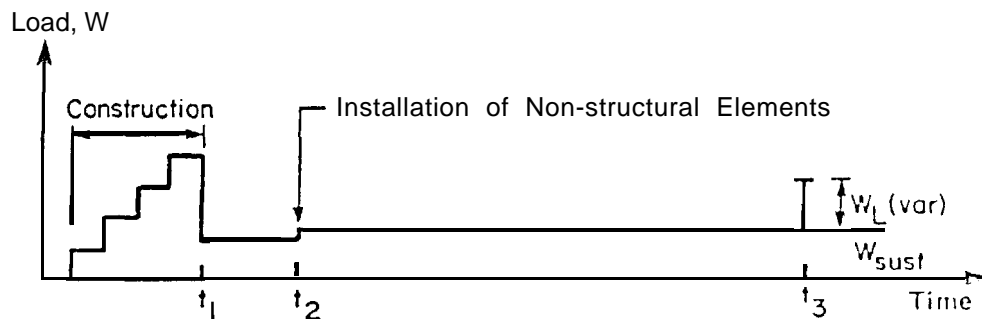
Fig. 4.4-Schematic load-time history

Bazant (1986)] give results that are quite similar to the original Grundy and Kabaila procedure. The maximum load during construction, including loads due to shoring and reshoring plus an allowance for construction live load, can be estimated using the following relationship:

$$w = k_1 \, k_2 R \, w_{slab} + \frac{w_{CL}}{N} \qquad (4.19)$$

where

k_1	=	allowance for error in theoretical load ratio R
k_2	=	allowance for weight of formwork
R	=	applied load/slab dead load ratio
	=	load ratio calculated by Grundy and Ka-

baila procedure
w_{slab} = slab dead load
w_{CL} = construction live load
N = number of shored and reshored levels

Gardner (1985) recommends $k_1 = k_2 = 1.1$. The construction live load may be taken as 50 psf (2.4 kPa) as recommended by ACI 347R. The factor k_1 accounts for errors in computing R due to variations in stiffnesses between the stories in the supporting system. The factor R has been shown to vary from 1.8 to 2.2, depending primarily on the number of stories of shores and reshores in the system. If the shoring system to be used is unknown, a value of $R = 2.0$ can be used in the calculation. Instead of a factor k_2 for formwork weight, a value of 10 psf is

Fig. 4.5-Simplified load-time histoly and corresponding deflection-time history

considered to be a reasonable allowance for most formwork systems.

At time t_2 in Fig. 4.4, a slight increase in the sustained load occurs as nonstructural elements are installed. The variable portion of live load may be considered as applied intermittently thereafter. One application of live load is shown at time t_3.
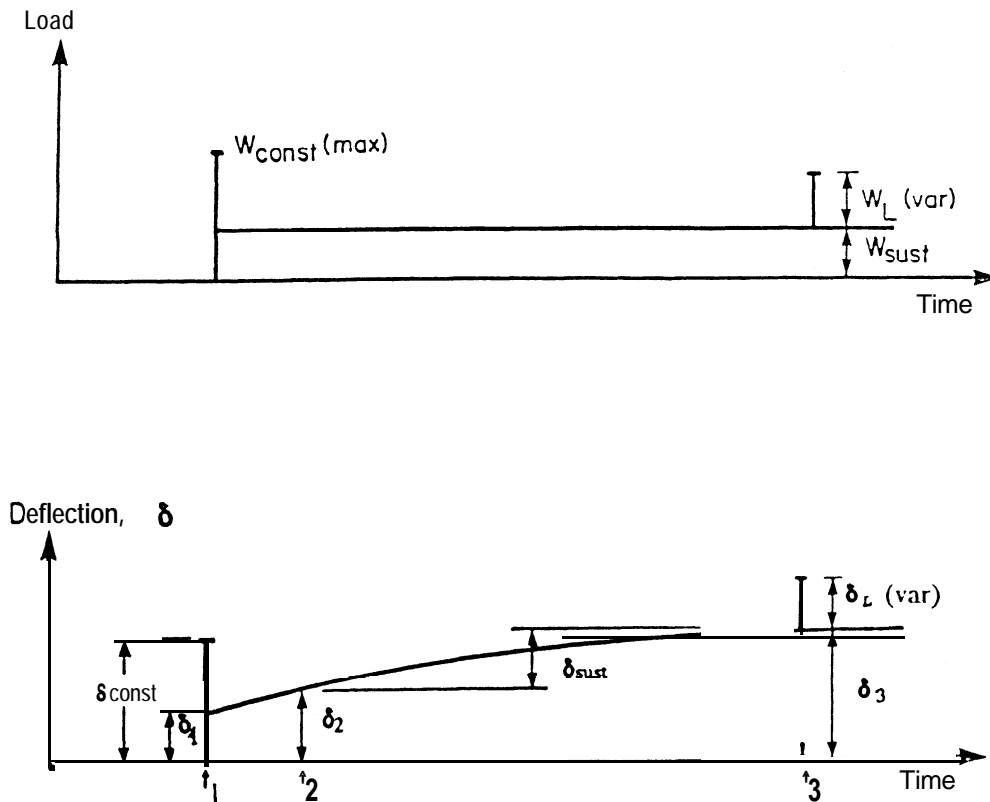
An analysis procedure based on this type of loading history and ACI 209R creep and shrinkage functions was developed by Graham and Scanlon (1986a), using the principle of superposition. Effects of partial creep recovery were considered. Analyses were also made for the simplified load-time history shown in Fig. 4.5 with the corresponding displacement-time history. Long-term sustained load deflections were obtained using multipliers calibrated with the more complex history of Fig. 4.4. Resulting multipliers are included in Table 4.1.

Based on the procedures suggested by Sbarounis (1984) and Graham and Scanlon (1986a), the following approach based on the simplified load-time history can be used to estimate long-term deflections in multi-story slab systems.

1. Estimate the maximum construction load expected $[w_{const}(max)]$ based on usual procedures for multi-story construction.

2. Calculate the corresponding immediate construc-

tion load deflection, δ_{const}.

3. Calculate the live load deflection by scaling the construction load deflection.

$$\delta_L = \frac{w_L}{w_{const}(\text{max})} \cdot \delta_{const} \cdot \frac{E_C(Const)}{E_c(L)}$$

where $E_c(Const)$ and $E_c(L)$ are modulus of elasticity values at application of construction load and live load, respectively.

4. Scale the construction load deflection to the sustained load level. Sustained load includes dead load plus any portion of the live load assumed to be sustained.

$$\delta_1 = \frac{w_{sust}}{w_{const}(\text{max})} \cdot \delta_{const} \cdot \frac{E_c(Const)}{E_c(Sust)}$$

where $E_c(Sust)$ is the modulus of elasticity at the time sustained load is applied (i.e., at end of construction period).

5. Calculate sustained load deflection at time of installation of non-structural elements.

$$\delta_2 = \lambda_l \delta_l$$

where λ_l = multiplier corresponding to time interval t_1

to t_2. *(The* time function given in Eq. 2.16 can be used to determine λ, i.e.,

$$m\lambda_1 = \frac{(t_2 - t_1)^{0.60}}{10 + (t_2 - t_1)^{0.60}} \cdot \lambda_t$$

6. Calculate ultimate sustained load deflection.

$$\delta_3 = A, \delta_1$$

where λ_t = long-term multiplier (Table 4.1).

7. Calculate the deflection due to the variable portion of live load, i.e., that portion of live load not assumed as sustained.

$$\delta_L(var) = K\,\delta_L \text{ (from step 3)}$$

where

$$K = \frac{variable\ live\ load}{total\ live\ load} = \frac{w_{L(var)}}{w_L}$$

8. Calculate increment in deflection after installation of nonstructural elements.

$$\delta_{inc} = \delta_3 + \delta_L(var) - \delta_2$$

9. Compare calculated deflections with appropriate permissible values.

4.7-Variability of deflections

ACI 435.4R, *Variability of Defections of Simply Supported Reinforced Concrete Beams,* reported that the variability of actual deflections under nominally identical conditions is often large. For simply supported beams under laboratory conditions it was reported that, using Branson's I-effective procedure, there is approximately a 90 percent probability that actual deflections of a particular beam will range between 80 percent and 130 percent of the calculated value. The variability of deflections in the field can be even greater.

Based on Monte Carlo simulation, Ramsay et al. (1979) indicated that the coefficient of variation for immediate deflection of beams ranged from 25 to 50 percent. The major source of variation was found to be flexural stiffness and tensile strength of concrete, particularly when the service load moment is close to the calculated cracking moment. Similar trends could presumably be expected for two-way slabs. Other sources of variability include variations of slab thickness and effective depth of reinforcing steel.

Jokinen and Scanlon (1985) presented results of an analysis of field-measured two-way slab deflections for a 28-story office tower in Edmonton, Alberta, Canada. Fig. 4.6 shows a plot of deflection versus time measurements for 40 nominally identical slab panels. The high variabil-

ity is evident, both during the construction period (first 35 days) and at approximately one year thereafter.

A histogram of one-year deflections, shown in Fig. 4.7, indicates a coefficient of variation of 29.9 percent for these slabs and a range of deflections from approximately the mean minus 50 percent to the mean plus 70 percent. Calculated deflections at one year based on three assumed values of modulus of rupture, and long-term multipliers proposed by Graham and Scanlon [1986(b)], are shown in Fig. 4.6. These results indicate that the best estimate of the mean deflection was obtained using an effective modulus of rupture of $4\sqrt{f_c'}$ psi ($0.33\sqrt{f_c'}$ MPa). The calculated deflection based on the ACI 318 specified value, $7.5\sqrt{f_c'}$ psi ($.62\sqrt{f_c'}$ MPa) was found to lie at the low end of the range of measured deflections. The calculations included effects of construction loads.

Sbarounis (1984) reported on deflection measurements taken after one year on 175 bays of a multi-story building in Chicago. Measured deflections had a mean value of 1.35 in. (34.3 mm) and a coefficient of variation of 21.2 percent. The range in measured deflections was 0.53 in. to 2.16 in. (13.5 to 54.9 mm), i.e., from the mean minus 60 percent to the mean plus 60 percent. Calculated values were close to the mean deflection.

A number of case studies of large deflections reported in the literature has been summarized in ACI 435.8R. These case studies, including examples from Australia, Scotland, Sweden, and the U.S., highlight the large number of factors that can cause variability in in-situ slab deflections.

4.8-Allowable deflections

ACI 318 specifies limits on calculated deflections for live load and incremental deflection after installation of nonstructural elements. No limit is specified for total deflection. However, on the assumption that nonstructural elements will be installed shortly after construction of the slab, the specified limit on incremental deflection indirectly controls the total deflection.

The specified deflection limits apply to calculated deflections. By calculating deflections based on unfactored design loads and expected material properties, the calculated deflection should be interpreted as an estimate of the mean deflection. Recognizing the variability of actual deflections as measured in the field, some variation from the calculated deflection is to be expected. If the calculated deflection is close to the allowable deflection, there is a high probability that the actual deflection will exceed the allowable limit.

Since the deflection limits are based on experience and past practice resulting in generally satisfactory behavior, it must be assumed that the variability of actual deflections is accounted for indirectly in the specified limits.

The primary concern of ACI 318 is public safety. The serviceability provisions are of a general nature intended to provide adequate serviceability for the majority of de-
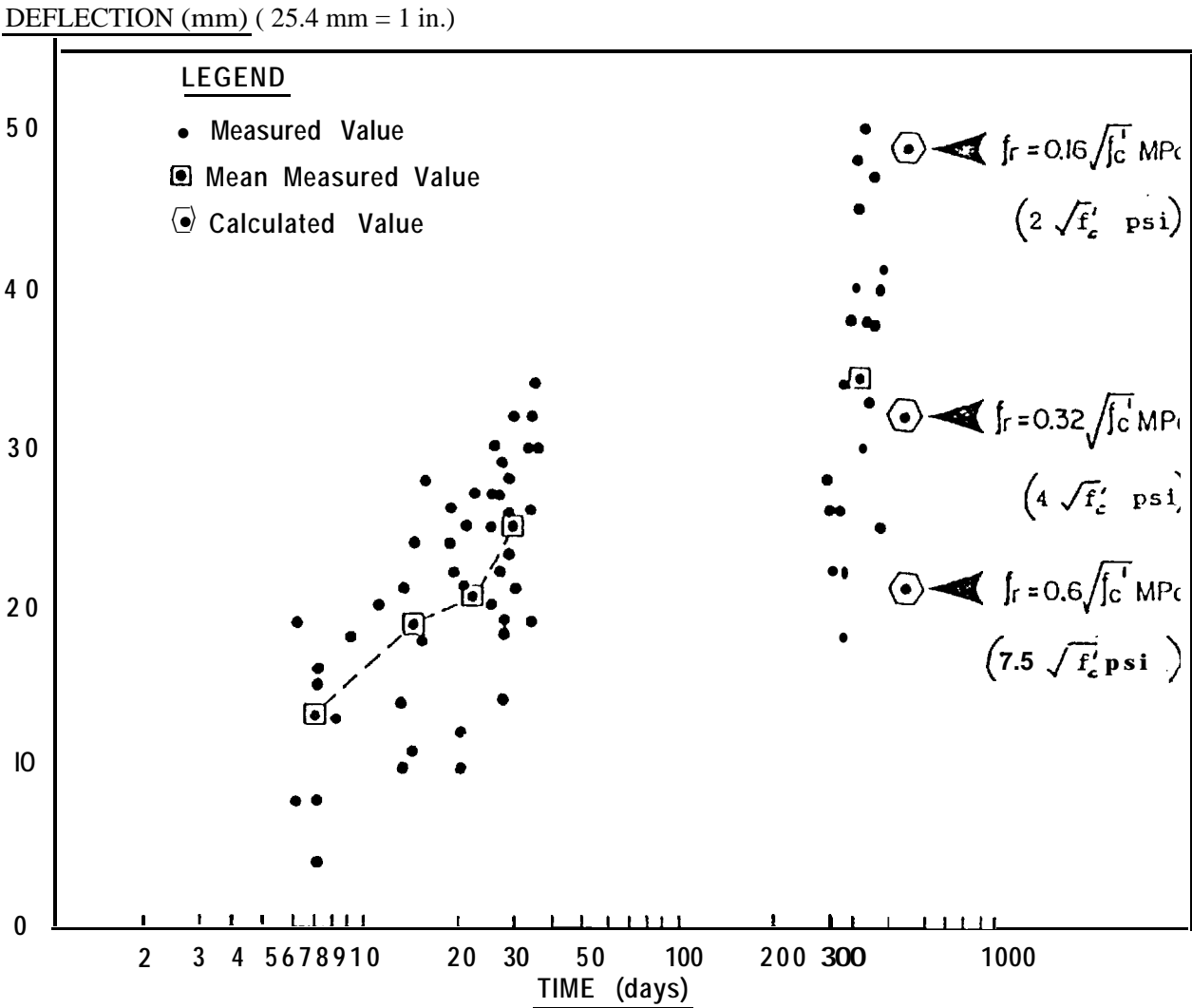
DEFLECTION (mm) (25.4 mm = 1 in.)

Fig. 4.6-Field-measured deflections for 40 nominally identical slab panels in 28-story building (Jokinen and Scanlon, 1985)

sign situations. Individual cases may require more stringent requirements than the limited treatment given in ACI 318. Guidance on appropriate deflection limits for a range of applications is given in ACI 435.3R (1984).

APPENDIX A4

Example A4.1-Deflection design example for long-term deflection of a two-way slab

The following example (Nawy, 1990) illustrates the application of the Equivalent Frame approach developed by Nilson and Walters (1975), along with the modulus of rupture and long-term multiplier given in ACI 318.

A 7-in. (178 mm) slab of a five panel by five panel floor system spanning 25 ft in the E-W direction (7.62 m) and 20 ft in the N-S direction (6.10 m) is shown in Fig. A4.1. The panel is monolithically supported by beams 15 in. x 27 in. in the E-W direction (381 mm x 686 mm) and

15 in. x 24 in. in the N-S direction (381 mm x 610 mm). The floor is subjected to a time-dependent deflection due to an equivalent uniform working load intensity $w = 450$ psf (21.5 kPa). Material properties of the floor are:

$$f'_c = 4000 \text{ psi (27.6 MPa)}$$
$$f_y = 60{,}000 \text{ psi (414 MPa)}$$
$$E_c = 3.6 \times 10^6 \text{ psi } (24.8 \times 10^6 \text{ kPa})$$

Assume

1. Net moment M_w from adjacent spans (ft-lb)

	E-W		N-S
Support 1:	20×10^3	Support 1:	40×10^3
Support 2:	5×10^3	Support 4:	20×10^3

2. Equivalent column stiffness $K_{cr} \approx 400\, E_1$ lb-in. per radian in both directions. Find the maximum central deflection of the panel due to the long-term loading and

FREQUENCY

$$n = 40$$
$$\bar{x} = 32.53 \text{ mm}$$
$$s = 9.72 \text{mm}$$
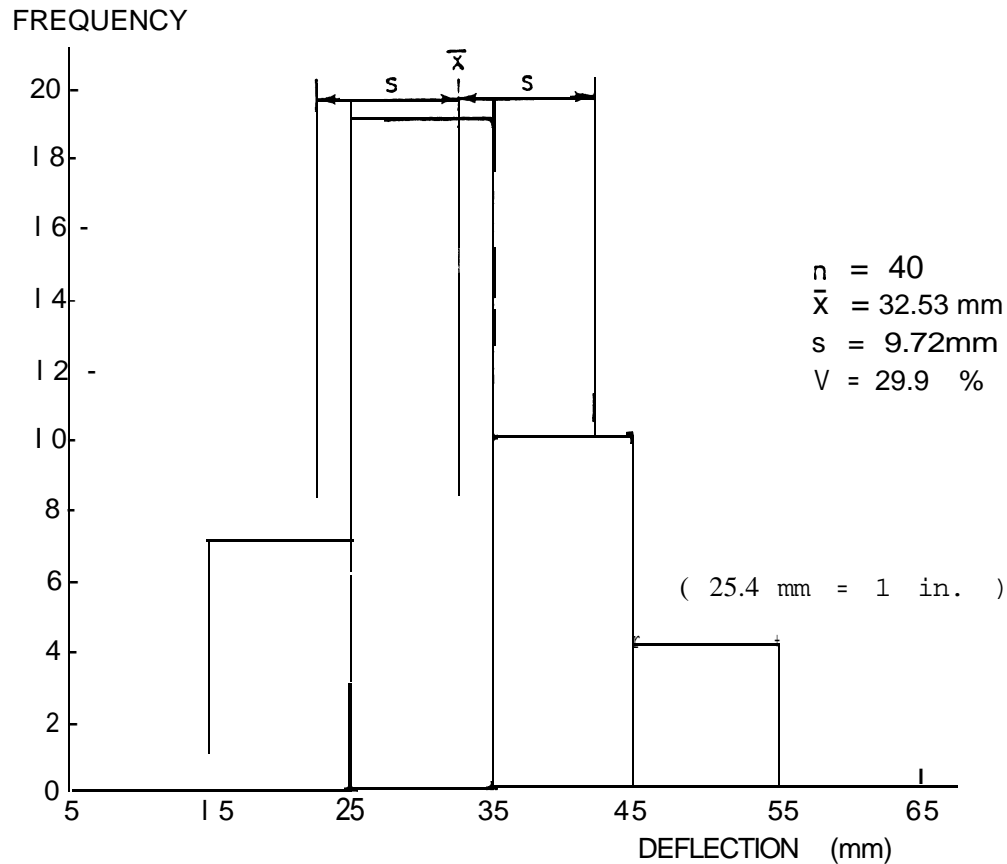$$V = 29.9 \%$$

(25.4 mm = 1 in.)

DEFLECTION (mm)

Fig. 4.7-Histogram of one year deflections (Jokinen and Scanlon, 1985)

determine if its magnitude is acceptable if the floor supports sensitive equipment which can be damaged by large deflections.

3. Cracked moment of inertia:
E-W: I_{cr} = 45,500 in.[4]
N-S: I_{cr} = 32,500 in.4

Solution:

Note: All calculations are rounded to three significant figures.

Calculate the gross moments of inertia (in.^4) of the sections in Fig. 8, namely, the total equivalent frame I_{cs} in part (b), the column strip beam I, in part (c), and the middle strip slab I_s in part (d). These variables are:

	I_{cs}	I_c	I_s	I_{CR}
E-W	63,600	53,750	3430	45,500
N-S	47,600	40,000	4290	32,500

Next, calculate factors $\alpha_1 \ell_2/\ell_1$ and $\alpha_2 \ell_1/\ell_2$. In both cases they are greater than 1.0. Hence, the factored moments coefficients (percent) obtained from the tables in Section 13.6 of ACI 318

	Column strip (+ and -)	Middle strip (+ and -)
E-W	81.0	19.0
N-S	67.5	32.5

E-W direction deflections (span = 25 ft)
Long-term w_w = 450 psf

$$\delta_{25}' \qquad \frac{450 \times 20(25)^4 \times 12^3}{384 \times 3.6 \times 10^6 \times 63,600} = 0.069 \text{ in.}$$

$$\delta_c \qquad = 0.069 \times 0.81 \frac{63,600}{53,700} = 0.066 \text{ in.}$$

$$\delta_s \qquad = 0.068 \times 0.19 \times \frac{63,600}{3430} = 0.243 \text{ in.}$$

Rotation at end 1 is

$$\theta_1 = \frac{M_1}{K_{ec}} = \frac{20 \times 10^3 \times 12}{400 \times 3.6 \times 10^6} = 1.67 \times 10^{-4} \text{ rad}$$

and the rotation at end 2 is

$$\theta_2 = \frac{M_2}{K_{ec}} = \frac{5 \times 10^3 \times 12}{400 \times 3.6 \times 10^6} = 0.42 \times 10^{-4} \text{ rad}$$

where θ is the rotation at one end if the other end is fixed.

δ'' = deflection adjustment due to rotation at supports 1 and 2 = $\theta \ell/8$

$$\delta'' = \frac{(1.67 + 0.42) \times 10^4 \times 300}{8} = 0.08 \text{ in.}$$
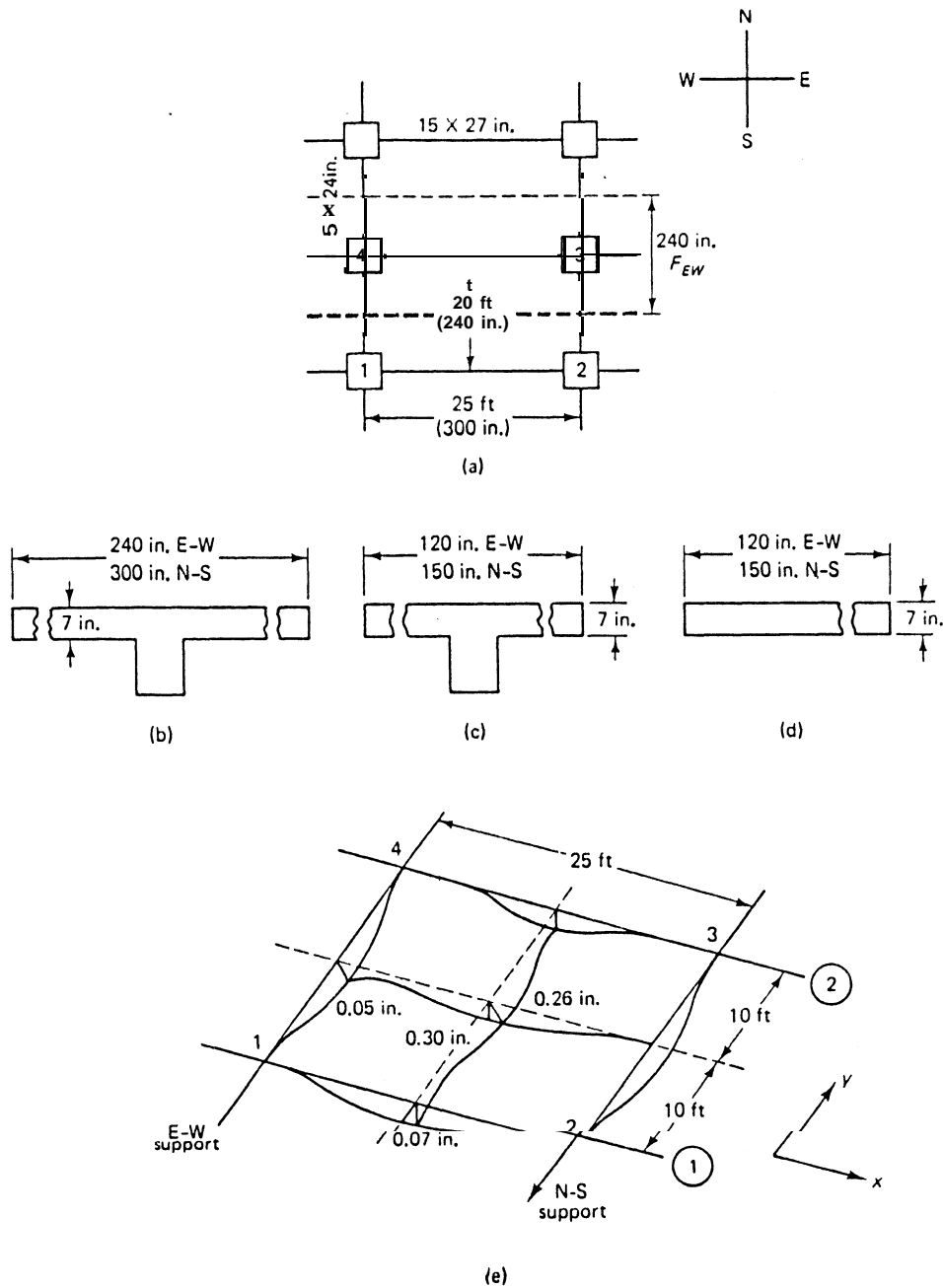
Fig. A4.1-Long-term deflection of two-way multi-panel slab on beams in Ex. A4.1, equivalent frame calculation method (Nawy, 1990 -courtesy Prentice Hall)

Therefore,

net δ_{cs} = 0.066 + 0.008 = 0.074   say 0.07 in.

net δ_{cs} = 0.243 + 0.008 = 0.251   say 0.25 in.

N-S direction deflections (span = 20 ft)

$$\delta_{20}' = \frac{450 \times 25(20)^4 \times 12^3}{384 \times 3.6 \times 10^6 \times 47,000} = 0.048 \text{ in}$$

$$\delta_c = 0.048 \times 0.675 \times \frac{47,000}{40,000} = 0.038 \text{ in.}$$

$$\delta_s = 0.048 \times 0.325 \times \frac{47,000}{4288} = 0.171 \text{ in.}$$

rotation $\theta_1 = \dfrac{M_1}{\overline{K^{ec}}} \dfrac{40 \times 10^3 \times 12}{400 \times 3.6 \ 10^6} = 3.3 \ 10^{-4} \text{ rad}$

rotation $\theta_4 = \dfrac{M_4}{K_{ec}} = \dfrac{20 \times 10^3 \times 12}{400 \times 3.6 \times 10^6} = 1.67 \times 10^{-4} \text{ rad}$

$$\delta'' \equiv \frac{\theta \ell_2}{8} = \frac{(3.3 + 1.67)10^{-4} \times 240}{8} = 0.015 \text{ in}$$

Therefore,

net δ_{cy} = 0.038 + 0.015 = 0.053 say 0.05 in.

$$\delta_{sy} = 0.171 + 0.015 = 0.186 \text{ say } 0.19 \text{ in.}$$

total central deflection $\Delta = \delta_{sx} + \delta_{cy} = \delta_{sy} + \delta_{cx}$

$\Delta_{E\text{-}W} = \delta_{sx} + \delta_{cy} = 0.25 + 0.05 = 0.30$ in.

$\Delta_{N\text{-}S} = \delta_{sy} + \delta_{cx} = 0.19 + 0.07 = 0.26$ in.

Hence, the average deflection at the center of the interior panel $\frac{1}{2}(\Delta_{E\text{-}W} + \Delta_{N\text{-}S}) = 0.28$ in. (7 mm).

Adjustment for cracked section: Use Branson's effective moment of inertia equation,

$$I_e = \left(\frac{M_{cr}}{M_a}\right)^3 I_g + \left[1 - \left|\frac{M_{cr}}{M_a}\right|^3 \right] I_{cr}$$

Calculation of ratio M_{cr}/M_a:

$$M_{cr} = \frac{f_r I_g}{y_t}$$

where f_r = modulus of rupture of concrete

y_t = distance of center of gravity of section from outer tension fibers

E-W (240-in. flange width): $y_t = 21.5$ in.

N-S (300 in. flange width): $y_t = 19.2$ in.

$$f_r = 7.5\sqrt{f_c'} = 7.4\sqrt{4000} = 474 \text{ psi}$$

Hence,

$$M_{cr}(E\text{-}W) = \frac{474 \times 63,600}{21.5} \times \frac{1}{12} = 1.17 \text{ x}10^5 \text{ ft-lb}$$

$$M_{cr}(N\text{-}S) = \frac{474 \times 47,000}{19.2} \times \frac{1}{12} = 0.97 \text{ x}10^5 \text{ ft-lb}$$

interior panel $M_a = \dfrac{w_s l^2}{16} = \dfrac{20 \times 450(25)^2}{16}$ for E-W

$= 3.52 \times 10^5$ ft-lb (M_a)

$\dfrac{25 \times 450(20)^2}{16}$ for N-S

$= 2.81 \times 10^5$ ft-lb

Note that the moment factor l/16 is used to be on the safe side, although the actual moment coefficients for two-way action would have been smaller.

E-W effective moment of inertia I_e

$$\frac{M_{cr}}{M_a} = \frac{1.17 \times 10^5}{3.52 \times 10^5} = 0.332$$

$$\left(\frac{M_{cr}}{M_a}\right)^3 = 0.037$$

$$I_e = 0.037 \times 63,600 + (1 - 0.037)45,500 = 46,200 \text{ in.}^4$$

N-S effective moment of inertia I_e

$$\frac{M_{cr}}{M_a} = \frac{0.97 \times 10^5}{2.81 \times 10^5} = 0.345$$

$$\left(\frac{M_{cr}}{M_a}\right)^3 = 0.041$$

$$I_e = 0.041 \times 47,000 + (1 - 0.041)32,500 = 33,100 \text{ in.}^4$$

$$\frac{I_g}{I_e} = \frac{1}{2}\left(\frac{63,600}{46,200} + \frac{47,000}{33,100}\right) = 1.40$$

Adjusted central deflection for cracked section effect

$= 1.40 \times 0.28 = 0.39$ in. (10 mm)

$$\frac{\ell}{\delta} = \frac{25 \, ft \times 12}{0.39} = 769 > 480 \quad \text{allowed in Table 4.2.}$$

Hence, the long-term central deflection is acceptable.

Example A4.2-Deflection calculation for a flat plate using the crossing beam method

An edge panel of 6 in. (150 mm) flat plate with multiple panels in each direction is shown in Fig. A4.2. The plate is supported on 16 in. x 16 in. (406 mm x 406 mm) columns. The slab is designed for an unfactored live load of 60 psf (2.87 kPa) in addition to its self-weight of 75 psf (3.59 kPa). Assume that the slab is subjected to significant in-plane restraint. Check the live load deflection and incremental deflection at mid-panel if non-structural components are installed one month after removal of shoring. Material properties are:

f_c' = 3000 psi (20.7 MPa)

f_y = 60,000 psi (414 MPa)

E_c = 3.12 x 10^{-6} psi (21,500 MPa)

Using Eq. 4.4, deflection of column and middle strips can be obtained from

$$\delta = \frac{5}{48} \frac{\ell_n^2}{E_c I_e} [M_m + 0.1 \, (M_1 + M_2)]$$

in which moments and I_e are computed for a strip of unit width.

The mid-panel deflection is computed as the sum of the column strip deflection in the N-S direction and the middle strip deflection i the E-W direction. Moments at unfactored load level due to dead plus live load are given in Table A4.1.

Cracking moment (M_{cr})

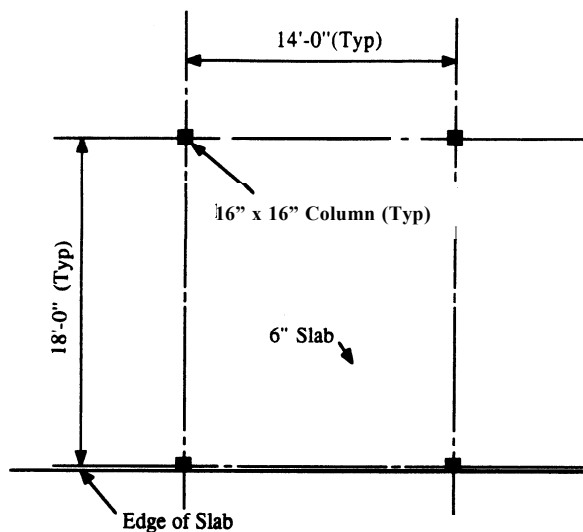f_r = 4 $\sqrt{f_c'}$ (significant restraint)

= 219 psi

Fig. A4.2-Plan of flat plate edge panel in Ex. A4.2, beam crossing calculation method

$$M_{cr} = \frac{f_r I_g}{y_t}$$

$$I_g = 1/12 \ (12) \ (6)^3 = 216 \ \text{in.}^4$$

$$y_t = 6/2 = 3 \ \text{in.}$$

$$M_{cr} = \frac{(219) \ (216)}{3} \left(\frac{1}{12,000}\right)$$

$$= 1.314 \ \text{ft. kips/ft}$$

Effective moment of inertia (I_e)

$$I_e = \left(\frac{M_{cr}}{M_a}\right)^3 I_g + \left[1 - \left(\frac{M_{cr}}{M_a}\right)^3\right] I_{cr}$$

(See Table 4.1 for tabulated values)

Average I_e for column strip = 52.2 in.^{4}

Average I_e for middle strip = 216 in.^{4}

Column strip deflection

$$\delta_c = \frac{(5) \ (16.7 \times 12)^2}{(48) \ (3,120,000) \ (52.2)} \ [2.93 + 0.1(-2.45 -$$
$$4.94)](12,000)$$
$$= 0.67 \ \text{in.}$$

Middle strip deflection

$$\delta_m = \frac{(5) \ (12.7 \times 12)^2}{(48) \ (3,120,000)(216)} \ [0.63 + 0.1(-0.72 - $$
$$0.72)] \ (12,000)$$
$$= 0.02 \ \text{in.}$$

Mid-panel deflection

$$\delta = \delta_c + \delta_m = 0.69 \ \text{in.}$$

Live load deflection

$$\delta_L = \left(\frac{w_L}{w_D + w_L}\right) 0.69 = \frac{(60)}{(135)} \ (0.69) = 0.31 \ \text{in.}$$

Span length on diagonal

$$= \sqrt{16.7^2 + 12.7^2} = 20.94 \ \text{ft.} = 251 \ \text{in.}$$

Permissible live load deflection

$$= \frac{\ell}{360} = \frac{251}{360}$$

$$= 0.70 \ \text{in.}$$
$$> 0.31 \ \text{in} \ . \ . \ . \ \text{OK for short-term deflection}$$

Incremental deflection

Use long-term multiplier = 2.5 applied to sustained load deflection.

Assume sustained load = 75 + 20 = 95 psf

$$\text{Instantaneous deflection} = \left(\frac{95}{135}\right)(0.69) = 0.49 \ \text{in.}$$

$$\text{Additional long-term deflection} = (2.5)(0.49) = 1.23 \ \text{in.}$$

$$\text{Long-term deflection at one month} = \left(\frac{0.5}{2.0}\right)(1.23) = 0.31 \ \text{in.}$$

Incremental deflection = 1.23 · 0.31 = 0.92 in.

$$\text{Additional live load deflection} = \left(\frac{40}{135}\right)(0.69) = 0.20 \ \text{in.}$$

Total = 1.12 in.

$$\text{Permissible deflection} = \frac{\ell}{480} = \frac{251}{480} = 0.53 \ \text{in.}$$

< 1.12 in. . . . NG for long-term deflection

Hence, camber the slab or revise the design if non-structural components are supported.

CHAPTER 5-REDUCING DEFLECTION OF CONCRETE MEMBERS*

5.l-Introduction

Building structures designed by limit states approach may have adequate strength but unsatisfactory serviceability response. Namely, they may exhibit excessive deflection. Thus, the size of many flexural members is in

---

* Principle author: R. S. Fling.

Table A4.1-Calculation of I_e for column and middle strips

	N-S column strip			E-W middle strip		
	Ext. Neg. (M_1)	Pos. (M_m)	Int. Neg. (M_2)	Neg. (M_1)	Pos. (M_m)	Neg. (M_2)
Moments (M_a) ft kips/ft	2.45	2.93	4.94	0.72 ($< M_{cr}$)	0.63 ($< M_{cr}$)	0.72 ($< M_{cr}$
$\left(\dfrac{M_{cr}}{M_a}\right)^3$	0.154	0.09	0.02	—	—	—
$1 - \left(\dfrac{M_{cr}}{M_a}\right)^3$	0.846	0.91	0.98	—	—	—
I_{cr} (in.^{4})	26.8	34.3	46.7	—	—	—
I_e	56.0	50.6	50.1	216 ($= I_g$)	216 ($= I_g$)	216 ($= I_g$)
I_e (average)	52.2			216		

many cases determined by deflection response rather than by strength. This Chapter proposes design procedures for reducing the expected deflection that will enable design engineers to proportion building structures to meet both strength and serviceability requirements. The result could be more economical structures compared to those designed with unnecessarily conservative deflection response. The discussion assumes that a competent design is prepared in accordance with *Building Code Requirements for Reinforced Concrete* (ACI 318) and construction follows good practices.

To properly evaluate options for reducing deflection, a design engineer must know the level of stress in the member under consideration, that is, whether the member is uncracked, partially cracked or fully cracked. Heavily reinforced members tend to be fully cracked because of the heavy loads they are subjected to. In this Chapter, only two limiting conditions are considered, uncracked members and fully cracked members. If the applied moment in the positive region is more than twice the cracking moment, considering the effect of flanges, the member may be considered as fully cracked. Frequently, a member is only partially cracked ($M_{cr} < M_a < 2M_{cr}$) and the statements about both limiting conditions are not strictly applicable. Engineering judgement and appropriate calculations should be made to assess the actual serviceability conditions of the beam. Chapter 2 and 3 of this report outline methods for computing the degree of cracking in a member.

In addition to the stress conditions, there may be physical or nonstructural constraints on the use of some options such as limits on increasing concrete dimensions. All options must be evaluated in terms of cost since some may increase the cost, and some may have offsetting considerations that reduce the cost, while still others may have little effect on cost. For each option presented, there is a discussion on the effect of implementation on deflection, the approximate range of potential reduction

of deflection, and appropriate situations in which the option should be considered. The options are arranged in three groups; Design techniques, Construction techniques, and Materials selection.

5.2-Design techniques

5.2.1 *Increasing section depth*-Increasing the depth may not be possible after schematic design of the possible after schematic design of the building has been established because such dimensional changes may affect the architectural and mechanical work. However, there are many instances where beam depth can be increased. The reduction in deflection is approximately proportional to the square of the ratio of effective depth, *d,* for cracked sections and to the cube of the ratio of total concrete depths for uncracked sections. This is based on the fact that the cracked moment of inertia, I_{cr} is expressed as,

$I_{cr} = nA_s(1-k)jd^2$ in reinforced concrete and
$I_{cr} = n_p A_{ps}d^2(1-1.6\sqrt{n_p\rho_p})$ in prestressed concrete. Hence,

$I_{cr} = (f)d^2$ or $I_{cr} = (f)d_p^2$ and the gross moment of inertia $I_g = bh^3/12$ for a rectangular section, namely $I_g = (f)d^3$. For example, if an 18 in.-deep, rectangular beam with an effective depth of 15.5 in. is increased to 20 in. deep, and all other parameters are kept the same, the cracked stiffness will increase by 27 percent [(17.5/15.5)2 = 1.27], and the uncracked stiffness will increase by 37 percent [$(20/18)^3$ = 1.37]. For heavily reinforced members, if the amount of reinforcement is reduced when the depth is increased, the cracked stiffness is increased only in proportion to the increase in depth or by 13 percent for this example. This can be seen from substituting for the reinforcement area its equivalent value M/f_sjd in the expression Icr= $A_s(1-k)jd^2$ giving $I = f(d)$. The increase in stiffness of an uncracked T-beam when it is made deeper will be less than that for a rectangular beam because the flanges do not change. Flanges tend to have

a fixed influence rather than a proportional influence on uncracked stiffness.

If, by increasing the depth, the concrete tensile stress in a member is reduced sufficiently so that it changes from a cracked, or partially cracked, to an uncracked member, the stiffness could increase dramatically. The uncracked stiffness can be as much as three times the partially cracked stiffness (Grossman, 1981).

5.2.2 *Increasing section width*-This option is not applicable to slabs or other members with physical constraints on their width. Where beams cannot be made deeper because of floor to floor height limitations, but can be made wider, the increase in stiffness is proportional to the increase in width if the member is uncracked. If the member is cracked and remains cracked after increasing the width, the increase in stiffness is very small. However, if a cracked member becomes uncracked because the width is increased, its stiffness increases appreciably, possibly by as much as a factor of three (Grossman, 1981).

5.2.3 *Addition of compression reinforcement*-Using ACI 318 procedures, compression reinforcement has some effect on immediate deflection as it can influence I_{cr}; thus I_e will be affected, as will the initial deflection, however small the influence is. But it can reduce additional long-term or incremental deflection up to about 50 percent (ACI 318, 1989). The effect on total deflection is somewhat less. The addition of compression reinforcement reduces the additional long-term deflection in the example to 0.50 in. or by 50 percent and the total deflection to 1.00 in. or by 33 percent.

Long-term deflection has two components, creep deflection and shrinkage warping. Compression reinforcement reduces deflection because concrete creep tends to transfer the compression force to the compression reinforcement which does not itself creep. The closer the reinforcement is to the compression face of the member, the more effective steel reinforcement is in reducing long-term creep deflection. Thus, compression reinforcement is more effective in deeper than in shallower beams or slabs if the concrete cover to the compression face of the member is of constant value. For some very shallow members, due to the requirements of minimum bar cover, compression reinforcement could be at or near the neutral axis and be almost totally ineffective in reducing long-term creep deflection.

Shrinkage warping occurs where the centroids of the steel reinforcement and the concrete do not coincide and the shrinkage of concrete, combined with the dimensional stability of steel reinforcement, warps the member in a fashion similar to a piece of bimetal subject to temperature variations. Compression reinforcement reduces shrinkage warping because it brings the centroid of the tension and compression reinforcement closer to the concrete neutral axis. While compression reinforcement reduces shrinkage and warping of all flexural members, it is especially effective for T-beams where the neutral axis is close to the compression face and far from the tension

reinforcement. If the T-beam has a thin slab subject to higher than normal shrinkage because of its high surface-to-volume ratio, then compression reinforcement will be more effective than for a rectangular beam. This will be true for ribbed slabs or joist systems as well.

5.2.4 *Addition of tension reinforcement*-For uncracked members, addition of tension reinforcement has hardly any effect on deflection. For fully cracked members, addition of tension reinforcement reduces both immediate and long-term deflection almost in proportion to the increase in the steel reinforcement area. This can be seen from the cracked moment of inertia, I_{cr}, defined in Section 5.2.1. For all practical purposes $I_{cr} \approx 0.9 A_s$ since the variation in the term $(1-k)j$ is usually small. For example, if the total deflection of a cracked member is 1.50 in. as in the previous example, increasing the tension reinforcement by 50 percent will reduce the deflection to about 1.10 in. However, the increased reinforcement area should still be less than the maximum permitted by ACl 318, namely a maximum of 0.75 times the balanced ratio ρ_b. This option is most useful for lightly reinforced solid and ribbed slabs. The option of adding more tension reinforcement is not available or is limited for heavily reinforced beams unless compression reinforcement is also added to balance the increase in tension bar area in excess of 0.75 ρ_b.

5.2.5 *Prestressing application*-Dead load deflection of reinforced concrete members may be reduced substantially by the addition of prestressing. However, deflections in prestressed concrete members due to live load and other transient loads are about the same as those in reinforced concrete members of the same stiffness, EI. If prestressing keeps the member in an uncracked state, without which it would otherwise crack, the live load deflection would be considerably smaller. If, however, the prestressed member size is reduced, as is usually the case in order to take advantage of prestressing, then the live load deflection becomes larger.

Consequently, the span/depth ratio in post-tensioned two-way floors is normally limited to 48 in lower floor slabs with light live load and 52 in roof slabs (ACI 318 Section R18.2.3, 1989). If the member has a high ratio of live to dead load, then the span/depth ratio must be proportionally reduced in order to give satisfactory deflection performance. A prestressing force sufficient to produce satisfactory deflection response should always be provided, regardless of whether the member is uncracked at service load or it is designed as partially prestressed with tolerable flexural crack width levels which are controlled by additional mild steel reinforcement.

5.2.6 *Revision of structure geometry*-Common solutions to reduce deflections include increasing the number of columns in order to reduce the length of the spans, adding cross members to create two-way systems, and increasing the size of columns to provide more end restraint to flexural members.

5.2.7 *Revision of deflection Limit criteria*-If deflection of a member is "excessive," the deflection limits may be

re-examined to determine if they are unnecessarily restrictive. If experience or analysis indicates that those limits (see Chapters 2 and 3) can be relaxed, then other action might not be required. Many building codes do not set absolute limits on deflection. An engineer might determine that the building occupancy, or construction conditions, such as a sloping roof, do not require the normal deflection limits.

5.3-Construction techniques

5.3.1 *Concrete curing to allow gain in strength-* Deflection response is determined by concrete strength at first loading, not by final concrete strength. If the construction schedule makes early loading of the concrete likely or desirable, then measures to ensure high-strength at first loading or construction loading can be effective. For example, if at the design compressive strength f'c of 4000 psi, the member would be uncracked as designed, but it is loaded when concrete strength is 2500 psi, it could be excessively cracked due to a lower modulus of rupture at the time of loading. Even though its final load-carrying capacity was satisfactory, the cracked member could still deflect several times more than a similar uncracked one. Furthermore, the modulus of elasticity of a 4000 psi concrete is higher than that of 2500 psi concrete (see Section 5.4 of this report for the effects of material selection on these parameters).

5.3.2 *Concrete curing to reduce shrinkage and creep-* Immediate deflection will not be greatly affected by concrete curing but additional long-term deflection will be reduced. Assuming the long-term component of deflection is evenly divided between shrinkage and creep, if shrinkage is reduced 20 percent by good curing, the additional long-term deflection due to shrinkage will be reduced by 10 percent. The effect will be most pronounced on members subject to high shrinkage such as those with a high surface/volume ratio (smaller members), those with thin flanges, and structures in arid atmospheres or members which are restrained. The effect of good curing on creep is similar to its effect on shrinkage.

5.3.3 *Control of shoring and reshoring procedures-* Many studies indicate that the shoring load on floors of multi-story buildings can be up to twice the dead weight of the concrete slab itself. Because the design super-imposed load is frequently less than the concrete self weight, the slab may be seriously overstressed and cracked due to shoring loads instead of remaining un-cracked as assumed by calculations based on design loads only. Thus, the flexural stiffness could be reduced to as little as one third of the value calculated assuming design loads only. Furthermore, the shoring loads may be imposed on the floor slabs before the concrete has reached its design strength (see discussion in Section 5.3.1).

Construction of formwork and shoring should ensure that a sag or negative camber is not built into the slab. Experience indicates that frequently the apparent deflection varies widely between slabs of identical design and construction. Some reasons for this may be that such slabs were not all built level or at the specified grade or the method and timing of form stripping was not uniformly applied. Also, construction loads may not have been applied uniformly.

5.3.4 *Delay of the first loading-*This allows the concrete to gain more strength before loading or helps to reach its design strength. Both the modulus of elasticity E_c and the modulus of **rupture** f_r will be increased. An increase in E_c increases the flexural stiffness. An increase in the modulus of rupture value, f_r, reduces the amount of cracking or even allows the member to remain un-cracked with an increase in flexural stiffness EI as noted in the next section.

5.3.5 *Delay in installation of deflection-sensitive elements or equipment-*Such delay in equipment installation will have no effect on immediate or total deflection, except as previously noted in 5.3.1. But incremental deflection will be reduced, namely the deflection occurring from the time a deflection-sensitive component is installed until it is removed or the deflection reaches its final value. For example, if the additional long-term deflection is 1.00 in., and installation of partitions is delayed for 3 months, the incremental deflection will be approximately 0.50 in. or about one-half as much as the total deflection.

5.3.6 *Location of deflection-sensitive equipment to avoid deflection problems-*Equipment such as printing presses, scientific equipment and the like must remain level and should be located at mid-span where the change in slope is very small with the increase in deflection. On the other hand, because the amplitude of vibration is highest at mid-span, vibration-sensitive equipment may be best located near the supports.

5.3.7 *Provision of architectural details to accommodate expected deflection-*Partitions that abut columns, as an example, may show the effect of deflection by separating horizontally from the column near the top even though the partition is not cracked or otherwise damaged. Architectural details should accommodate such movements. Likewise, windows, walls, partitions, and other non-structural elements supported by or located under deflecting concrete members should be provided with slip joints in order to accommodate the expected deflections or differential deflections between concrete members above and below the non-structural elements.

5.3.8 *Building camber into floor slabs-*Built in camber has no effect on the computed deflection of a slab. However, cambering is effective for installation of partitions and equipment, if the objective is to have a level floor slab after deflection takes place. For best results, deflection must be carefully calculated using the appropriate modulus of concrete E_c value and the correct moment of inertia I. Overestimating the deflection value can lead the designer to specify unreasonable overcambering. Hence, the pattern and value of cambering at several locations has to be specified and the results monitored during construction. Procedures have to be revised as necessary for slabs which are to be constructed

at a later date.

5.3.9 *Ensuring that top bars are not displaced downward*-Downward displacement of top bars always reduces strength. The effect on deflection in uncracked members is minimal. But its effect on cracked members, namely those that are heavily loaded, is in proportion to the square of the ratio of change in effective depths for cantilevers but much less for continuous spans. This reduced effect in continuous members is because the flexural stiffness and resulting deflection of the member is determined primarily by member stiffness at the midspan section. Thus, the deflection of cantilevers is particularly sensitive to misplacement of the top reinforcing bars. Deflection could increase, in continuous members, if the reduction in strength at negative moment regions results in redistribution of moments.

5.4-Materials selection

5.4.1 *Selection of materials for mix design that reduce shrinkage and creep or increase the moduli of elasticity and rupture*-Materials having an effect on these properties include aggregates, cement, silica fume, and admixtures. Lower water/cement ratio, a lower slump and changes in other materials proportions can reduce shrinkage and creep or increase the moduli of elasticity or rupture.

5.4.2 *Use of concretes with a higher modulus of elasticity*-Using AC1 318 procedures, the stiffness of an uncracked member increases in proportion to the elastic modulus which varies in proportion to the square root of the cylinder strength. (ACI 318, 1989, Sections 9.5.2.2 and 8.5) The stiffness of a cracked section is affected little by a change in the modulus of elasticity.

5.4.3 *Use of concretes with a higher modulus of rupture* -Concrete with a higher modulus of rupture does not necessarily increase the stiffness of uncracked members and highly cracked members. Stiffness of partially cracked members increases because of the reduction of the degree of cracking. The increase in stiffness (decrease in deflection) depends on steel reinforcement percentage, the increase in modulus of rupture, and the magnitude of applied moment.

5.4.4 *Addition of short discrete fibers to the concrete mix*--Such materials have been reported to reduce shrinkage and increase the cracking strength, both of which might reduce deflection (Alsayed, 1993).

5.5-Summary

Table 5.1 summarizes some of the preventive measures needed to reduce or control deflection. This table can serve as a general guide to the design engineer but is not all inclusive, and engineering judgement has to be exercised in the choice of the most effective parameters that control deflection behavior.

<div align="center">

REFERENCES

</div>

Chapter 2

"Building Code Requirements for Reinforced Con-

crete and Commentary," ACI 318, American Concrete Institute, Detroit, Michigan, 1989, 353 pp.

"Prediction of Creep, Shrinkage, and Temperature Effects in Concrete Structures," SP-27, American Concrete Institute, Detroit, 1971, pp. 51-93; SP-76, 1982, pp. 193-300.

"Prediction of Creep, Shrinkage and Temperature Effects in Concrete Structures," American Concrete Institute, ACI-209R-92, *Manual of Concrete Practice,* 1994, pp. l-47.

"State-of-the-Art Report on High Strength Concrete," ACI JOURNAL, *Proceedings,* V. 81, No. 4, July-August 1984, pp. 364-410.

"State-of-the-Art Report on Temperature-Induced Deflections of Reinforced Concrete Members," SP-86, American Concrete Institute, Detroit, 1985, pp. 1-14.

ACI Committee 435, Building Code Subcommittee, "Proposed Revisions by Committee 435 to AC1 Building Code and Commentary Provisions on Deflections," ACI JOURNAL, *Proceedings,* V. 75, No. 6, June 1978, pp. 229-238.

ACI Committee 435, Subcommittee 7, "Deflections of Continous Concrete Beams," ACI JOURNAL, *Proceedings,* V. 70, No. 12, Dec. 1973, pp. 781-787.

ACI Committee 435, Subcommittee 2, "Variability of Deflections of Simply Supported Reinforced Concrete Beams," ACI JOURNAL, *Proceedings,* V. 69, No. 1, Jan. 1972, pp. 29.35.

"Prediction of Creep, Shrinkage, and Temperature Effects in Concrete Structures," SP-27, American Concrete Institute, Detroit, 1971, pp. 51-93.

ACI Committee 435, Subcommittee 1, "Allowable Deflections," ACI JOURNAL, *Proceedings,* V. 65, No. 6, June 1968, pp. 433-444.

ACI Committee 435, "Deflections of Reinforced Concrete Flexural Members", ACI JOURNAL, *Proceedings* V. 63, No. 6, June 1966, pp. 637-674.

Ahmad, S.H., and Shah, S.P., "Stress-Strain Curves of Concrete Confined by Spiral Reinforcement," ACI JOURNAL, *Proceedings,* V. 79, No. 6, Nov.-Dec. 1982, pp. 484.490.

Al-Zaid, R., Al-Shaikh, A.H., and Abu-Hussein, M., "Effect of Loading Type on the Effective Moment of Inertia of Reinforced Concrete Beams," *ACI Structural Journal,* V. 88, No. 2, March-April 1991, pp. 184-190.

ASCE Task Committee on Finite Element Analysis of Reinforced Concrete Structures, "Finite Element Analysis of Reinforced Concrete," ASCE, 1982, New York, 545 pp.

Bazant, Z.P, Panula, L., "Creep and Shrinkage Characterization for Analyzing Prestressed Concrete Structures," *PCI Journal,* V. 25, No. 3, May-June 1980, pp. 86-122.

Beeby, A.W., "Short Term Deformations of Reinforced Concrete Members," *Cement and Concrete Association Technical Report,* TRA 408, London, Mar. 1968.

Branson, D.E., Chapter 2-"Deflections", *Handbook of Concrete Engineering,* Second Edition, Van Nortrand

Table 5.1-Deflection reducing options

Option	Effect on section stiffness	
	Cracked	Uncracked
Design techniques		
1. Deeper members	$(h^*/h)^3$ for rectangular beams. Less for T-beams.	$(d^*/d)^2$ or (d^*/d). If change to uncracked section, up to 300 percent.
2. Wider members	(b^*/b)	Small unless changed to uncracked section.
3. Add A_s'	Up to 50 percent for Δ_{LT}. No effect for Δ_i.	Up to 50 percent for Δ_{LT}. No effect for Δ_i.
4. Add A_s	No effect.	A_s^*/A_s.
5. Add prestress	Reduces dead load deflection to nearly zero.	Reduces dead load deflection to nearly zero and member to uncracked.
6. Structural geometry	Large effect.	Large effect.
7. Revise criteria	See text.	See text.
Construction techniques		
8. Cure: f_c'	Same as higher E_c and f_r	Same as higher E_c and f_r and could change to uncracked section.
9. Cure: ϵ_{sh} and ϵ_{cr}	For long-term deflection $(\epsilon_{sh}^*/\epsilon_{sh})$ and $(\epsilon_{cr}^*/\epsilon_{cr})$.	For long-term deflection $(\epsilon_{sh}^*/\epsilon_{sh})$ and $(\epsilon_{cr}^*/\epsilon_{cr})$.
10. Choring	Large effect, see text.	Large effect, see text.
11. Delay first loading	Similar to options in Section 5.4.	Similar to options in Section 5.4.
12. Delay installation	Up to 50 percent+ depending on time delay.	Up to 50 percent+ depending on time delay.
13. Locate equipment	See text.	See text.
14. Architectural details	See text.	See text.
15. Camber	See text.	See text.
16. Top bars	No effect.	Up to $(d^*/d)^2$ for cantilevers.
Materials		
17. Materials	See Section 5.4.	See Section 5.4.
18. Mix design	See Sections 5.4.2 and 5.4.3.	See Sections 5.4.2 and 5.4.3.
19. Higher E_c	(E_c^*/E_c) or $(f_c'^*/f_c')^{0.5}$.	Small.
20. Higher f_r	None.	Significant.
21. Use fiber reinforcement.	See Sections 5.3.2 and 5.4.4.	See Sections 5.3.2 and 5.4.4.

* = a superscript denoting parameters that have been changed to reduce deflection.
Δ = deflection.
ϵ = strains; ϵ_{sh} = shrinkage strain; and ϵ_{cr} = creep strain.
Other symbols are the same as those specified in the ACI 318-89 (Revised 1992) code.

Reinhold Co., New York, Editor, M. Fintel, 1985, pp. 53-78.

Branson, D.E., and Trost, H., "Unified Procedures for Predicting the Deflection and Centroidal Axis Location of Partially Cracked Non-Prestressed Members," ACI JOURNAL, *Proceedings,* V. 79, No. 2, Mar.-Apr. 1982, pp. 119-130.

Branson, D.E., *Deformation of Concrete Structures,* McGraw Hill Book Co., Advanced Book Program, New York, 1977, 546 pp.

Branson, D.E., and Cristianson, M.L., "Time-Dependent Concrete Properties Related to Design-Strength and Elastic Properties, Creep and Shrinkage," ACI Special Publication, SP-27, 1971, pp. 257-277.

Branson, D.E., and Kripanarayanan, KM., "Loss of Prestress, Camber and Deflection of Non-Composite and Composite Prestressed Concrete Structures," *PCI Journal,* V. 16, Sept.-Oct. 1971, pp. 22-52.

Branson, D.E., "Compression Steel Effect on Long-Time Deflections," ACI JOURNAL, *Proceedings,* V. 68,

No. 8, Aug. 1971, pp. 555-559.

Branson, D.E., "Instantaneous and Time-Dependent Deflections of Simple and Continous Reinforced Concrete Beams," *HPR Publication* No.7, Part 1, Alabama Highway Department, U.S. Bureau of Public Roads, Aug. 1963, pp. l-78.

Carrasquillo, R.L., Nilson, A.H., and Slate, F.O., "Properties of High Strengh Concrete Subjected to Short Term Loads," ACI JOURNAL, *Proceedings,* V. 78, No. 3, May-June 1981, pp. 171-178.

CEB Commission IV, Deformations, Portland Cement Association, Foreign Literature Study 547, 1968.

Comite-International du Beton (CEB) - Federation Internationale de la Pricontrainte (FIP), *Model Code for Concrete Structures,* 1990, P.O. Box 88, CH-1015, Lausanne.

Ghali, A., "Deflection Prediction in Two-Way Floors," *ACI Structural Journal,* V. 86, No. 5, Sept.- Oct. 1989, pp. 551-562.

Ghali, A., and Favre, R., *Concrete Structures: Stresses and Deformations,* Chapman and Hall, London and New York, 1986, 352 pp.

Grossman, J.S., "Simplified Computations for Effective Moment of Inertia (Ie) and Minimum Thickness to Avoid Deflection Computations," ACI JOURNAL, *Proceedings,* V. 78, No. 6, Nov.-Dec., 1981, pp. 423-439. Also, Author Closure, ACI JOURNAL, *Proceedings,* V. 79, No. 5, Sept.-Oct., 1982, pp. 414-419.

Grossman, J.S., "Reinforced Concrete Design," *Building Structural Design Handbook,* R.N. White and C.G. Salmon, editors, John Wiley & Sons, New York, 1987, Ch. 22, pp 699-786.

Hsu, C.T., "A Simple Nonlinear Analysis of Continuous Reinforced Concrete Beams," *Journal of Engineering and Applied Science,* V. 2, No. 4, 1983, pp. 267-276.

Hsu, C.T., and Mirza, M.S., "A Study of Post-Yielding Deflection in Simply Supported Reinforced Concrete Beams," ACI SP-43, *Deflection of Concrete Structures,* American Concrete Institute, 1974, pp. 333-355, Closure, ACI JOURNAL, April 1975, pp. 179.

Luebkaman, C.H., Nilson, A.H., and Slate, F.O., "Sustained Load Deflection of High Strength Concrete Beams," *Research Report* No. 85-2, Dept. of Structural Engineering, Cornell University, February 1985.

Martin, I., "Effects of Environmental Conditions on Thermal Variations and Shrinkage of Concrete Structures in the United States," SP-27, 1971, pp. 279-300.

Martinez, S., Nilson, A.H., and Slate, F.O., "Spirally-Reinforced High Strength Concrete Columns," *Research Report* No. 82-10, Department of Structural Engineering, Cornell University, Ithaca, August 1982.

Meyers, B.L., and Thomas, E.W., Chapter 11, "Elasticity, Shrinkage, Creep, and Thermal Movement of Concrete," *Handbook of Structural Concrete,* MaGraw Hill, New York, Editors, Kong, Evans, Cohen, and Roll, 1983, pp. 11.1-11.33.

Nagataki, S., and Yonekura, A., "Studies of the Volume Changes of High Strength Concretes with Superplasticizer," *Journal,* Japan Prestressed Concrete Engineering Association, V. 20, 1978, pp. 26-33.

Nawy, E.G., *Reinforced Concrete — A Fundamental Approach,* Second Edition, Prentice Hall, 1990, 738 pp.

Nawy, E.G., "Structural Elements: Strength, Serviceability and Ductility," *Handbook of Structural Concrete,* McGraw Hill, New York, 1983, pp. 12.1-12.86.

Nawy, E.G., and Balaguru, P.N., "High Strength Concrete," *Handbook of Structural Concrete,* McGraw Hill, New York, 1983, pp. 5.1-5.33.

Nawy, E.G., and Neuworth, G., "Fiber Glass Reinforced Concrete Slabs and Beams," *Structural Division Journal,* ASCE, New York, pp. 421-440.

Ngab, AS., Nilson, A.H., and Slate, F.O., "Shrinkage and Creep of High Strength Concrete," ACI JOURNAL, *Proceedings,* V. 78, No. 4, July-August 1981, pp. 255-261.

Nilson, A.H., "Design Implications of Current Research on High Strength Concrete," American Concrete Institute, SP-87, 1985, pp. 85-117.

Nilson, A.H., Hover, K.C., and Paulson, K.A., "Immediate and Long-Term Deflection of High Strength Concrete Beams," *Report* 89-3, Cornell University, Department of Structural Engineering, May 1989,230 pp.

Park, R., and Paulay, T., *Reinforced Concrete Structures,* John Wiley & Sons, Inc., New York, 1975,769 PP.

Pfeifer, D.W.; Magura, D.D.; Russell, H.G.; and Corley, W.G., "Time Dependent Deformations in a 70 Story Structure," SP-37, American Concrete Institute, 1971, pp. 159-185.

Portland Cement Association, "Notes on ACI 318-83 Building Code Requirements for Reinforced Concrete with Design Applications," Skokie, Illinois, 1984.

Russell, H.G., and Corley, W.G., "Time-Dependent Behavior of Columns in Water Tower Place," SP-55, American Concrete Institue, 1978, pp. 347-373.

Saucier, K.L., Tynes, W.O., and Smith, E.F., "High Compressive-Strength Concrete-Report 3, Summary Report," *Miscellaneous Paper* No. 6-520, U.S. Army Engineer Waterways Experiment Station, Vicksburg, September 1965, 87 pp.

Swamy, R.N., and Anand, K.L., "Shrinkage and Creep of High Strength Concrete," *Civil Engineering and Public Works Review,* V. 68, No. 807, Oct. 1973, pp. 859-865, 867-868.

Teychenne, D.C., Parrot, L.J., and Pomeroy, C.D., "The Estimation of the Elastic Modulus of Concrete for the Design of Structures," Current paper No. CP23/78, Building Research Establishment, Garston, Watford, 1978, 11 pp.

Yu, W.W., and Winter, G., "Instantaneous and Long-Term Deflections of Reinforced Concrete Beams Under Working Loads," ACI JOURNAL, *Proceedings,* V. 57, No. 1, 1960, pp. 29-50.

Wang, C.K., and Salmon, C.G., *Reinforced Concrete Design* 5th Edition, Harper Collins, 1992, pp. 1030.

Chapter 3

ACI Committee 318, "Building Code Requirements for Reinforced Concrete (318-89) and Commentary-ACI 318R-89," American Concrete Institute, Detroit, 1989.

ACI Committee 209, "Prediction of Creep, Shrinkage, and Temperature Effects in Concrete Structures," American Concrete Institute, SP-76, 1982, pp. 193-300.

ACI Committee 435, Subcommittee 5, Scordelis, A.C., Branson, D.E., and Sozen, M.A., "Deflections of Prestressed Concrete Members," Manual of *Concrete Practice,* ACI 435.1R-63 (Reapproved 1979), pp. 2-14, and ACI Journal, *Proceedings,* V. 60, No. 12, Dec. 1963, pp. 1697-1728.

ACI Committee 435, "Deflections of Reinforced Concrete Flexural Members," ACI Journal, *Proceedings* V. 63, No. 6, part 1, June 1966, *ACI Manual of Concrete Practice,* Part 2: Structural Design, Structural Specifications, Structural Analysis, 1967, 1972, pp. 637-674.

ACI Committee 209, Subcommittee 2, and Committee 209, Prediction of Creep, Shrinkage and Temperature Effects in Concrete Structures, in "Designing for Effects of Creep, Shrinkage and Temperature in Concrete Structures," SP-27, 1971, pp. 51-93.

ACI - ASCE Joint Committee 423, *Prestressed Concrete Report,* "Estimating Prestress Losses", *Concrete International,* V. 1, No. 6, June 1979.

ACI Committee 435, *Designing Concrete Structures For Serviceability and Safety,* SP-133, American Concrete Institute, Detroit, 1993, pp. 346.

Aswad, A., "Time-Dependent Deflections of Prestressed Members: Rational and Approximate Methods," ACI Symposium on Creep and Shrinkage, February 22, 1989, Atlanta, GA.

Aswad, A., "Rational Deformation Prediction of Prestressed Members," SP-86, American Concrete Institute, Detroit, 1985, pp. 263-280.

Aswad, A., "Experience with Pre- and Post-Cracking Deflections of Pretensioned Members," ACI SP-133, American Concrete Institute, Detroit, 1992, pp. 207-224.

ACI Committee 435, Subcommittee 2, and Committee 435 "Variability of Deflections of Simply Supported Reinforced Concrete Beams," ACI Journal, *Proceedings* V. 69, No. 1, Jan. 1972, p. 29-35, with discussion, D. E. Branson, ACI Journal, *Proceedings,* V. 69, No. 7, July 1972, pp. 449-450.

Bazant, Z. P., "Prediction of Concrete Creep Effects Using Age-Adjusted Effective Modulus Method," ACI Journal, *Proceedings,* V. 69, No. 4, April 1972, pp. 212-217.

Branson, D. E., and Trost, H., "Application of the I-Effective Method in Calculating Deflections of Partially Prestressed Members," *PCI Journal,* V. 27, No. 6, Dec. 1982, pp. 86-111.

Branson, D.E., and Ozell, A.M., "Camber in Prestressed Concrete Beams," V. 57, No. 12, June 1961, pp. 1549-1574.

Branson, D.E., and Christianson, M.L., "Time-Dependent Concrete Properties Related to Design-Strength and Elastic Properties, Creep, and Shrinkage," SP 27, American Concrete Institute, Detroit, 1971, pp. 257-277.

Branson, D.E., and Kripanarayanan, K.M., "Loss of Prestress, Camber and Deflection of Non-composite and Composite Prestressed Concrete Structures,"PCI Journal, V. 16, Sept.-Oct. 1971, pp. 22-52.

Branson, D.E., "Compression Steel Effect on Long-Time Deflections," ACI Journal, *Proceedings,* V. 68, No. 8, Aug. 1971, pp. 323-363.

Branson, D.E., and Shaikh, A.F., "Deflection of Partially Prestressed Members," SP-86, American Concrete Institute, Detroit, 1985, pp. 323-363.

Branson, D. E., *Deformation of Concrete Structures,* New York: McGraw Hill, 1977, pp. 546.

Branson, D. E., "The Deformation of Non-Composite and Composite Prestressed Concrete Members," In *Deflection of Concrete Structures,* SP-43, American Concrete Institute, Detroit, 1974, pp. 83-127.

Branson, D. E., and Trost, H., "Unified Procedures for Predicting the Deflection and Centroidal Axis Location of Partially Cracked Nonprestressed and Prestressed Concrete Members," ACI Journal, *Proceedings,* V. 79, No. 5, Oct. 1982, pp. 62-77.

Branson, D.E., "Instantaneous and Time-dependent Deflections of Simple and Continuous Reinforced Concrete Beams," *HPR Publication 7,* Part 1, l-78, Alabama Highway Department, Bureau of Public Roads, Aug. 1963.

Branson, D.E., "Design Procedures for Computing Deflections," ACI Journal, *Proceedings,* V. 65, No. 9, Sept. 1968, pp. 730-742.

Branson, D.E., "The Deformation of Non-composite and Composite Prestressed Concrete Members," *Deflections of Concrete Structures,* SP-43, American Concrete Institute, Detroit, MI, 1970.

Collins, M.P. and Mitchell, D., "Shear and Torsion Design of Prestressed and Non-Prestressed Concrete Beams," *PCI Journal,* V. 25, No. 5, September-October 1980.

Comite' Euro-International du Beton (CEB) - Federation Internationale de la Precontrainte (FIP), *Model Code for Concrete Structures,* 1990, CEB, 6 rue Lauriston, F-75116, Paris.

Dilger, W.H., "Creep Analysis of Prestressed Concrete Structures Using Creep-Transformed Section Properties," *PCI Journal,* V. 27, No. 1, Jan.-Feb. 1982.

Elbadry, M.M. and Ghali, A., "Serviceability Design of Continuous Prestressed Concrete Structures," *PCI Journal,* V. 34, V.l, January-February, 1989, pp. 54-91.

Ghali, A., "A Unified Approach for Serviceability Design of Prestressed and Nonprestressed Reinforced Concrete Structures," *PCI Journal,* Vol. 31, No. 2, March-April 1986, 300 pp.

Ghali, A. and Favre, R., *Concrete Structures: Stresses and Deformations,* Chapman and Hall, London and New York, 1986, 300 pp.

Ghali, A., and Neville, A.M., *Structural Analysis-A*

Unified Classical and Matrix Approach, 3rd Edition, Chapman & Hall, New York, 1989, pp. 608409.

Herbert, T.J., "Computer Analysis of Deflections and Stresses in Stage Constructed Concrete Bridges," *PCI Journal,* V. 35, No. 3, May-June 1990, pp. 52-63.

Libby, J.R., *Modem Prestressed Concrete,* 3rd Edition, Van Nostrand Reinhold Company, New York, 1984, 635 p.

Martin, D.L., "A Rational Method for Estimating Camber and Deflection of Precast Prestressed Members," *PCI Journal,* V. 22, No. 1, January-February, 1977, pp. 100-108.

Mirza, M.S., and Sabnis, G.M., "Deflections of One-Way Slabs and Beams," Proceedings of Symposium, ACI Canadian Capital Chapter, Montreal, Canada, Oct. 1971, pp. 53-87.

Fling, R.S., "Practical Considerations in Computing Deflection of Reinforced Concrete," SP-133, American Concrete Institute, Detroit, 1993, pp. 69-92.

Naaman, A.E., *Prestressed Concrete Analysis and Design-Fundamentals,* First edition, McGraw Hill Book Co., New York, N.Y., 1982, 670 pp.

Naaman, A.E., "Time Dependent Deflection of Prestressed Beams by Pressure Line Method," *PCI Journal,* V. 28, No. 2, April 1983, pp. 98-119.

Naaman, A.E., "Partially Prestressed Concrete: Review and Recommendations," *Journal of the Prestressed Concrete Institute 30* (1985), pp. 30-71.

Nawy, E.G., and Potyondy, J.G., "Deflection Behavior of Spirally Confined Pretensioned Prestressed Concrete Flanged Beams," *PCI Journal,* V. 16, June 1971, pp. 44 - 59.

Nawy, E.G., and Potyondy, J.G., "Flexural Cracking Behavior of Pretensioned Prestressed Concrete I- and T-Beams," ACI JOURNAL, *Proceedings,* V. 68, 1971, pp. 335-360.

Nawy, E.G. and Potyondy, J.G., authors' closure and discussion by D. E. Branson of "Flexural Cracking Behavior of Pretensioned Prestressed Concrete I- and T-Beams," ACI JOURNAL, *Proceedings,* V. 68, No. 5, May 1971, discussion and closure, ACI JOURNAL, *Proceedings* V. 68, No. 11, Nov. 1971, pp. 873-877.

Nawy, E.G., and Huang, P.T., "Crack and Deflection Control of Pretensioned Prestressed Beams," *Journal of the Prestressed Concrete Institute,* V. 22 (1971), pp. 30-47.

Nawy, E.G., and Chiang, J.Y., "Serviceability Behavior of Post-Tensioned Beams," *Journal of the Prestressed Concrete Institute,* V. 25, 1980, pp. 74-95.

Nawy, E.G., *Prestressed Concrete-A Fundamental Approach,* Prentice Hall, Englewood Cliffs, N.J., 1989, 738 pp.

Nawy, E.G. and Balaguru, P.N., "High Strength Concrete," *Handbook of Structural Concrete,* McGraw Hill, New York, 1983, pp. 5.1-5.33.

Nilson, A.H., *Design of Prestressed Concrete, New* York: Wiley, 1987, pp 592.

Neville, A. M., and Dilger, W., *Creep of Concrete: Plain, Reinforced, and Prestressed,* North-Holland Publishing Company, Amsterdam, 1970, 622 pp.

Prestressed Concrete Institute, *PCI Design Handbook,* Chicago, Illinois, Fourth Edition, 1993.

PCI Committee on Prestress Losses, "Recommendations for Estimating Prestress Losses," *Journal of the Prestressed Concrete Institute,* V. 20, No. 4, July-August 1975.

Rangan, B.V., "Serviceability Design in Current Australian Code," SP-133, American Concrete Institute, Detroit 1993, pp. 93-110.

Shaikh, A.F. and Branson, D.E., "Non-Tensioned Steel in Prestressed Concrete Beams," *PCI Journal,* V. 15, No. 1, Feb. 1970, pp. 14-36.

Sirosh, S.N. and Ghali, N., "Reinforced Concrete Beam-Columns and Beams on Elastic Foundation," *Journal of Structural Engineering,* ASCE, V. 115, No.3, March 1989, pp. 666-682.

Tadros, M.K., "Expedient Service Load Analysis of Cracked Prestressed Concrete Sections," *PCI Journal, V.* 27, No. 6, Nov.-Dec. 1982, pp. 86-101.

Tadros, M.K., Ghali, A., and Dilger, W.H., "Effect of Non-Prestressed Steel on Prestressed Loss and Deflection," *PCI Journal,* Vol. 22, No. 2, March 1977, pp. 50.

Tadros, M.K., 'Expedient Service Load Analysis of Cracked Prestressed Concrete Sections," *PCI Journal,* V. *27,* Nov.-Dec. 1982, pp. 86-111. Also, see Discussion by Nilson, Branson, Shaikh, et al., *PCI Journal,* V. 28, No. 6, Nov.-Dec. 1983.

Tadros, M.K., and Sulieman, H., Discussion of "Unified Procedures for Predicting Deflections," by Branson and Trost, *PCI Journal,* V. 28, No. 6, Nov.-Dec., 1983, pp. 131-136.

Tadros, M.K., Ghali, A., and Meyer, A.W., "Prestress Loss and Deflection of Precast Concrete Members," *PCI Journal,* V. 30, No. 1, January-February 1985.

Tadros, M.K., and Ghah, A., "Deflection of Cracked Prestressed Concrete Members" SP-86, American Concrete Institute, Detroit, pp. 137-166.

Trost, H., "The Calculation of Deflections of Reinforced Concrete Members-A Rational Approach," SP-76, American Concrete Institute, Detroit, Michigan, 1982, pp. 89-108.

Chapter 4

"Prediction of Creep, Shrinkage, and Temperature Effects in Concrete Structures," ACI 209R-82 (Revised 1986), American Concrete Institute, Detroit, 1982.

"Control of Cracking in Concrete Structures," ACI 224R-80 (Revised 1984), American Concrete Institute, Detroit, 1980.

"Building Code Requirements for Reinforced Concrete (AC1 318-89)(Revised 1992) and Commentary-ACI 318R-89 (Revised 1992)," American Concrete Institute, Detroit, 1992, 345 pp.

"Recommended Practice for Concrete Formwork," ACI 347-78, American Concrete Institute, Detroit, 1978.

"Allowable Deflections," ACI 435.3R-68 (Reapproved 1989), American Concrete Institute, Detroit, 1968, 12 pp.

"Variability of Deflections of Simply Supported Reinforced Concrete Beams," AC1 435.4R-72 (Reapproved 1989), American Concrete Institute, Detroit, 1972, 7 pp.

"Deflection of Two-Way Reinforced Concrete Floor Systems: State-of-the-Art Report," ACI 435.6R-74 (Reapproved 1989), American Concrete Institute, Detroit, 1974, 24 pp.

"Observed Deflection of Reinforced Concrete Slab Systems, and Causes of Large Deflections," ACI 435, 8R-85 (Reapproved 1991), American Concrete Institute, Detroit, 1985.

"Flexural Strength of Concrete Using Simple Beam with Center Point Loading," ASTM C 293-79, American Society for Testing and Materials.

Aguinaga-Zapata, M., and Bazant, Z.P.," Creep Deflections in Slab Buildings and Forces in Shores During Construction," ACI JOURNAL, *Proceedings,* V. 83, No. 5, 1986, pp. 719-726.

ASCE Task Committee on Finite Element Analysis of Reinforced Concrete Structures, "Finite Element Analysis of Reinforced Concrete," American Society of Civil Engineers, New York, 1982, 553 pp.

Branson, D.E.,"Instantaneous and Time-Dependent Deflections of Simple and Continuous Reinforced Concrete Beams," *HPR Publication 7,* Part 1, Alabama Highway Department, Bureau of Public of Roads, Aug., 1963, pp. l-78.

Branson, D.E.,"Deformation of Concrete Structures," McGraw-Hill Book Company, New York, 1977, 546 pp.

Cook, R.D., "Concepts and Applications of Finite Element Analysis," John Wiley and Sons, 1974.

Gallagher, R. H., "Finite Element Analysis: Fundamentals," Prentice-Hall, Inc., New Jersey, 1975.

Gardner, N.J., "Shoring, Re-shoring and Safety," *Concrete International,* V. 7, No. 4, 1985, pp. 28-34.

Ghali, A., "Deflection Prediction in Two-Way Floors," *ACI Structural Journal,* V. 86, NO. 5, 1989, pp. 551-562.

Ghali, A., "Deflection of Prestressed Concrete Two-Way Floor Systems," *ACI Structural Journal,* V. 87, No. 1, 1989, pp. 60-65.

Ghali, A., and Favre, R., "Concrete Structures: Stresses and Deformations," Chapman and Hall, London and New York, 1986, 350 pp.

Ghosh, S.K,"Deflections of Two-Way Reinforced Concrete Slab Systems," *Proceedings,* International Conference on Forming Economical Concrete Buildings, Portland Cement Association, Skokie, 1982, pp. 29.1-29.21.

Gilbert, R.I.,"Deflection Control of Slabs Using Allowable Span to Depth Ratios," ACI JOURNAL, *Proceedings,* V. 82, No. 1, Jan.-Feb. 1985, pp. 67-77.

Gilbert, R.I.,"Determination of Slab Thickness in Suspended Post-Tensioned Floor Systems," V. 86, No. 5, Sep.-Oct. 1989, pp. 602-607.

Graham, C.J., and Scanlon, A., "Deflection of Reinforced Concrete Slabs under Construction Loading," SP-86, American Concrete Institute, Detroit, 1986.

Graham, C.J., and Scanlon, A., "Long Time Multipliers for Estimating Two-Way Slab Deflections," ACI JOURNAL, *Proceedings,* V. 83, No. 5, 1986, pp. 899-908.

Grossman, J.S., "Simplified Computations for Effective Moment of Inertia *Ie* and Minimum Thickness to Avoid Deflection Computations," ACI JOURNAL, *Proceedings,* V. 78, No. 6, Nov.-Dec. 1981, pp. 423-439.

Grossman, J.S., Chapter 22, *Building Structural Design Handbook,* R.N. White and C.G. Salmon editors, John Wiley and Sons, 1987.

Grundy, P., and Kabila, A., "Construction Loads on Slabs with Shored Formwork in Multi-story Buildings," ACI JOURNAL, *Proceedings,* V. 60, No. 12, December 1963, pp. 1729-1738.

Jensen, V.P., "Solutions for Certain Rectangular Slabs Continuous Over Flexible Supports," University of Illinois *Engineering Experimental Station Bulletin* No. 303, 1938.

Jokinen, E.P., and Scanlon, A., "Field Measured Two-Way Slab Deflections," *Proceedings,* 1985 Annual Conference, CSCE, Saskatoon, Canada, May 1985.

Kripanarayanan, K.M., and Branson, D.E., "Short-Time Deflections of Flat Plates, Flat Slabs, and Two-Way Slabs," ACI JOURNAL, *Proceedings,* V. 73, No. 12, December 1976, pp. 686-690.

Lin, T. Y., "Load-Balancing Method for Design and Analysis of Prestressed Concrete Structures," ACI JOURNAL, *Procedings,* V. 60, 1963, pp. 719-742.

Liu, X., Chen, W.F., and Bowman, M.D., "Construction Load Analysis for Concrete Structures," *Journal of Structural Engineering, V. 111, No. 5,1985, pp. 1019-1036.*

Meyers, B.L. and Thomas, E.W., Chapter 11, "Elasticity, Shrinkage, Creep and Thermal Movement of Concrete," *Handbook of Structural Concrete,* McGraw Hill, New York, 1983, pp. 11.1-11.33.

Nawy, E.G., *Reinforced Concrete-A Fundamental Approach,* 2nd edition, Prentice-Hall, 1990, 738 pp.

Nawy, E.G., *Prestressed Concrete-A Fundamental Approach,* Prentice Hall, 1989, 739 pp.

Nawy, E.G., and Neuewrth, G., "Fiber Glass Reinforced Concrete Slabs and Beams," Structural Division, ASCE *Journal,* 1977, pp. 421-440.

Nilson, A.H., and Walters, D.B. Jr., "Deflection of Two-Way Floor Systems by the Equivalent Frame Method," ACI JOURNAL, *Proceedings,* V. 72, No. 5, May 1975, pp. 210-218.

"Design of Post-Tensioned Slabs," Post-Tensioning Institute, Glenview Illinois, 1976, 52 pp.

Ramsay, R.J., Mina. S.A., and Macgregor, J.G., "Monte Carlo Study of Short Time Deflections of Reinforced Concrete Beams," ACI JOURNAL, *Proceedings,* V. 76, No. 8, August 1979, pp. 897-918.

Rangan, B.V., "Prediction of Long-Term Deflections of Flat Plates and Slabs," ACI JOURNAL, *Proceedings,* V. 73, No. 4, April 1976, pp. 223-226.

Rangan, B.V., "Control of Beam Deflections by Allowable Span to Depth Ratios," ACI JOURNAL, *Proceedings,* V. 79, No. 5, Sept.-Oct. 1982, pp. 372-377.

Sbarounis, J.A., "Multi-story Flat Plate Buildings -

Construction Loads and Immediate Deflections," *Concrete International,* V. 6., No. 2, February 1984, pp. 70-77.

Sbarounis, J.A., "Multi-story Flat Plate Buildings: Measured and Computed One-Year Deflections," *Concrete International,* V. 6, No. 8, August 1984, pp. 31-35.

Scanlon, A., and Murray D. W., "Practical Calculation of Two-Way Slab Deflections," *Concrete International,* November 1982, pp. 43-50.

Simmonds, S.H., "Deflection Considerations in the Design of Slabs," ASCE National Meeting on Transportation Engineering, Boston, Mass., July 1970, 9 pp.

Tam, K.S.S., and Scanlon, A., "Deflection of Two-Way Slabs Subjected to Restrained Volume Change and Transverse Loads," ACI JOURNAL, *Proceedings,* V. 83, No. 5, 1986, pp. 737-744.

Timoshenko, S. and Woinowsky-Krieger, S., *Theory of Plates and Shells,* McGraw-Hill Book Co., New York, 1959.

Thompson, D.P., and Scanlon, A., "Minimum Thickness Requirements for Control of Two-Way Slab Deflections," *ACI Structural Journal,* V. 85, No. 1, Jan.-Feb. 1986, pp. 12-22.

Vanderbilt, M.D., Sozen, M.A. and Siess, C.P., "Deflections of Multiple-Panel Reinforced Concrete Floor Slabs," *Proceedings,* ASCE, V. 91, No. ST4 Part 1, August 1965, pp. 77-101.

Zienkiewicz, O.C., *The Finite Element Method,* McGraw-Hill Book Co., 1977.

Chapter 5

"Building Code Requirements for Reinforced Concrete (ACI 318-89)(Revised 1992) and Commentary-ACI318R-89 (Revised 1992)," American Concrete Institute, Detroit, 1992, 345 pp.

Alsayed, S.H., "Flexural Deflection of Reinforced Fibrous Concrete Beams," *ACI Structural Journal,* V. **90,** No. 1, Jan.-Feb. 1993, pp. 72-76.

Grossman, Jacob S., "Simplified Computation for Effective Moment of Inertia, *Ie* and Minimum Thickness to Avoid Deflection Computations," ACI JOURNAL, *Proceedings,* V. 78, Nov.-Dec. 1981, pp. 423-439.

APPENDIX B—DETAILS OF THE SECTION CURVATURE METHOD FOR CALCULATING DEFLECTIONS[*]

This appendix presents a general method for calculating displacements (translations and rotations) in prestressed and nonprestressed reinforced concrete plane frames and beams. The method is based on analysis of strain distribution at individual sections to determine axial strain and curvature under prescribed loading conditions.

B1—Introduction

The body of this report discusses control of deflection by different means, including the choice of thickness of members, the selection of the material, and the construction techniques. It also discusses simplified calculation methods. The method in this appendix represents a more comprehensive method for the calculation of deformations in plane frames. Starting with the calculation of axial strain and curvature at individual sections, the variation of these parameters over the length of members is determined and used to calculate the translations or the rotations at any section. Thus, the comprehensive analysis requires more calculations than the simplified methods; it also requires more given (or assumed) data. It accounts for the time-dependent effects of creep and shrinkage of concrete and relaxation of prestressing steel, using time-dependent material parameters that need to be included in the given data. The comprehensive analysis is recommended when the deflection is critical and accuracy is necessary. In this case, the analysis gives at any section of a plane frame strain distribution that can be used to calculate displacement components, composed of translations in two orthogonal directions and a rotation. Thus, the analysis can give vertical deflections as well as horizontal drifts.

The general method in this appendix determines the displacements (translations and rotations) in prestressed and nonprestressed reinforced concrete plane frames. The general method is based on an analysis of strain distribution at a section considering the effects of a normal force and a moment caused by applied loads, prestressing, creep and shrinkage of concrete, and relaxation of prestressing steel. The calculated axial strain and the curvature at various sections of the frame can then be used to calculate displacement by virtual work or other classical techniques. The sectional analysis can accommodate the effects of creep and shrinkage of concrete and relaxation of the prestressing steel. A sensitivity analysis of the uncertainties can be performed to determine the effect of varying the time-dependent parameters on the calculated displacements.

The sectional analysis is intended for service conditions. A linear stress-strain relationship can be assumed for the concrete under service conditions, provided that the concrete stress does not exceed about half the compressive strength. At a crack location, the concrete section in tension is ignored. At an uncracked location, reinforcement bonded to the concrete causes increased stiffness, which should be

considered in the analysis of displacements (see Section B7). A linear stress-strain relationship is also assumed for the reinforcement. The method in this appendix can be applied not only for steel reinforcement but also for other reinforcement materials, such as fiber-reinforced polymers (Hall and Ghali 1997; ISIS Canada 2001)

Cracking changes the distribution of internal forces in statically indeterminate structures. For example, sections that crack over the supports of continuous beams result in reduced negative moments at these sections and increased positive moments at midspans. This redistribution of bending moments can be important in deflection calculations.

The procedure presented in this appendix is intended to compute deformations in service; it does not track the behavior as the load approaches ultimate. Approximations are involved for nonlinear effects when the concrete stress exceeds one-half its compressive strength and when unbonded post-tensioning is used. Strain compatibility of unbonded tendons and the adjacent concrete is not satisfied (Ariyawardena and Ghali 2002).

B1.1 *Notation*—

A	=	cross-sectional area
B	=	first moment of cross-sectional area
C_t	=	ratio of creep strain to the initial strain (occurring immediately after stress application)
dA	=	elemental area
E	=	modulus of elasticity
f_{ct}	=	tensile strength of concrete
I	=	second moment of cross-sectional area
I_e	=	effective second moment of cross-sectional area
ℓ	=	member length
M	=	bending moment
N	=	normal force
n	=	ratio of modulus of elasticity of reinforcement to modulus of elasticity of concrete
P	=	absolute value of prestressing force
t	=	time
y	=	distance measured downward from a horizontal x-axis
β	=	coefficient to account for the effects of bond quality of reinforcement, cyclic loading, and sustained loading on tension stiffening
γ	=	$d\sigma/dy$ = slope of stress diagram
δ	=	deflection or camber
ε	=	strain
ε_O	=	strain at reference point O
ε_{SH}	=	unrestrained shrinkage of concrete
κ	=	dimensionless coefficient used to calculate curvatures due to creep and shrinkage in reinforced nonprestressed sections (See Section B5.3)
σ	=	stress
σ_O	=	stress at reference point O
χ	=	aging coefficient
χ_r	=	reduction multiplier of the intrinsic relaxation
ϕ	=	curvature (= $d\varepsilon/dy$ = slope of strain diagram)
$\Delta\sigma_p$	=	intrinsic relaxation
$\Delta\sigma_{pr}$	=	reduced relaxation

Subscripts
1 and 2 =   uncracked state and cracked state, with concrete
            in tension ignored, respectively
c   =   concrete
cr   =   cracking
g   =   gross concrete cross section
m   =   mean value interpolated between States 1 and 2
ns   =   nonprestressing steel
ps   =   prestressing steel

B2—Background
Calculation of deflections of prestressed or nonprestressed reinforced concrete members is complicated by several factors, including shrinkage and creep of concrete, relaxation of prestressing reinforcement, and cracking. The analysis presented in this appendix can be used to determine the initial and the time-dependent stresses, strains, and displacement at service loads for prestressed or nonprestressed reinforced concrete members for which the internal forces are known. The procedure accounts for cracking; equilibrium and compatibility requirements of basic mechanics are satisfied.

The accuracy of deformation calculations for reinforced concrete structures depends upon the thoroughness of the analysis method and the accuracy of the parameters used as given data. These parameters include the moduli of elasticity of concrete, nonprestressing and prestressing reinforcements, the creep coefficient of concrete, the unrestrained shrinkage of concrete, relaxation of the prestressing reinforcement, and, when cracking occurs, the tensile strength of the concrete. It is impossible to eliminate the error caused by the uncertainty of the input parameters because they depend upon variables, such as the properties of the concrete, the ambient temperature, and the relative humidity. An analysis satisfying the two basic requirements of mechanics, equilibrium and compatibility, can reduce the error in the calculations. This appendix presents such a method for structural concrete frames. A study of the sensitivity of the calculated displacements to the values of the input parameters is presented in Ghali, Favre, and Elbadry (2002); a website for this book provides three computer programs to assist in the calculations.

For statically determinant structures, the equilibrium requires that the stress resultants at any cross section are not to be changed by the time-dependent effects of creep, shrinkage, and relaxation, and that the stress resultants be equal to the known normal force *N* and the bending moment *M*. Compatibility requires that the strains in bonded reinforcement and concrete are equal. For prestressing steel, this requirement applies to the change in strain occurring after transfer of the prestress force to the concrete. Most of this appendix deals with the analysis of stress and strain distributions in a cross section of a member. After the strain distribution has been determined, calculation of the deflected shape of the structure represents a geometry problem that has been covered in many textbooks (Ghali and Neville 1997); also refer to Section B8. The procedure of analysis presented in this appendix can be used to evaluate the validity of simplified analyses that do not adhere to the requirements of equilibrium and compatibility, such as use of a multiplier to

the initial deflection to give the deflection due to creep and shrinkage combined.

The analysis method can determine the upper and the lower bounds of probable deflections by varying the input parameters and repetition of the calculation. In statically indeterminate structures, the time-dependent effects can develop changes in the stress resultants; computation of these changes is discussed in Ghali, Favre, and Elbadry (2002).

B3—Cross-sectional analysis outline
Cross-sectional analysis is applicable for initial and time-dependent strains and stresses in prestressed and nonprestressed reinforced concrete structures. Cracking may occur depending on the amount of prestressing provided. The analysis assumes that structures are composed of members, for which plane cross sections remain plane after deformation. The strain distribution over the cross section, or a part of the cross section in the case of composite cross section, can be defined by two parameters: the normal strain ε_O at an arbitrary reference point *O* and the curvature ϕ, that is, the gradient of the strain over the depth of the section. The parameters ε_O and ϕ can be used to calculate displacement (translations and rotations) by established structural analysis methods, such as virtual work or moment area.

B4—Material properties
This section defines the material parameters required as input in the calculation of displacement. The parameters are:
E_c =   the modulus of elasticity of concrete;
C_t =   the creep coefficient;
χ =   the aging coefficient;
ε_{SH} =   the free shrinkage of concrete; and
$\Delta\sigma_p$ =   the intrinsic relaxation of the prestressing steel.
Guidance on the values of E_c, C_t, ε_{SH}, χ, and $\Delta\sigma_p$ to be used in design are given in ACI 209R, CEB-FIP (1990), and Magura, Sozen, and Siess (1964). Refer to Section B10 for example values of these parameters.

B4.1 *Creep*—The lines AB and BC in Fig. B4.1(a) represent the variation of a stress increment σ_c, introduced on concrete at time t_0, and sustained to time *t*. The corresponding variation of strain is represented by curve EFG in Fig. B4.1(b). The total corresponding strain, instantaneous plus creep, at time *t* can be expressed by:

$$\varepsilon_c(t) = \frac{\sigma_c}{E_c(t_0)}[1 + C_t(t, t_0)] \quad \text{(B4-1)}$$

where $E_c(t_0)$ is the modulus of elasticity of concrete at time t_0. $C_t(t,t_0)$ is the creep coefficient, which is equal to the creep strain in the period t_0 to *t* divided by the instantaneous strain.

When the stress increment σ_c is introduced gradually over the period t_0 to *t*, represented by Curve ADC in Fig. B4.1(a), the total strain at time *t* is (refer to Curve EHI in Fig. B4.1(b)):

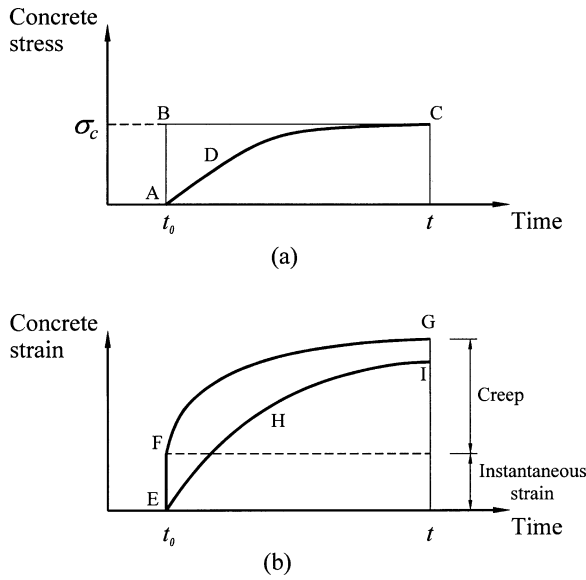$$\varepsilon_c(t) = \frac{\sigma_c}{E_c(t_0)}[1 + \chi C_t(t, t_0)] \quad \text{(B4-2)}$$

(a)

(b)

Fig. B4.1—Variation of stress and strain with time: (a) stress; and (b) strain.

$$\varepsilon_c(t) = \frac{\sigma_c}{\overline{E}_c(t, t_0)} \qquad \text{(B4-3)}$$

where χ is the aging coefficient, and $\overline{E}_c(t,t_0)$ is the age-adjusted modulus of elasticity of concrete.

Examples of stresses that are introduced gradually include time-dependent effects of shrinkage, prestress loss, and support settlement. The aging coefficient is mainly a function of t_0 and t (Ghali, Favre, and Elbadry 2002); a value of 0.8 can be used in most cases because χ varies between 0.7 and 0.9. Tabulated values of χ are given in ACI 209R. The aging coefficient χ is used as a multiplier to the creep coefficient, $C_t(t, t_0)$, as shown in Eq. (B4-2). The aging coefficient was introduced by Trost (1967) and Bažant (1975) to calculate the total strain, including creep, due to a gradually introduced stress increment, as represented by Curve ADC in Fig. B4.1(a).

B4.2 *Shrinkage*—The strain that results from unrestrained shrinkage of concrete between time t_0 and t, $\varepsilon_{SH}(t,t_0)$, depends mainly upon the size and the shape of the member, the properties of concrete, the ambient air humidity, and the ages of concrete at t_0 and t (ACI 209R). The same parameters also influence the value of the creep coefficient $C_t(t,t_0)$. For the analysis of deformations in a specified period t_0 to t, the given data include the value of the hypothetical shrinkage that would occur in the period if the concrete were free to shrink. This value is:

$$\varepsilon_{SH}(t,t_0) = \varepsilon_{SH}(t,t_s) - \varepsilon_{SH}(t_0,t_s) \qquad \text{(B4-4)}$$

where the time t_s is the start of drying shrinkage. When the analysis is for ultimate shrinkage and creep, $t = \infty$.

B4.3 *Relaxation of prestressing steel*—The loss of tensile stress in a tendon that is elongated and then maintained at a constant length and temperature is referred to as the intrinsic relaxation and is denoted $\Delta\sigma_p$. The value $\Delta\sigma_p$ depends on the
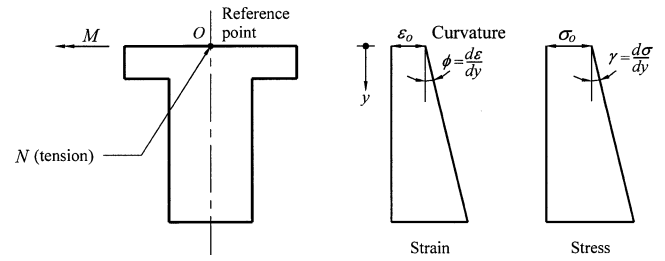

Fig. B5.1—Stress and strain distribution in a cross section subjected to normal force N *and a bending moment* M. *This figure also defines positive directions for all parameters.*

properties of the steel and the magnitude of the initial stress in the tendon. In concrete members, relaxation in a prestressing tendon is less than the intrinsic relaxation because of the additional reduction in stress due to creep and shrinkage that occur simultaneously with stress relaxation. The reduced relaxation value to be used when calculating time-dependent stresses and deformations is

$$\Delta\sigma_{pr} = \chi_r \Delta\sigma_p \qquad \text{(B4-5)}$$

where χ_r is a function of the initial steel stress and the total prestress change (Ghali et al. 2002); a value of $\chi_r = 0.8$ is a reasonable value to use in practice.

B5—Sectional analysis

The procedure in Section B5.2 satisfies equilibrium and strain compatibility at all reinforcement layers and applies to prestressing and nonprestressing reinforcement in cracked or uncracked sections. In a section post-tensioned by a unbonded internal or external tendon, the change in strain in the tendon due to loads applied after prestressing or due to creep, shrinkage, or relaxation is not compatible with the change in strain in the adjacent concrete. The procedure presented in Section B7.2 ignores this incompatibility; thus, it implies an approximation when applied to a structure having unbonded internal or external prestressed tendons (Ariyawardena and Ghali 2002).

B5.1 *Review of basic equations*—The following is the derivation of equations for the distribution of stress σ and strain ε over a homogeneous elastic cross section subjected to a normal force N at an arbitrary reference point O combined with a moment M about a horizontal axis through O (Fig. B5.1). Assuming that a plane cross section remains plane, the stress and strain variations over the depth are expressed by equations of straight lines:

$$\varepsilon = \varepsilon_O + y\phi \qquad \text{(B5-1a)}$$

$$\sigma = \sigma_O + y\gamma \qquad \text{(B5-1b)}$$

where y is a distance of any fiber, measured from the reference horizontal axis through O, and ε and σ are strain and stress at any fiber. The strain parameters ε_O and ϕ define the strain distribution; ε_O is the strain value at O; $\phi = d\varepsilon/dy$ = curvature.

Similarly, the stress parameters σ_O and γ define the stress distribution; σ_O is stress value at O; $\gamma = d\sigma/dy$ is the slope of the stress diagram. Assuming a linear stress-strain relationship, the strain and the stress parameters are related by

$$\sigma_O = E\varepsilon_O \qquad\qquad (B5\text{-}2a)$$

$$\gamma = E\phi \qquad\qquad (B5\text{-}2b)$$

where E is the modulus of elasticity of the homogeneous material.

The stress resultants are:

$$N = \int \sigma \, dA \qquad\qquad (B5\text{-}3a)$$

$$M = \int \sigma y \, dA \qquad\qquad (B5\text{-}3b)$$

Substitution of Eq. (B5-1a) and (B5-1b) into (B5-3a) and (B5-3b), respectively, gives the stress resultants

$$N = A\sigma_O + B\gamma \qquad\qquad (B5\text{-}4a)$$

$$M = B\sigma_O + I\gamma \qquad\qquad (B5\text{-}4b)$$

where A, B, and I are the cross-sectional area and its first and second moments about a horizontal axis through O, respectively. Thus,

$$A = \int dA; \; B = \int y \, dA; \; I = \int y^2 \, dA.$$

When N and M are known, the corresponding strain and stress parameters can be determined by solution of Eq. (B5-4a) and (B5-4b) and by using Eq. (5-2a) and (5-2b):

$$\sigma_O = \frac{IN - BM}{AI - B^2} \qquad\qquad (B5\text{-}5a)$$

$$\gamma = \frac{-BN + AM}{AI - B^2} \qquad\qquad (B5\text{-}5b)$$

$$\varepsilon_O = \frac{IN - BM}{E(AI - B^2)} \qquad\qquad (B5\text{-}6a)$$

$$\phi = \frac{-BN + AM}{E(AI - B^2)} \qquad\qquad (B5\text{-}6b)$$

When O is chosen at the centroid, $B = 0$, and Eq. (B5-5a), (B5-5b), (B5-6a), and (B5-6b) take the more familiar forms

$$\sigma_O = \frac{N}{A} \qquad\qquad (B5\text{-}7a)$$

$$\gamma = \frac{M}{I} \qquad\qquad (B5\text{-}7b)$$

$$\varepsilon_O = \frac{N}{EA} \qquad\qquad (B5\text{-}8a)$$

$$\phi = \frac{M}{EI} \qquad\qquad (B5\text{-}8b)$$

Choosing O at a fixed point (for example, the top fiber) rather than the centroid has the advantage that the location of the centroid does not have to be determined for the uncracked and cracked stages. The equations in this section will be used for the structural concrete section, with A, B, and I being properties of the transformed section, which is the area of the concrete plus the area of the reinforcement multiplied by the modular ratio (E_{ns} or E_{ps} for reinforcement divided by E_c or $\overline{E}_c$ for concrete); where E_{ns} and E_{ps} are the moduli of elasticity of nonprestressing and prestressing reinforcement, respectively; and E_c and $\overline{E}_c$ are modulus and age-adjusted modulus of concrete, respectively. The transformed section has modulus of elasticity equal to that of concrete. When cracking occurs, only the area of concrete in compression is included in the transformed section.

B5.2 *Instantaneous and time-dependent stress and strain*—This section describes a procedure to analyze immediate increments of strains $\varepsilon(t_0)$ and stresses $\sigma(t_0)$ in a prestressed or nonprestressed section and the changes in these values in a period t_0 to t. The times t_0 and t represent instances in multistage construction when a load or prestressing is applied, or when the support conditions are modified. The term immediate means initial before occurrence of creep, shrinkage, and relaxation.

The given data are as follows (Fig. B5.2):
- Gross concrete dimensions of the section, areas A_{ps} and A_{ns} (with subscripts ps and ns referring to prestressing and nonprestressing reinforcement, respectively);
- Coordinates y defining the location of each area;
- Magnitudes of normal force N and bending moment M introduced at t_0;
- Elasticity moduli $E_c(t_0)$, E_{ps}, and E_{ns};
- Creep and aging coefficients of concrete $C_t(t,t_0)$ and $\chi(t,t_0)$, respectively; and
- Unrestrained shrinkage of concrete $\varepsilon_{SH}(t,t_0)$, and reduced relaxation $\Delta\sigma_{pr}$.

The values of N and M, respectively, represent the total normal force at the reference point O, and the bending moment introduced at t_0 including any statically indeterminate effects of loads and prestressing. It is assumed that just before introducing N and M, the section is subjected to linearly varying strain and stress defined by the values at O and the derivatives with respect to y.

As an example, consider the cross section at the midspan of the post-tensioned, simple beam subjected at time t_0 to a prestressing force P, and the member self-weight per unit length q in Fig. B5.3(a) illustrates the meaning of the
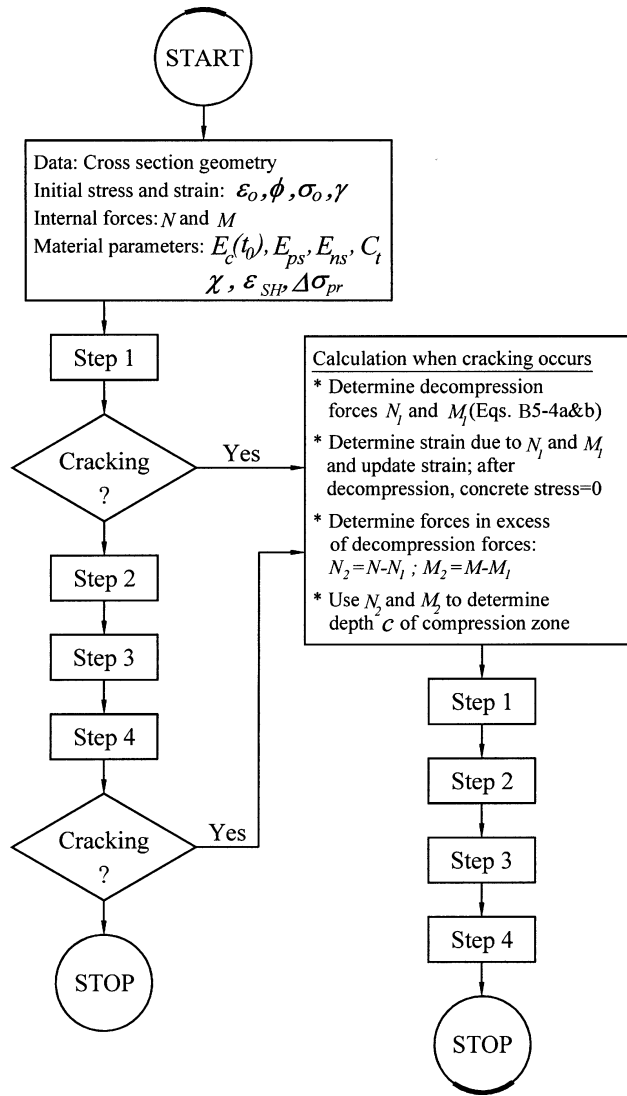
Fig. B5.2—Analysis of instantaneous and time-dependent strain and stress in a cross section for a single time interval in a multistage construction.

Fig. B5.3—Examples explaining the meaning of symbols N and M, Eq. (5-9a) and (5-9b): (a) post-tensioned simple beam; (b) pretensioned simple beam; and (c) continuous post-tensioned beam.

If the beam is continuous over two symmetrical spans (Fig. B5.3(c)), the values of N and M introduced at midspan at t_0 are

$$N = -P \qquad (B5\text{-}10a)$$

$$M = -y_{ps}P + \frac{q\ell^2}{8} + \overline{M} \qquad (B5\text{-}10b)$$

where $\overline{M}$ is the statically indeterminate moment due to prestressing. N and M are resultants, at t_0, of the stress change in concrete and nonprestressing steel.

The analysis, which assumes cracking does not occur, is performed in four steps. Figure B5.2 indicates additional analysis required to account for cracking, as discussed in Section B6.

Step 1—Calculate the instantaneous strain parameters, $\Delta\varepsilon_O(t_0)$ and $\Delta\phi(t_0)$, using Eq. (B5-6a) and (B5-6b) and substituting for A, B, and I the properties of a transformed section composed of A_c plus $n_{ns}(t_0)A_{ns}$ and $n_{ps}(t_0)A_{ps}$, where n_{ns} or n_{ps} is the ratio of modulus of elasticity of nonprestressing E_{ns} or prestressing E_{ps}, reinforcement divided by $E_c(t_0)$; A_{ps} includes only the cross-sectional area of reinforcement prestressed earlier than t_0. The instantaneous changes in stress parameters $\Delta\sigma_O(t_0)$ and $\Delta\gamma(t_0)$ are calculated by Eq. (B5-2a) and (B5-2b), substituting $E_c(t_0)$ for E.

symbols N and M. The values of N and M introduced at midspan section at t_0 are

$$N = -P \qquad (B5\text{-}9a)$$

$$M = -y_{ps}P + \frac{q\ell^2}{8} \qquad (B5\text{-}9b)$$

where P is the absolute value of the jacking prestress force less friction loss; and y_{ps} and ℓ are defined in Fig. B5.3(a). The parameters N and M are resultants of the instantaneous stress change in concrete, excluding the cross-sectional area of the prestressing duct, and in the nonprestressing steel.

If the beam is pretensioned (Fig. B5.3(b)), Eq. (B5-9a) and (B5-9b) give values of N and M, but with P being the absolute value of the force in the tendon at t_0, immediately before prestress transfer. Furthermore, N and M represent resultants of stress changes at transfer in the concrete and in the nonprestressing and the prestressing steels.
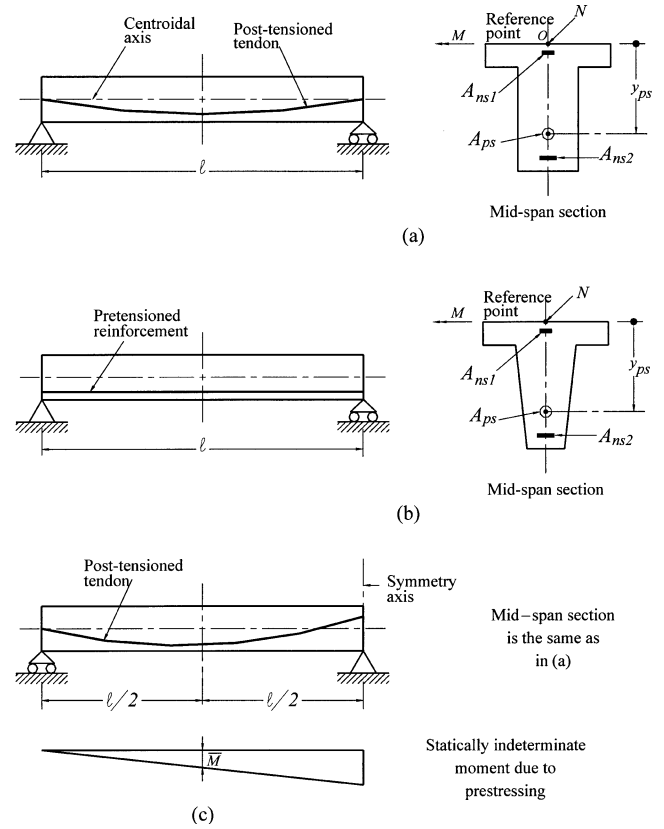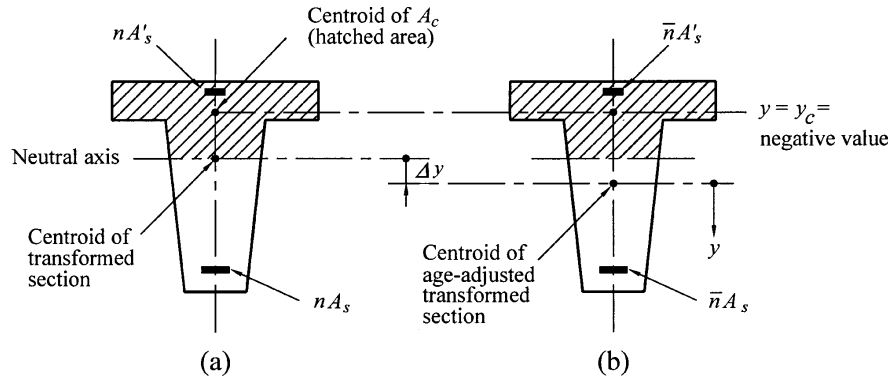
Fig. B5.4—*Properties of the transformed section at* t_0 *and the age-adjusted transformed section: (a) cracked section at* t_0; *and (b) age-adjusted transformed section.*

Step 2—Determine parameters for the hypothetical strain change that would occur, in the period t_0 to t, if creep and shrinkage were unrestrained, using:

$$\Delta\varepsilon_{O\,free}(t,t_0) = \varepsilon_{SH}(t,t_0) + C_t\Delta\varepsilon_O(t,t_0) \qquad \text{(B5-11a)}$$

$$\Delta\phi_{free} = C_t(t,t_0)\Delta\phi(t_0) \qquad \text{(B5-11b)}$$

If the initial stress is not zero, creep due to stresses introduced earlier than t_0 should be added, and the creep coefficients should be included in the input. ACI 209R, Ghali, Favre, and Elbadry (2002), and CEB-FIP (1990) give guidance on creep-coefficient values.

Step 3—Calculate the two parameters defining the distribution of a hypothetical stress gradually introduced between t_0 and t to prevent the strain change calculated in Step 2, using Eq. (B5-2a) and (B5-2b).

$$\sigma_{O\,restraint} = -\overline{E}_c\Delta\varepsilon_{O\,free} \qquad \text{(B5-12a)}$$

$$\gamma_{restraint} = -\overline{E}_c\Delta\phi_{free} \qquad \text{(B5-12b)}$$

where $\overline{E}_c$ is the age-adjusted modulus of elasticity of concrete.

$$\overline{E}_c(t,t_0) = E_c(t_0)/[1 + \chi C_t(t,t_0)] \qquad \text{(B5-13)}$$

Step 4—Calculate A, B, and I for concrete alone, without reinforcement, and substitute these values together with $\sigma_{O\,restraint}$ and $\gamma_{restraint}$ in Eq. (B5-4a) and (B5-4b) to obtain the resultants of stress required to prevent creep and shrinkage deformations

$$\Delta N_{creep,\,shrinkage} = A_{concrete}\sigma_{O\,restraint} + \qquad \text{(B5-14a)}$$
$$B_{concrete}\gamma_{restraint}$$

$$\Delta M_{creep,\,shrinkage} = B_{concrete}\sigma_{O\,restraint} + \qquad \text{(B5-14b)}$$
$$I_{concrete}\gamma_{restraint}$$

Determine the stress resultants that cancel the effect of the prestressing steel relaxation

$$\Delta N_{relax} = A_{ps}\Delta\sigma_{pr} \qquad \text{(B5-15a)}$$

$$\Delta M_{relax} = A_{ps}y_{ps}\Delta\sigma_{pr} \qquad \text{(B5-15b)}$$

The sum of the two normal forces and the two bending moments calculated in this step (Eq. (B5-14) and (B5-15)) represent fictitious forces ΔN and ΔM, which would prevent deformations due to creep, shrinkage, and relaxation.

Eliminate the fictitious restraint by application of $-\Delta N$ and $-\Delta M$ on the age-adjusted transformed section (whose properties are $\overline{A}$, $\overline{B}$, and $\overline{I}$). The age-adjusted transformed section is composed of A_c, $\overline{n}_{ns}A_{ns}$ and $\overline{n}_{ps}A_{ps}$; where $\overline{n}_{ns}$ or $\overline{n}_{ps}$ is the modulus of elasticity of reinforcement divided by $\overline{E}_c(t,t_0)$. Calculate the changes in strain and stress parameters (changes in ε_O, ϕ, σ_O, γ) by substitution of $-\Delta N$, $-\Delta M$, $\overline{E}_c(t,t_0)$, $\overline{A}$, $\overline{B}$, and $\overline{I}$ in Eq. (B5-5a), (B5-5b), (B5-6a), and (B5-6b).

Update the initial stress parameters by adding the stress parameters determined in Steps 1, 3, and 4. Update the initial strain parameters by adding the strain parameters determined in Steps 1 and 4.

B5.3 *Commentary on the general procedure and on a special case (nonprestressed sections subjected to* M *without* N)—The general procedure gives the two parameters ε_O, ϕ defining the strain distribution in an uncracked prestressed or nonprestressed section subjected to N and M. When cracking occurs, an additional step is required; refer to Section B6. Calculation of displacement in a plane frame from the strain parameters is a classical geometry problem that can be solved more easily by virtual work or other methods. Transverse deflection in beams can be determined from the curvature ϕ only (without the need for ε_O). The equations presented below, which are derived from the general procedure in Section B5.2, give the immediate and the long-term curvatures at nonprestressed reinforced concrete sections subjected to bending moment M.

Consider a nonprestressed reinforced concrete cross section (Fig. B5.4) subjected at time t_0 to a bending moment M, without normal force. The general procedure of analysis in Section B5.2 reduces to Eq. (B11-1) to (B11-3) for initial

curvature $\phi(t_0)$ and the curvature changes $(\Delta\phi)_{creep}$ and $(\Delta\phi)_{shrinkage}$ due to creep and shrinkage occurring between t_0 and t. The long-term curvature at time t is the sum of the curvatures determined by the three equations

$$\phi(t_0) = \frac{I_g}{I}\phi_c \qquad \text{(B5-16)}$$

$$(\Delta\phi)_{creep} = \phi(t_0)C_t\kappa_{creep} \qquad \text{(B5-17)}$$

$$(\Delta\phi)_{shrinkage} = -\frac{\varepsilon_{cs}}{d}\kappa_{shrinkage} \qquad \text{(B5-18)}$$

where ϕ_c is the instantaneous curvature at an uncracked homogenous concrete section (without reinforcement)

$$\phi_c = \frac{M}{E_c(t_0)I_g} \qquad \text{(B5-19)}$$

where

$E_c(t_0)$ = the modulus of elasticity of concrete at time t_0;
C_t and ε_{SH} = the creep coefficient and the unrestrained shrinkage of concrete in the period t_0 to t, respectively;
d = the distance from extreme compression fiber to the centroid of the tension reinforcement;
I_g = moment of inertia of the gross concrete section about its centroidal axis, neglecting reinforcement; and
κ_{creep} and $\kappa_{shrinkage}$ = dimensionless coefficients depending on properties of the section.

$$\kappa_{creep} = \frac{I_c + A_c y_c \Delta y}{\overline{I}} \qquad \text{(B5-20)}$$

$$\kappa_{shrinkage} = \frac{A_c y_c d}{\overline{I}} \qquad \text{(B5-21)}$$

where

I = the moment of inertia about the centroidal axis of the transformed section composed of concrete area A_c plus $n[= E_s/E_c(t_0)]$ multiplied by the area of reinforcement;
$\overline{I}$ = moment of inertia about the centroidal axis of the age-adjusted transformed section composed of concrete area A_c plus $\overline{n}(= \overline{E}_s/\overline{E}_c)$ multiplied by areas of reinforcements;
I_c = moment of inertia of the concrete area A_c about the centroidal axis of the age-adjusted transformed section;
$\overline{E}_c$ = the age-adjusted modulus of elasticity of concrete (Eq. (B5-13));
Δy = the y-coordinate of the centroid of the age-adjusted transformed section, measured downward from the

neutral axis at t_0 (the centroidal axis of the transformed section at t_0); and
y_c = the y-coordinate of the centroid of A_c, measured downward from the centroid of the age-adjusted transformed section.

In most cases, the tension steel area A_s near the bottom fiber is larger than the compression steel area A_s' and the values of Δy and y_c are positive and negative, respectively (Fig. B5.4(a) and (b)).

The symbol A_c means the active area of concrete at time t_0. Thus, when the previous equations are used for a cracked section, A_c is the area of concrete within the compression zone at time t_0. Derivation of the equations in this Appendix from the general procedure in Section B5.2 and graphs for the coefficients κ_{creep} and $\kappa_{shrinkage}$ are available (Ghali, Favre, and Elbadry 2002).

B6—Calculation when cracking occurs

If at the end of Step 1 of the general procedure it is determined that cracking occurs (the extreme fiber stress exceeds the tensile strength of concrete), the calculations indicated in Fig. B5.2 become necessary. Partition M and N into two parts, such that $M = M_1 + M_2$ and $N = N_1 + N_2$. The pair N_1 and M_1 (decompression forces, a part of the pair M and N) represents the stress resultants that will bring to zero the concrete stresses existing before the introduction of M and N; the pair N_2 and M_2 represents the remainder. With N_1 and M_1, the section is uncracked. Cracking is produced only by N_2 combined with M_2. For the analysis, two loading stages need to be considered: 1) N_1 and M_1 applied on an uncracked section; and 2) N_2 and M_2 applied on a cracked section, in which the concrete outside the compression zone is ignored. The strains in the two stages are added to give the total instantaneous change. The values of N_1 and M_1 can be calculated by Eq. (B5-4a) and (B5-4b), substituting for σ and γ, the initial stress parameters with reversed sign and for A, B, and I properties of the uncracked transformed section. After N_1 and M_1 have been determined, N_2 and M_2 are calculated by $N_2 = N - N_1$ and $M_2 = M - M_1$.

Performing Steps 2, 3, and 4 for the cracked section gives the time-dependent changes in strain and stress. Numerical examples and a computer program based on the detailed method of analysis presented previously can be found in Section B10 and in Ghali, Favre, and Elbadry (2002); a computer program can be used to perform the analysis (Ghali and Elbadry 1986 and 2001).

Section B7—Tension-stiffening

The normal strain ε_{O2} and the curvature ϕ_2 calculated for a cracked section represent the state at a crack location. Away from the crack location, concrete bonded to the reinforcement tends to restrain deformations and reduce the normal strain and the curvature. This is called tension-stiffening. Empirical approaches have been proposed to account for the tension stiffening effect on the displacements. These procedures use the mean values of strain parameters ε_{Om} and ϕ_m to calculate displacements. The mean parameters have

intermediate values between the strain parameters in uncracked and the cracked states.

B7.1 *Branson's effective moment of inertia*—For a member subjected to bending moment without a normal force, only the curvature ϕ_m is required to calculate transverse deflection. For a nonprestressed reinforced concrete section subjected to bending moment M without normal force, Branson's equations (Branson 1977) for mean curvature are:

$$\phi_m = \frac{M}{EI_e} \qquad (B7\text{-}1a)$$

$$I_e = \left(\frac{M_{cr}}{M}\right)^4 I_g + \left[1 - \left(\frac{M_{cr}}{M}\right)^4\right] I_2 \qquad (B\text{-}7\text{-}1b)$$

where
I_e = the effective moment of inertia;
I_g = the second moment of gross concrete area about its centroidal axis, ignoring the presence of reinforcement;
I_2 = the second moment of area of the transformed cracked section about its centroidal axis;
M_{cr} = cracking moment; and
M = the moment on the section.

B7.2 *CEB-FIP approach*—For any prestressed or nonprestressed reinforced section, the mean strain parameters ε_{Om} and ϕ_m can be determined by interpolation between uncracked and cracked states

$$\varepsilon_{Om} = (1 - \zeta)\varepsilon_{O1} - \zeta\varepsilon_{O2} \qquad (B7\text{-}2a)$$

$$\phi_m = (1 - \zeta)\phi_1 + \zeta\phi_2 \qquad (B7\text{-}2b)$$

where
ε_{O1} and ϕ_1 = strain parameters calculated using the uncracked transformed section;
ε_{O2} and ϕ_2 = strain parameters calculated using the cracked transformed section
ζ = an empirical interpolation coefficient, expressed by CEB-FIP Model Code MC-90 (1990) as follows:

$$\zeta = 1 - \beta\left(\frac{f_{ct}}{\sigma_{1\,max}}\right)^2 \text{ (when } \sigma_{1\,max} > f_{ct}\text{, cracked)} \qquad (B7\text{-}3)$$

$$\zeta = 0 \text{ (when } \sigma_{1\,max} < f_{ct}\text{, uncracked)} \qquad (B7\text{-}4)$$

where
f_{ct} = the tensile strength of concrete;
$\sigma_{1\,max}$ = calculated tensile stress at extreme fiber when cracking is ignored; and
β = coefficient to account for the effects of bond quality of reinforcement, cyclic loading, and sustained loading on tension stiffening.

In most cases, $\beta = 0.5$ can be used when deformed bars are employed and cyclic or sustained loads are applied.

B7.3 *Other tension stiffening approaches*—The complete stress-strain curve for concrete in tension has been used by many researchers to model the tension-stiffening effect (Gilbert and Warner 1978; Polak and Vecchio 1993; Scanlon and Murray 1974). This approach can be incorporated into the section curvature procedure by appropriate modification of the transformed-section properties. Introduction of the nonlinear stress-strain relationship would involve an iterative solution. Gilbert and Warner (1998) have modeled the effect by increasing the effective stiffness of the reinforcing steel, while Kaufmann and Marti (1998) have introduced a tension-chord model based on assumed bond stress distribution between cracks.

B8—Deflection and change in length of a frame member

The following equation can be used to calculate the transverse deflection δ_{center} at midlength of a straight member of a frame

$$\delta_{center} = \frac{\ell^2}{96}(\phi_{m1} + 10\phi_{m2} + \phi_{m3}) \qquad (B8\text{-}1)$$

where
ℓ = the member length; and
ϕ_{m1}, ϕ_{m2}, and ϕ_{m3} = mean curvatures at one end, at the center, and at the other end, respectively.

Similarly, the rotation at member ends θ_{end} and the change in member length $\Delta\ell$ can be determined by:

$$\theta_{end1} = \frac{\ell}{6}(\phi_{m1} + 2\phi_{m2}) \text{ and} \qquad (B8\text{-}2)$$

$$\theta_{end2} = \frac{\ell}{6}(2\phi_{m2} + \phi_{m3})$$

$$\Delta\ell = \frac{\ell}{6}(\varepsilon_{Om1} + 4\varepsilon_{Om2} + \varepsilon_{Om3}) \qquad (B8\text{-}3)$$

where ε_{Om1}, ε_{Om2}, and ε_{Om3} are mean normal strains at one end, at the center, and at the other end, respectively.

The deflection δ_{center} and the rotation θ_{end} are measured from the chord, which is the straight line joining the two ends.

Equations (B8-1) to (B8-3) assume parabolic or straight line variations of ϕ_m and ε_{Om} over the length of a frame member. The method of virtual work (Ghali and Neville 1997) gives the translation in any direction and the rotation at any section of a frame having any variation of ϕ_m and ε_{Om}. Equations (B8-4) to (B8-6), which are derived by virtual work, can be used instead of Eq. (B8-1) to (B8-3) with any variation of ϕ_m and ε_{Om} over the length of a frame member:

$$\delta_{center} = \frac{1}{2}\int_0^{\ell/2} \phi_m x\,dx + \frac{\ell}{2}\int_{\ell/2}^{\ell} \phi_m\left(1 - \frac{x}{\ell}\right)dx \qquad (B8\text{-}4)$$

$$\theta_{end1} = \int_0^\ell \phi_m \left(1 - \frac{x}{\ell}\right)dx \text{ and } \theta_{end2} = \int_0^\ell \phi_m \left(\frac{x}{\ell}\right)dx \quad \text{(B8-5)}$$

$$\Delta\ell = \int_0^\ell \varepsilon_{Om}dx \quad \text{(B8-6)}$$

where x is the distance from End 1 to any section of the member.

When ϕ_m and ε_{Om} vary as a second-degree parabola (or as a straight line), Eq. (B8-4) to (B8-6) reduce to Eq. (B8-1) to (B8-3). The deflection at end 2 from the tangent to the elastic line at End 1 for any member of a plane frame is

$$\delta_{End\ 2\ relative\ to\ End\ 1} \int_0^\ell \phi_m (\ell - x)dx \quad \text{(B8-7)}$$

An example of the use of this equation is to determine the side sway at the top end of a column that is fixed at the bottom (End 1). When cracking occurs at some sections, the integrals in Eq. (B8-4) to (B8-7) can be conveniently evaluated numerically.

B9—Summary and conclusions

The section curvature method presented in this appendix can be used to calculate the immediate and the long-term strain distributions in prestressed or nonprestressed reinforced concrete sections subjected to a normal force and a bending moment. The strain value ε_O at an arbitrary reference location and the slope ϕ of the strain diagram (the curvature), when determined at various sections, can be used to calculate the change in length or the deflections of individual members or the displacements of plane frames.

The deflections of cracked members are calculated from the mean strain ε_{Om} and mean curvature ϕ_m determined by interpolation between ε_{O1} and ε_{O2} and between ϕ_1 and ϕ_2, where the subscript 1 refers to values calculated by ignoring cracking, and the subscript 2 refers to values calculated by ignoring the concrete in tension. The interpolation is done empirically.

The analysis presented in this appendix accounts for the time-dependent loss of prestress due to creep and shrinkage without making a prior estimate of the loss. In fact, the analysis results include the time-dependent change in stress in the prestressing steel. The analysis procedure involves four steps demonstrated by the examples in Section B10. The validity of the analysis is demonstrated by comparison with published data in Ghali and Azarnejad (1999).

B10—Examples

Example 1—Uncracked section: A prestress force $P = 315$ kip and a bending moment $M = 3450$ kip-in. are applied at age t_0 on the rectangular post-tensioned concrete section shown in Fig. B10.1. Calculate the stress, the strain, and the curvatures at age t_0 and at a later time t given the following data: $E_c(t_0) = 4350$ ksi; $E_{ns} = E_{ps} = 29 \times 10^3$ ksi; uniform

unrestrained shrinkage, $\varepsilon_{SH}(t,t_0) = -240 \times 10^{-6}$; $C_t(t,t_0) = 3$; $\chi_r = 0.8$; reduced relaxation $\Delta\sigma_{pr} = -12$ ksi. If the section analyzed is at the center of a simple beam of span 61 ft, what are the midspan deflections at time t_0 and t? Assume parabolic variation of curvature with zero values at the ends. (This is close to the actual variation when the load is uniform and the tendon profile is parabolic with zero eccentricity at the ends.)

Step 1—Select the reference point O at top fiber. The transformed section properties at time t_0 are: [gross-section area – duct + $(n-1)A_{ns}$; with $n = E_{ns}/E_c(t_0)$]:

A = 593.3 in.^{2}
B = 14,250 in.^{3}
I = 462,100 in.^{4}

The values of N and M applied at t_0 are:

N = –315 kip
M = 3450 – 315 (42.0) = –9780 kip-in.

The initial strain and stress parameters are (Eq. (B5-5a), (B5-5b), (B5-6a), and (B5-6b)):

$\sigma_O(t_0)$ = –0.087 ksi
$\gamma(t_0)$ = –0.0185 kip/in.^{3}
$\varepsilon_O(t_0)$ = –20.0 × 10^{-6}
$\phi(t_0)$ = –4.25 × 10^{-6} in.$^{-1}$

Step 2—Changes in strain parameters for unrestrained creep and shrinkage (Eq. (B5-11a) and (B5-11b)):

$\Delta\varepsilon_{O\ free} = -240 \times 10^{-6} + 3(-20 \times 10^{-6}) = -300 \times 10^{-6}$
$\Delta\phi_{free} = 3(-4.25 \times 10^{-6}) = -12.75 \times 10^{-6}$ in.$^{-1}$

Step 3—The age-adjusted modulus of elasticity (Eq. (B5-13)), $\overline{E}_c = 1279$ ksi. The stress that can prevent the strain change determined in Step 2 (Eq. (B5-12a) and (B5-12b)):

$\sigma_{O\ restraint}$ = –1279 (–300 × 10^{-6}) = 0.3837 ksi
$\gamma_{restraint}$ = –1279 (–12.75 × 10^{-6}) = 16.3 × 10^{-3} kip/in.^{3}

Step 4—Cross-sectional properties of concrete (gross-sectional area – A_{ps} – A_{ns}):

$A_{concrete}$ = 570.4 in.^{2}
$B_{concrete}$ = 13,640 in.^{3}
$I_{concrete}$ = 434,300 in.^{4}

Add the resultants of $\sigma_{restraint}$ (Eq. (B5-14a) and (B5-14b)) to the forces that cancel the effect of prestressed steel relaxation (Eq. (B5-15a) and (B5-15b)) to obtain the total restraining forces.

ΔN = 418.2 kip
ΔM = 11,350 kip-in.

Properties of the age-adjusted transformed section [gross-section area + $(\overline{n} - 1)(A_{ps} + A_{ns})$, with $\overline{n} = (E_{ns}$ or $E_{ps})/\overline{E}_c$]:

$\overline{A}$ = 697.8 in.^{2}
$\overline{B}$ = 17,800 in.^{3}
$\overline{I}$ = 615,800 in.^{4}

Changes in strain and stress due to $-\Delta N$ and $-\Delta M$ applied on the age-adjusted transformed section (Eq. (B5-5a), (B5-5b), (B5-6a), and (5B-6b)):

$\Delta\varepsilon_O(t,t_0)$ = –385 × 10^{-6}
$\Delta\phi(t,t_0)$ = –3.29 × 10^{-6} in.$^{-1}$
$\Delta\sigma_O(t,t_0)$ = 0.3837 + 1279(–385 × 10^{-6}) = –0.108 ksi
$\Delta\gamma(t,t_0)$ = 16.3 × 10^{-3} + 1279(–3.29 × 10^{-6}) = 0.0121 kip/in.^{3}

The values $\sigma_{O\ restraint}$ and $\gamma_{restraint}$ calculated in Step 3 are included in the last two equations.
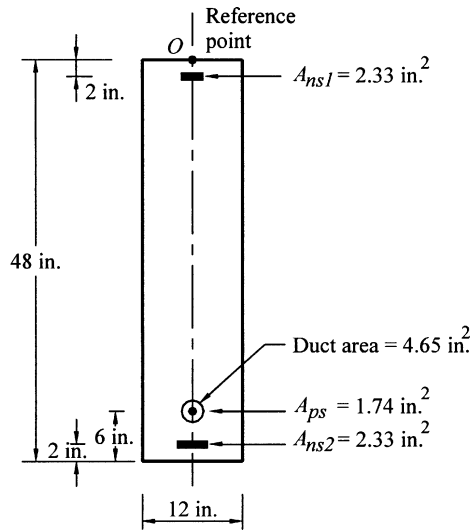
Fig. B10.1—Beam cross section of Examples 1 and 2.

The strain and stress parameters at time t (add the values determined in this step and in Step 1):

$$\varepsilon_O(t) = (-20 - 385)10^{-6} = -405 \times 10^{-6}$$
$$\phi(t) = (-4.25 - 3.29)10^{-6} = -7.53 \times 10^{-6} \text{ in.}^{-1}$$
$$\sigma_O(t) = -0.087 - 0.108 = -0.195 \text{ ksi}$$
$$\gamma(t) = -0.0185 + 0.0121 = -0.00641 \text{ kip/m}^3$$

Deflection: The immediate and the long-term deflection at the center of span (Eq. (B8-5)):

$$\delta_{center}(t_0) = \frac{(61 \times 12)^2}{96}[10(-4.25 \times 10^{-6})] = -0.24 \text{ in.}$$

$$\delta_{center}(t) = \frac{(61 \times 12)^2}{96}[10(-7.53 \times 10^{-6})] = -0.42 \text{ in.}$$

The curvatures at the two ends are ignored for simplicity of presentation. If these curvatures are calculated and Eq. (B8-5) is used, $\delta_{center}(t)$ would be –0.40 in. The minus sign means upward deflections.

Several parameters given as input are dependent upon t_0 and t. As mentioned earlier, in practice the analysis should be preceded by selecting the appropriate values of the parameters (ACI 209R; CEB-FIP [1990]; and Magura, Sozen, and Siess [1964]).

Example 2—Cracked Section: For the section of Example 1 (Fig. B10.1), determine the axial strain and the curvature at time t immediately after application of an additional bending moment $M = 6000$ kip-in. (for example, caused by live load). Assume that at time t, the modulus of elasticity of concrete $E_c(t) = 4600$ ksi and $f_{ct} = 0.36$ ksi.

The properties of the transformed uncracked section at time t [gross-sectional area + $(n - 1)$ $(A_{ns} + A_{ps})$; with $n = (E_{ns}$ or $E_{ps})/E_c(t)$]:

$$A_1 = 605.8 \text{ in.}^2$$
$$B_1 = 14{,}800 \text{ in.}^3$$
$$I_1 = 484{,}800 \text{ in.}^4$$

The immediate changes in strain parameters assuming no cracking (Eq. (B5-6a) and (B5-6b)):

$$\Delta\varepsilon_{O1} = -258 \times 10^{-6}$$
$$\Delta\phi_1 = 10.57 \times 10^{-6} \text{ in.}^{-1}$$

Change in stress at the bottom fiber = 1.146 ksi

Stress at the bottom fiber just before live load application (determined by substituting $\sigma_O(t)$ and $\gamma(t)$ calculated in Example 1 in Eq. (B5-1), with $y = 48$ in.) = –0.502 ksi

Updated stress at bottom fiber at time $t = \sigma_{1\ max} = 0.644$ ksi

This stress is greater than f_{ct}, which indicates that cracking occurs. Substituting A_1, B_1, and I_1 and the values of $-\sigma_O(t)$ and $-\gamma(t)$ determined in Example 1 in Eq. (B5-4) gives the decompression forces:

$$N_1 = 212.7 \text{ kip}$$
$$N_2 = -212.7 \text{ kip}$$
$$M_1 = 5983 \text{ kip-in.}$$
$$M_2 = 6000 - 5983 = 17 \text{ kip-in.}$$

Substitution of A_1, B_1, I_1, N_1, and M_1 in Eq. (B5-6a) and (B5-6b) gives the immediate changes in strain parameters in the decompression stage:

$$\Delta\varepsilon_{O1} = 42 \times 10^{-6}$$
$$\Delta\phi_1 = 1.39 \times 10^{-6} \text{ in.}^{-1}$$

With N_2 and M_2 applied on a reinforced concrete cracked section, determine the depth of the compression zone; $c = 22.9$ in. Determination of c is a standard analysis discussed in many books, including Ghali, Favre, and Elbadry (2002). Properties of the cracked section, ignoring concrete in tension are:

$$A_2 = 308.1 \text{ in.}^2$$
$$B_2 = 4288 \text{ in.}^3$$
$$I_2 = 98{,}240 \text{ in.}^4$$

Substituting A_2, B_2, I_2, N_2, and M_2 in Eq. (B5-6a) and (B5-6b) gives the immediate changes in strain parameters, with the concrete in tension ignored:

$$\Delta\varepsilon_{O2} = -383 \times 10^{-6}$$
$$\Delta\phi_2 = 16.77 \times 10^{-6} \text{ in.}^{-1}$$

The interpolation coefficient (Eq. (B7-3)):

$$\zeta = 1 - 0.5\left(\frac{0.360}{0.644}\right)^2 = 0.844$$

The mean strain parameters (Eq. (B7-2)):

$$\Delta\varepsilon_{Om} = (1 - 0.844)(-258)10^{-6} + 0.844(42 - 383)10^{-6} = -328 \times 10^{-6}$$
$$\Delta\phi_m = (1 - 0.844)(10.57)10^{-6} + 0.844(1.39 + 16.77)10^{-6} = 16.97 \times 10^{-6}$$

The updated curvature and deflection at center of span, immediately after live load application:

Curvature after live load application = $(-7.53 + 16.97) 10^{-6} = 9.44 \times 10^{-6} \text{ in.}^{-1}$; and

Deflection after live load application (Eq. B8-5) =

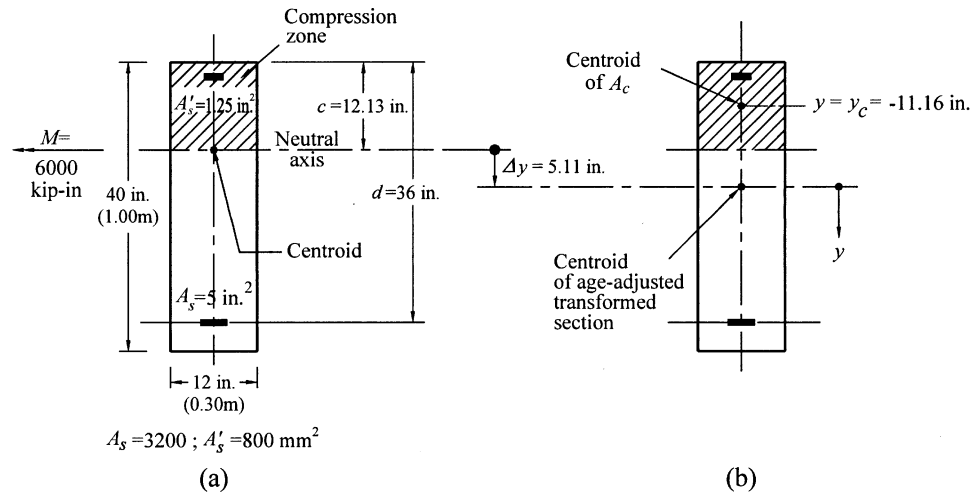$$\frac{(61 \times 12)^2}{96}[10(9.44 \times 10^{-6})] = 0.53 \text{ in.}$$

Fig. B10.2—Example section subjected to moment: (a) cracked section at age t₀ (neutral axis through centroid of transformed section); and (b) properties of age-adjusted transformed section.

Example 3—Nonprestressed section in flexure: Determine the curvature $\phi(t_0)$ and $\phi(t)$ for a rectangular cracked section shown in Fig. B10.2. Given data:

$E_c(t_0)$ = 3625 ksi (25.00 GPa)
E_s = 29,000 ksi (200 GPa)
C_t = 2.0
$\overline{E}_c$ = 1390 ksi (9.59 GPa)
ε_{SH} = -300×10^{-6}
M = 6000 kip-in. (452 kN-m)
n = $E_s/E_c(t_0) = 8.00$
$\overline{n}$ = $E_s/\overline{E}_c = 20.86$
I_g = 64,000 in.^{4}

Depth of compression zone for a rectangular section (Fig. B10.2a) is:

$$c = \frac{-a_2 + \sqrt{a_2^2 - 4a_1a_3}}{2a_1}$$

where
a_1 = $b/2$
a_2 = $nA_s + (n-1)A_s'$
a_3 = $-nA_s d - (n-1)A_s'd_s'$
This gives:
a_1 = 6 in.
a_2 = 48.75 in.^{2}
a_3 = -1475 in.^{3}
c = 12.13 in.

The centroid of the transformed section at t_0 coincides with the bottom edge of the compression zone. Other geometrical properties of the section are:
I = 30,510 in.^{4}
A_c = 144.4 in.^{2}

The centroid of the age-adjusted transformed section is at:
Δy = 5.11 in.
$\overline{I}$ = 61,020 in.^{4}
y_c = -11.16 in.
I_c = 19,670 in.^{4}

Equations (B5-17) to (B5-21) give:

$$\kappa_{creep} = \frac{19,760 + 144.4(-11.16)(5.11)}{61,020} = 0.189$$

$$\kappa_{shrinkage} = \frac{144.4(-11.16)(36)}{61,020} = 0.950$$

$$\phi_c = \frac{6000}{3625(64,000)} = 26.86 \times 10^{-6} \text{ in.}^{-1}$$

The initial curvature at time t_0:

$$\phi(t_0) = \frac{64,000}{30,509}(25.86 \times 10^{-6}) - 54.25 \times 10^{-6} \text{ in.}^{-1}$$

$$(\Delta\phi)_{creep} = 54.25 \times 10^{-6}(2.00)(0.189) = 20.51 \times 10^{-6} \text{ in.}^{-1}$$

$$(\Delta\phi)_{shrinkage} = \frac{(-300 \times 10^{-6})}{36}(0.950) = 7.92 \times 10^{-6} \text{ in.}^{-1}$$

The long-time curvature at time t:

$$\phi(t) = (54.25 + 20.51 + 7.92) \times 10^{-6} = 82.7 \times 10^{-6} \text{ in.}^{-1}$$

B11—References
B11.1 *Referenced standards and reports*—The following standards and reports listed were the latest editions at the time this document was prepared. Because these documents are revised frequently, the reader is advised to contact the sponsoring group to refer to the latest version.

American Concrete Institute
209R   Prediction of Creep, Shrinkage, and Temperature Effects in Concrete Structures
318/318R Building Code Requirements for Structural Concrete and Commentary

These publications may be obtained from:

American Concrete Institute
P.O. Box 9094
Farmington Hills, MI 48333-9094

B11.2 *Cited references*—
Ariyawardena, N., and Ghali, A., 2002, "Prestressing with Unbonded or External Tendons: Analysis and Computer Model," *Journal of Structural Engineering*, ASCE, V. 128, No. 12, pp. 1493-1501.

Bažant, Z. P., 1975, "Prediction of Concrete Creep Effects Using Age-Adjusted Effective Modulus Method," ACI JOURNAL, *Proceedings* V. 69, No. 4, Apr., pp. 212-217.

Branson, D. E., 1977, *Deformation of Concrete Structures*, McGraw-Hill, New York, 546 pp.

CEB-FIB, 1990, *Model Code for Concrete Structures*, CEB, Thomas Telford, London.

Ghali, A., and Azarnejad, A., 1999, "Deflection Prediction of Members of Any Concrete Strength," *ACI Structural Journal*, V. 96, No. 5, Sept.-Oct., pp. 807-816.

Ghali, A., and Elbadry, M., 1986 and 2000, *User's Manual and Computer Program CRACK*, Research Report CE85-1, Department of Civil Engineering, University of Calgary, Calgary, Alberta, Canada, Feb. Updated and renamed version: "Reinforced and Prestressed Members, Computer program RPM," American Concrete Institute, software code 076AG2.CP.

Ghali, A.; Favre, R.; and Elbadry, M., 2002, *Concrete Structures: Stresses and Deformations*, 3rd Edition, Spon Press, London and New York, website: www.sponpress.com/concretestructures.

Ghali, A., and Neville, A. M., 2003, *Structural Analysis: A Unified Classical and Matrix Approach*, 5th Edition, Spon Press, London and New York, 844 pp.

Gilbert, R. I., and Warner, R. F., 1978, "Tension Stiffening in Reinforced Concrete Slabs," *Journal of the Structural Division*, V. 104, No. ST.

Hall, T. S., and Ghali, A., 1997, "Prediction of the Flexural Behavior of Concrete Members Reinforced with GFRP Bars," *Society for the Advancement of Material and Process Engineering,* V. 42, pp. 298-310.

ISIS Canada, 2001, "Reinforcing New Structures with Fiber Reinforced Polymers*,*" *Design Manual* No. 3.

Kaufmann, W., and Marti, P., 1998, "Structural Concrete: Cracked Membrane Model," *Journal of Structural Engineering*, V. 124, No. 12, pp. 1467-1475.

Magura, D.; Sozen, M. A.; and Siess, C. P., 1964, "A Study of Stress Relaxation in Prestressing Reinforcement," *PCI Journal*, V. 9, No. 2, pp. 13-57.

Polak, M. A., and Vecchio, F. J., 1993, "Nonlinear Analysis of Reinforced Concrete Shells," *Journal of Structural Engineering*, V. 119, No. 12, pp. 3439-3462.

Scanlon, A., and Murray, D. W., 1974, "Time Dependent Reinforced Concrete Slab Deflections," *Journal of the Structural Division*, V. 100, No. ST9, pp. 1911-1924.

Trost, H., 1967, "Auswirkungen des Superpositionsprinzips auf Kriech-und Relaxations—Probleme bei Beton und Spannbeton," *Beton-und Stahlbetonbau*, V. 62, No. 10, pp. 230-238.

ACI Committee 435 during creation of Appendix B

Andrew Scanlon[*]
Chair

Debrethann R. Cagley-Orsak
Secretary

John H. Allen	N. John Gardner[*]	Vilas S. Mujumdar
Alex Aswad	Amin Ghali*	Hani H. A. Nassif
Abdeldjelil Belarbi	S. K. Ghosh	Edward G. Nawy
Brahim Benmokrane	Anand B. Gogate	Maria A. Polak[*]
Donald R. Buettner	Hidayat N. Grouni	Madhwesh Raghavendrachar
Finley A. Charney	Robert W. Hamilton	B. Vijaya Rangan
Ramesh M. Desai	Paul C. Hoffman	Charles G. Salmon
Luis Garcia Dutari	Cheng-Tzu T. Hsu	Mark P. Sarkisian
Mamdouh M. El-Badry[*]	Shivaprasad Kudlapur	Richard H. Scott
A. Samer Ezeldin	Peter Lenkei	A. Fattah Shaikh
Russell S. Fling	Faris A. Malhas	Himat T. Solanki
Simon H. C. Foo	Bernard L. Meyers	Susanto Teng

[*]Members who prepared Appendix B.

CONVERSION FACTORS---INCH-POUND TO SI (METRIC)*

To convert from	to	multiply by

Length

inch	millimeter (mm)	25.4E†
foot	meter (m)	0.3048E
yard	meter (m)	0.9144E
mile (statute)	kilometer (km)	1.609

Area

square inch	square millimeter (mm^2)	645.1
square foot	square meter (m^2)	0.0929
square yard	square meter (m^2)	0.8361

Volume (capacity)

ounce	milliliters (m L)	29.57
gallon	cubic meter (m^3)	0.003785
cubic inch	cubic millimeter (mm3)	16390
cubic foot	cubic meter (m3)	0.02832
cubic yard	cubic meter (m^3)‡	0.7646

Force

kilogram-force	newton (N)	9.807
kip-force	kilo newton (kN)	4.448
pound-force	newton (N)	4.448

Pressure or stress (force per area)

kilogram-force/square meter.	pascal (Pa)	9.807
kip-force/square inch (ksi)	megapascal (MPa)	6.895
newton/square meter (N/m^2)	pascal (Pa)	1.000E
pound-force/square foot	pascal (Pa)	47.88
pound-force/square inch (psi)	kilopascal (kPa)	6.895

Bending moment or torque

inch-pound-force	newton-meter $(N \bullet m)$	0.1130
foot-pound-force	newton-meter (N.m)	1.356
meter-kilogram-force	newton-meter (N.m)	9.807

Mass

ounce-mass (avoirdupois)	gram (g)	28.34
pound-mass (avoirdupois)	kilogram (kg)	0.4536
ton (metric)	megagram (mg)	1.000E
ton (short, 2000 lbm)	kilogram (kg)	907.2

Mass per volume

pound-mass/cubic foot	kilogram/cubic meter (kg/m^3)	16.02
pound-mass/cubic yard	kilogram/cubic meter (kg/m^3)	0.5933
pound-mass/gallon	kilogram/cubic meter (kg/m^3)	119.8

Temperature §

degrees Fahrenheit (F)	degrees Celsius (C)	$t_C \quad (t_F - 32)/1.8$
degrees Celsius (C)	degrees Fahrenheit (F)	$t_F = 1.8 t_C + 32$

---

*This selected list gives practical conversion factors of units found in concrete technology. The reference sources for information on SI units and more exact conversion factors are ASTM E 380 and E 621. Symbols of metric units are given in parenthesis.

† E Indicates that the factor given is exact.

‡One liter (cubic decimeter) equals 0.001 m^3 or 1000 cm^3.

§ These equations convert one temperature reading to another and include the necessary scale corrections. To convert a difference in temperature from Fahrenheit degrees to Celsius degrees, divide by 1.8 only. i.e., a change from 70 to 88 F represents a change of 18 F or 18/1.8 = 10 C deg.